THE REGULATION OF SIGNALING IN
HEMATOPOIETIC STEM CELL MAINTENANCE

by

Jae Young Lee

A dissertation submitted in partial fulfillment
of the requirements for the degree of
Doctor of Philosophy
(Cell and Developmental Biology)
in The University of Michigan
2010

Doctoral Committee:

       Professor Sean J. Morrison, Chair
       Professor Eric R. Fearon
       Assistant Professor Diane C. Fingar
       Assistant Professor Ivan P. Maillard

ACKNOWLEDGMENTS

I wish to genuinely thank my mentor Sean Morrison for giving me a glimpse of what it means to pursue science at the highest level. His tireless passion and dedication to the hunt for new knowledge will be a great source of inspiration for me throughout the next phase of my scientific training and beyond.

I would like to thank Daisuke Nakada for his invaluable help on the Pten project as described in Chapter 2. He worked painstakingly to optimize techniques for Western blotting and immunofluorescence staining of hematopoietic stem cells and I have learned much from him. We worked together on many experiments and we are co-authors on a manuscript currently under review.

I would like to thank Fei Liu for all of his hard work on the FIP200 project. I performed many of the initial replicates of experiments described in Chapter 3, and Fei worked diligently to complete the data sets. I am second author on a manuscript we prepared together, and that manuscript is currently under review.

I want to thank current and former Morrison lab members for their intellectual contributions to my work and for their friendship during my 4 years in the lab. I thank Jeff Magee for our discussions and for serving as an outstanding physician-scientist role model. Jeff is currently examining the role of Pten in the regulation of neonatal hematopoietic stem cells, and he has helped me collect samples for future microarray studies. I thank Melih Acar for his expertise on many matters and for providing me with a testing ground for new ideas. I also thank Sergei Chuikov, Boaz Levi, Shenghui He, Lei

TABLE OF CONTENTS

LIST OF TABLES

LIST OF FIGURES

ABSTRACT

Hematopoietic stem cells (HSCs) maintain themselves throughout life by undergoing self-renewing divisions and by differentiating to generate all the blood and immune system cells in the body. Tumor suppressors play an important role in regulating signaling pathways that maintain HSCs while avoiding leukemogenesis. Deficiency in the tumor suppressor *Pten* depletes HSCs but expands leukemia-initiating cells. Understanding this mechanistic difference could lead to anti-leukemia therapies with less toxicity to HSCs. Indeed, the mTOR inhibitor, rapamycin, blocks HSC depletion and leukemogenesis in *Pten*-deficient cells, raising the question of how mTOR activation depletes HSCs. In contrast to what occurs after *FoxO1/3/4* deletion, we found that the depletion of *Pten*-deficient HSCs was not caused by oxidative stress and could not be blocked by N-acetyl-cysteine. Instead, *Pten* deletion induced the expression of $p16^{Ink4a}$ and p53 in HSCs, and $p19^{Arf}$ and p53 in other hematopoietic cells. Rapamycin treatment attenuated these increases. Analysis of compound mutant mice indicated that p53 suppressed leukemogenesis and promoted HSC depletion after *Pten* deletion. $p16^{Ink4a}$ also promoted HSC depletion but had a limited role suppressing leukemogenesis. $p19^{Arf}$ suppressed leukemogenesis but did not deplete HSCs. *Pten* deficiency and *FoxO* deficiency therefore deplete HSCs by different mechanisms. These results provide functional evidence that mTOR activation depletes stem cells by inducing a tumor suppressor response.

Little is known about whether autophagic processes are active in HSCs and whether they contribute to HSC maintenance. FIP200 plays important roles in mammalian autophagy and other cellular functions, but its role in hematopoiesis has not been examined. We found that conditional deletion of *FIP200* in hematopoietic cells led to impaired autophagy in the fetal liver, severe anemia, and perinatal lethality. FIP200 was also cell-autonomously required for the maintenance of fetal HSCs as *FIP200*-deleted HSCs were unable to reconstitute lethally irradiated recipients. *FIP200* ablation increased the rate of cell-cycling in HSCs, which may have contributed to HSC depletion. Interestingly, *FIP200*-deleted HSCs exhibited increased mitochondrial mass and elevated reactive oxygen species levels. Our data identify FIP200 as a key intrinsic regulator of fetal HSCs and implicate a potential role for autophagy in the maintenance of fetal hematopoiesis and HSCs.

CHAPTER 1

INTRODUCTION: THE REGULATION OF SIGNALING IN HEMATOPOIETIC STEM CELL MAINTENANCE

Stem cells are responsible for the regeneration of cells in tissues as diverse as blood, brain, breast, intestine, and skin. The regenerative demands of replacing all blood and immune cells by hematopoietic stem cells (HSCs) are especially astounding. It is estimated that over the course of our lives, HSCs are responsible for generating 10^{16} hematopoietic cells, equivalent to roughly 10 times our body weight (MacKey, 2001) despite the fact that HSCs represent approximately 0.003% of bone marrow cells under steady-state conditions (Harrison and Zhong, 1992; Kiel et al., 2005). In certain contexts, such as development or response to injury, the regenerative demands are even higher.

HSCs maintain themselves throughout life by undergoing self-renewing divisions in which at least one of the daughter cells retains the multipotency of HSCs. Age-related hematopoietic morbidities such as anemia, decreased immunity, and bone marrow failure are all thought to reflect a progressive decline of HSC function with age (Sharpless and DePinho, 2007). Furthermore, leukemic cells can maintain themselves through ectopic or over-activation of HSC self-renewal pathways (Lessard and Sauvageau, 2003). Thus, understanding of the mechanisms that maintain HSCs also has the potential to provide fundamental insights into aging and cancer. One critical signaling pathway that regulates HSC maintenance is the PI-3kinase pathway.

1

PI-3kinase signaling

Cells can sense whether environmental conditions are suitable for cell growth and cell division by activating signaling cascades in response to ligand-receptor interactions. One such class of interactions involves those between growth factors and their respective receptor tyrosine kinases (Schlessinger, 2000). Upon growth factor binding to the extracellular domain of the receptor, structural changes activate these receptors by increased autophosphorylation of the cytoplasmic domain (Schlessinger, 2000). Activated receptors directly interact with and activate phosphotidylinositide 3-kinases (PI-3kinase) which promote cell growth, proliferation, and survival through a variety of downstream mechanisms (Yuan and Cantley, 2008) (see Figure 1.1 for a schematic). Activated receptor tyrosine kinases can also phosphorylate scaffolding adaptors such as Insulin Receptor Substrate 1 (IRS-1), which in turn can also activate PI-3kinases. Class I PI-3kinases function by converting phosphatidylinositol-4,5-bisphosphate (PIP2) into phosphatidylinositol-3,4,5-trisphosphate (PIP3) (Yuan and Cantley, 2008) and downstream signaling proteins containing pleckstrin-homology domains, such as Phosphoinositide-Depdendent Kinase 1 (PDK1) and Akt, are then recruited to sites of activated PI3-kinase by directly binding to PIP3. This recruitment to the plasma membrane then facilitates the activating phosphorylation of the T308 residue in Akt by PDK1.

Akt/mTOR signaling

The serine/threonine kinase Akt represents a critical node in the promotion of cell growth, proliferation and survival because numerous targets are phosphorylated by Akt.

The function of many of these targets are inactivated by Akt phosphorylation, including the Tuberous Sclerosis Complex (TSC) (Inoki et al., 2002; Tang et al., 1999), which is a critical negative regulator of the mammalian target of rapamycin (mTOR) kinase, and is composed of TSC1 and TSC2. The TSC complex negatively regulates mTOR by hydrolyzing the active GTP-bound form of Rheb into the inactive GDP-bound form (Inoki et al., 2002). Inhibition of the TSC complex by Akt therefore results in the activation of mTOR.

mTOR functions as the catalytic subunit in a complex formed with regulatory associated protein of mTOR (Raptor), mammalian lethal with Sec13 protein 8/G-protein b-subunit like protein (mLST8/GβL), proline-rich Akt substrate 40 kDa (PRAS40), and DEP-domain-containing mTOR-interacting protein (Deptor) to form mTORC1, which is directly inhibited by the drug rapamycin (Fingar and Blenis, 2004; Guertin and Sabatini, 2007; Laplante and Sabatini, 2009). mTORC1 promotes cell growth and proliferation by inhibiting catabolic processes such as autophagy (Codogno and Meijer, 2005), and by activating numerous anabolic processes, including protein synthesis, by phosphorylating the p70 ribosomal S6 kinase and the eukaryotic initiation factor 4E-binding protein 1 (4EBP1) (Fingar et al., 2002; Inoki et al., 2002). Activated S6 kinase can also inhibit IRS-1, forming a negative feedback loop that results in the attenuation of the PI-3kinase signaling pathway (Zick, 2005). mTOR also forms a second complex with rapamycin-insensitive companion of mTOR (Rictor), mammalian stress-activated protein kinase interacting protein (mSIN1), protein observed with Rictor-1 (Proctor-1), mLST8, and Deptor, to form mTORC2, which can be indirectly inhibited by rapamycin in certain cell types, including hematopoietic cells (Fingar and Blenis, 2004; Guertin and Sabatini,

2007; Sarbassov et al., 2006). In comparison to mTORC1, relatively little is known about mTORC2, especially of the signaling pathways upstream of mTORC2 activation or inhibition. Regardless, growth factors can stimulate mTORC2 activity (Guertin and Sabatini, 2007) and activated mTORC2 also promotes cell survival and proliferation by positively regulating Akt through phosphorylation of the S473 residue (Sarbassov et al., 2005).

Pten and the PI-3kinase/Akt/mTOR pathway in HSC maintenance

Phosphatase and tensin homolog (Pten) is a dual specificity protein and lipid phosphatase that attenuates PI-3kinase pathway signaling by dephosphorylating PIP3 to PIP2 (Maehama and Dixon, 1998), and its function reduces Akt, mTORC1, and S6 kinase activities. In this way, Pten functions as a tumor suppressor, and Pten deficiency increases the growth, proliferation, and survival of many cells (Sun et al., 1999). Consistent with this, inactivating mutations or silencing of *Pten* are frequently observed in diverse cancers (Di Cristofano and Pandolfi, 2000).

Regulation of the PI-3kinase/Akt/mTOR signaling axis is central to the maintenance of HSCs. Serial transplantation experiments in lethally irradiated mice have demonstrated the extensive self-renewal potential of HSCs, but at steady state, most HSCs in adult mice are quiescent and enter the cell cycle infrequently (Cheshier et al., 1999; Foudi et al., 2008; Kiel et al., 2007). Although the potential of HSCs to self-renew exceeds what is physiologically required during a normal life span, adult HSCs are quickly depleted when forced to undergo repeated rounds of cell division (Orford and Scadden, 2008). These observations are consistent with earlier reports indicating that the

vast majority of long-term multilineage reconstituting potential of HSCs resides within the quiescent fraction (Fleming et al., 1993), and with more recent reports that a slowly cycling population of HSCs possesses greater reconstituting activity than cycling HSCs (Foudi et al., 2008; Wilson et al., 2008). Activation of the PI-3kinase/Akt/mTOR signaling axis drives HSCs into cell cycle.

Conditional deletion of *Pten* in the mouse hematopoietic system by Mx-1-Cre drives HSCs into cell-cycle, leading to a transient increase in the number of HSCs (Yilmaz et al., 2006; Zhang et al., 2006). Over the course of several weeks, *Pten*-deleted HSCs become depleted, and unlike control HSCs, *Pten*-deleted HSCs are unable to sustain long-term multilineage reconstitution in lethally irradiated recipients (Yilmaz et al., 2006). *Pten* deletion also leads to the generation of leukemia-initiating cells as *Pten*-deleted mice rapidly develop myeloproliferative disease (MPD) and transplantable acute myeloid leukemia (AML) and T-cell acute lymphoblastic leukemia (T-ALL) (Yilmaz et al., 2006; Zhang et al., 2006). Interestingly, it is possible to exploit the mechanistic differences between normal HSC maintenance and leukemia-initiating cell maintenance by administering the mTOR inhibitor rapamycin. Treatment with rapamycin immediately after *Pten* deletion prevents leukemogenesis, and restores the function of *Pten*-deleted HSCs (Yilmaz et al., 2006). This demonstrates that both leukemogenesis and HSC depletion following *Pten*-deletion are mediated by mTOR hyperactivation.

Activating the PI-3kinase/Akt/mTOR pathway with mutations other than *Pten* deficiency has similar effects on HSCs. Bone marrow progenitors infected with a constitutively active myristoylated Akt (myr-Akt) display higher rates of cell cycling, and become exhausted over time in transplantation models (Kharas et al., 2010). Mice

transplanted with myr-Akt infected bone marrow also develop MPD, AML, and T-ALL by 8 weeks after transplantation (Kharas et al., 2010). Loss of Tsc1 results in the acute loss of HSC quiescence, increased proliferation and eventual depletion of HSCs in an mTOR-dependent manner (Chen et al., 2008; Gan et al., 2008). In contrast to *Pten* deletion, the loss of Tsc1 does not result in leukemogenesis. Whereas *Tsc1* deletion using Rosa26-CreER results in MPD (Gan et al., 2008), Mx-1-Cre driven deletion results in a curious reduction of the myeloid compartment (Chen et al., 2008). Overexpression of Rheb2, which is inhibited by the TSC complex, leads to increased mTORC1 activity and the transient expansion of progenitors but a decrease in long-term reconstituting ability (Campbell et al., 2009). *Pml*-deficient mice also display loss of HSC quiescence that results in a temporary increase but long-term decline in HSC activity (Ito et al., 2008). Consistent with the role of Pml as a negative regulator of mTOR (Bernardi et al., 2006), rapamycin treatment prevents the exhaustion of *Pml*-deficient HSCs (Ito et al., 2008). Although Pml loss alone does not induce leukemogenesis, the maintenance of leukemia-initiating cells in a retrovirally tranduced BCR-ABL chronic myeloid leukemia model are also dependent on Pml (Ito et al., 2008). Stimulation with interferon-α also increases the number of HSCs that entered the cell cycle, and HSCs display a higher level of activated Akt by flow cytometry (Essers et al., 2009). Chronic stimulation with interferon-α also renders HSCs unable to compete in reconstitution experiments (Essers et al., 2009). Thus, activation of the PI-3kinse/Akt/mTOR pathway drives HSCs out of quiescence and ultimately leads to their depletion.

Recent work suggests that hyperactivation of mTOR may be a generalized mechanism that depletes stem cells in tissues other than the hematopoietic system.

Persistent ectopic Wnt1 stimulation in the epidermis leads to acute growth of hair follicles, but depletes epithelial stem cells by senescence which results in the loss of hair growth (Castilho et al., 2009). This depletion is mediated by activated mTOR signaling as rapamycin restores epithelial stem cells and hair growth despite persistent Wnt1 stimulation (Castilho et al., 2009).

FoxOs and the suppression of oxidative damage in HSCs

Members of the Forkhead O (FoxO) subfamily of transcription factors, including FoxO1, FoxO3a, and FoxO4, comprise another important class of Akt targets that becomes inactivated upon phosphorylation by Akt (Manning and Cantley, 2007). When active, FoxO transcription factors reside in the nucleus and promote the expression of various target genes involved in cellular functions such as cell cycle arrest, stress resistance, apoptosis, and detoxification of reactive oxygen species (ROS). Activated Akt phosphorylates each of the FoxO transcription factors on conserved residues, resulting in a 14-3-3 protein dependent exclusion from the nucleus and subsequent degradation in the cytoplasm (Biggs et al., 1999; Brunet et al., 1999; Manning and Cantley, 2007). This reduces the expression of antioxidant enzymes and increases intracellular levels of ROS.

HSCs are highly sensitive to the toxic effects of ROS (Ito et al., 2004; Ito et al., 2006). When FoxO1, FoxO3a, and FoxO4 are conditionally deleted from the hematopoietic system, HSCs display an increase in ROS and become depleted (Tothova et al., 2007). Aspects of HSC function can be partially rescued by treatment with the antioxidant, N-Acetyl-cysteine (NAC), indicating that oxidative stress contributes to the depletion of HSCs after the loss of FoxO transcription factors (Tothova et al., 2007).

FoxO3a is especially important for HSC maintenance as the loss of FoxO3a alone can increase ROS levels and deplete HSCs (Miyamoto et al., 2007; Yalcin et al., 2008).

A central question that arose in the field as a result of these observations is whether PI-3kinase/Akt pathway activation depletes HSCs as a consequence of FoxO inactivation and increases in oxidative damage, or whether mTOR activation depletes HSCs through other unknown mechanisms (Orford and Scadden, 2008; Tothova and Gilliland, 2007). One possibility is that *Pten* deletion depletes HSCs through an Akt mediated inactivation of FoxO transcription factors that decreases the expression of antioxidant enzymes and results in an elevation of intracellular ROS. In support of this idea, deletion of *Tsc1* results in an increase in mitochondrial biogenesis and ROS levels within HSCs, and treatment with NAC restores the reconstitution defects of *Tsc1*-deleted marrow (Chen et al., 2008). In contrast, constitutively active Akt also depletes HSCs without increasing ROS levels, and NAC is unable to rescue defects in colony forming ability (Kharas et al., 2010). Therefore, activation of specific components within the PI-3kinase/Akt/mTOR pathway sometimes leads to the depletion of HSCs through increased oxidative stress, and sometimes does not. It remained to be tested whether *Pten* deletion could result in HSC depletion through oxidative stress, and whether antioxidant treatment could rescue the function of *Pten*-deleted HSCs.

Tumor suppressor pathways

An alternative mechanism that could account for the depletion of HSCs after *Pten* deletion involves the compensatory activation of other tumor suppressors and cell-cycle inhibitors in response to the oncogenic stress of persistently activated PI-

3kinase/Akt/mTOR signaling. A brief overview of major tumor suppressor pathways is provided below.

Cell-cycle progression requires the activation of cyclin-dependent kinases (CDKs) by association with cyclin subunits (Sherr and Roberts, 1999). Triggering exit from quiescence first involves the activation of CDK4 and CDK6 by D-type cyclins. Next, the DNA replication checkpoint is successfully negotiated by activation of CDK2/cyclin E and CDK2/cyclin A kinases, then activation of CDK1/cyclin B initiates mitosis. p53, p16^{Ink4a}, and p19^{Arf} negatively regulate progression through the cell-cycle by directly functioning as a CDK inhibitor (like p16^{Ink4a}), or by promoting the expression of other CDK inhibitors (like p53 and p19^{Arf}) (Bringold and Serrano, 2000). These CDK inhibitors (CKIs) generally fall into two groups (Ink4 family and Cip/Kip family) that activate parallel senescence pathways (Ink4/Rb and p19^{Arf}/p53/p21^{Cip1}). The Ink4 family, which is comprised of p16^{Ink4a}, p15^{Ink4b}, p18^{Ink4c}, and p19^{Ink4d}, function by inhibiting CDK4 and CDK6, and therefore maintain the retinoblastoma tumor suppressor (Rb) in its unphosphorylated, active state (Ruas and Peters, 1998; Sherr, 2004).

In addition to *p16^{Ink4a}*, the *Cdkn2a* locus also encodes *p19^{Arf}*, which has a distinct promoter and first exon, but shares the second and third exons with p16^{Ink4a} in an alternate reading frame. One of the most well characterized functions of p19^{Arf} is inhibition of Mdm2 and thus stabilization of p53, though p53-independent functions of p19^{Arf} exist (Kim and Sharpless, 2006; Sherr, 2006). Nevertheless, an important transcriptional target of p53 is p21^{Cip1} (el-Deiry et al., 1993), of the Cip/Kip family that also includes p27^{Kip1} and p57^{Kip2}. Cip/Kip members inhibit CDK2/E-A complexes and thus induce cell-cycle arrest.

Oncogenic stresses activate tumor suppressive programs

Functional tumor suppressor pathways successfully limit cancer growth because pro-growth signals in major signaling pathways often trigger mechanisms that constrain cell proliferation. One example is induction of p53, which promotes the activation of several apoptotic programs at multiple levels (Fridman and Lowe, 2003; Vogelstein et al., 2000). Evan et al. (1992) initially demonstrated that oncogenic c-Myc activation in Rat-1 fibroblasts induces apoptosis (Evan et al., 1992). Later studies in mouse embryonic fibroblasts (MEFs) showed that apoptosis occurs through the induction p19^{Arf} to stabilize p53 (Zindy et al., 1998). Expression of other oncogenes such as E1A in MEFs also leads to a p53-dependent apoptosis that also requires p19^{Arf} (de Stanchina et al., 1998). Even in HSCs, losing the tumor suppressor Fbxw7, which inhibits c-Myc (Minella and Clurman, 2005), leads to increased cycling and premature HSC depletion due to p53-dependent apoptosis (Matsuoka et al., 2008). Thus, p53 can be activated in response to oncogenic stress and result in apoptosis.

Beyond apoptosis, senescence appears to be another common response in cells exposed to oncogenic stress (Lowe et al., 2004). As with apoptosis, p53 is also a major regulator of the senescence response, along with the tumor suppressors p16^{Ink4a} and p19^{Arf}. The first report of oncogene-induced senescence was described by Serrano et al. (1997) where over-expression of oncogenic Ras in cultured cells leads to a permanent cell cycle arrest and an accumulation of p16^{Ink4a} and p53 (Serrano et al., 1997). Cells that are deficient for either p16^{Ink4a}/p19^{Arf} or p53 do not undergo senescence, even under

enforced expression of oncogenic Ras, suggesting that senescence pathways may have evolved as tumor suppressive mechanisms (Serrano et al., 1997).

These observations were later confirmed in studies of multiple human and mouse cancers, demonstrating that senescence is tumor suppressive under physiological conditions *in vivo*. Human nevi harbor oncogenic mutations in *BRAF* but also show signs of senescence, suggesting that senescence blocks the development of melanomas from these lesions (Michaloglou et al., 2005). Oncogenic Ras signaling in mouse lymphoma and mouse lung adenoma models also triggers senescence to limit the growth of pre-neoplastic lesions (Braig et al., 2005; Collado et al., 2005). Benign human neurofibromas from *NF1* mutant patients are also senescent, and disrupted NF1 signaling in human fibroblasts leads to senescence via Ras hyperactivation (Courtois-Cox et al., 2006). Acute reactivation of p53 in mouse models of hepatocellular carcinoma, lymphoma, and sarcoma rapidly induces senescence and leads to significant regression and in some cases partial clearance of these lesions by immune cells (Ventura et al., 2007; Xue et al., 2007). In all of these studies, p16^{Ink4a} or p53 are the central mediators of senescence in the pre-neoplastic lesions.

Activation of tumor suppressor pathways after *Pten* deletion

Losing Pten is sufficient to trigger the activation or expression of various anti-proliferative tumor suppressors. Deleting *Pten* from the mouse prostate leads to the development of benign prostatic intraepithelial neoplasia that show signs of senescence and elevated levels of p53 and p21^{Cip1} (Chen et al., 2005). Furthermore, follow up studies in MEFs distinguished the senescence response that is induced as a result of Pten

inactivation, termed Pten-loss-induced cellular senescence (PICS), from classical oncogene-induced senescence. First, the onset of PICS is characterized by an increased translation of p53. Second, the onset of PICS does not require a sustained hyperproliferative phase or a DNA damage response (Alimonti et al., 2010). Similarly, deletion of *PTEN* from human epithelial cells increases p53 and p21^{CIP1} levels and leads to a senescence-like growth arrest (Kim et al., 2007). In MEFS, simply activating mTOR signaling by Tsc1 loss also leads to p53 accumulation and sensitization to p53-dependent apoptosis during stress (Lee et al., 2007). Treatment with rapamycin abrogates p53 accumulation and protects cells from apoptosis. Pten and p53 inactivation cooperate in the generation of bladder cancer (Puzio-Kuter et al., 2009) and also glioblastomas by promoting the maintenance of highly undifferentiated, self-renewing cells (Zheng et al., 2008). Pten inactivation also collaborates with p16^{Ink4a}/p19^{Arf} loss in the generation of multiple types of cancers, including histiocytic sarcoma in both mice and humans (Carrasco et al., 2006; You et al., 2002). Therefore, inactivation of Pten is sufficient to induce tumor suppressors in the p16^{Ink4a} and p19^{Arf}/p53/p21^{Cip1} pathways in multiple tissues. This raises the question of what consequences this might have for stem cell function.

Tumor suppressors and stem cell maintenance

Although tumor suppressors are known for their ability to suppress cancer development, many also limit stem cell function. Specifically, gatekeeping tumor suppressors reduce stem cell function by promoting senescence, cell death, or other unknown mechanisms (Pardal et al., 2005). Alternatively, oncogenes and proto-

oncogenes tend to promote stem cell function by endowing cells with the ability to cycle. Thus, a careful balance of tumor suppressor and proto-oncogene activity is essential to provide sufficient protection against tumorigenesis while retaining the regenerative capacity of stem cells.

Some proto-oncogenes promote stem cell self-renewal by negatively regulating the expression of gatekeeping tumor suppressors. In neural stem cells, one way Bmi-1 promotes self-renewal is by inhibiting the expression of $p16^{Ink4a}$ and $p19^{Arf}$ (Molofsky et al., 2005; Molofsky et al., 2003). Loss of Bmi-1 triggers the upregulation of $p16^{Ink4a}$ and $p19^{Arf}$ expression in neural stem cells and results in neural stem cell depletion. Deletion of either $p16^{Ink4a}$ or $p19^{Arf}$ results in a substantial but partial rescue of $Bmi-1^{-/-}$ neural stem cells, indicating that other mechanisms also deplete neural stem cells in the absence of Bmi-1. HSC function in Bmi-1$^{-/-}$ mice is also limited by both p16^{Ink4a} and p19^{Arf}, though cell extrinsic effects and perturbations in other pathways also contribute to HSC depletion in the absence of Bmi-1 (Lessard and Sauvageau, 2003; Liu et al., 2009a; Oguro et al., 2006; Park et al., 2003). The high mobility group protein Hmga2 also promotes the maintenance of neural stem cells in fetal and young adult mice by repressing p16^{Ink4a} and p19^{Arf} (Nishino et al., 2008).

Other stimuli also deplete stem cells by increasing the expression of tumor suppressors. Myelosuppressive treatments such as non-lethal ionizing radiation or busulfan exposure result in sustained damage to HSC self-renewal with a prolonged elevation of p21^{Cip1}, p19^{Arf}, and p16^{Ink4a} (Meng et al., 2003; Wang et al., 2006). Furthermore, oxidative damage caused by Atm loss is thought to compromise HSC function through p16^{Ink4a} and p19^{Arf} induction (Ito et al., 2004; Ito et al., 2006). Aging

also results in the increased expression of both p16^{Ink4a} and p19^{Arf} in almost all mouse tissues, and p16^{Ink4a} expression increases in many aged human tissues (Krishnamurthy et al., 2004; Zindy et al., 1997). p16^{Ink4a} expression also increases in aged HSCs, neural stem cells, and pancreatic β-cells, and this coincides with a decline in proliferative potential that is partially rescued by p16^{Ink4a} deficiency (Janzen et al., 2006; Krishnamurthy et al., 2006; Molofsky et al., 2006). Therefore, increased expression of gatekeeping tumor suppressors either by oncogene inactivation or other stimuli decreases stem cell function.

Since activation of gatekeeping tumor suppressors generally results in suppression of stem cell activity, one could predict that the loss of these tumor suppressors would enhance stem cell function. Consistent with this idea, the loss of another member of the Ink4 family, p18^{Ink4c}, results in an expansion of the HSC pool and enhanced competitiveness during serial reconstitution (Yu et al., 2006; Yuan et al., 2004). Combined loss of p16^{Ink4a} and p19^{Arf} increases the serial reconstituting capacity of HSCs, though losing p19^{Arf} alone does not (Stepanova and Sorrentino, 2005). The loss of p53 increases the frequency of HSCs both by immunophenotype and function (TeKippe et al., 2003), and hematopoietic reconstitution following myeloablative treatment is enhanced in the absence of p53 (Wlodarski et al., 1998). Furthermore, the gene dosage of p53 is inversely correlated with engraftment activity from aged p53$^{+/-}$, p53$^{+/+}$, and p53$^{+/m}$ hypermorphic mice, which express a truncated but hyperactive form of p53 (Dumble et al., 2007). These effects on HSCs by p53 loss may be mediated through enhanced cell cycling (Liu et al., 2009b). Loss of all three Rb family members, Rb, p107, and p130 increases HSC cycling, though the effects on HSC maintenance remain uncertain

(Viatour et al., 2008). In contrast, loss of p21[Cip1] promotes the exhaustion of HSCs under the stresses of myeloablation or serial transplantation in mice of mixed background (Cheng et al., 2000), though these effects appear to be minimal when assessed in backcrossed C57BL/6 mice (van Os et al., 2007). Overall, loss of gatekeeping tumor suppressors enhances HSC function, suggesting that their function is to limit HSC activity.

Taken together, activation of the PI-3kinase/Akt/mTOR pathway drives HSCs out of quiescence and can be oncogenic in the hematopoietic system. Gatekeeper tumor suppressors can be activated in response to oncogenic stress, but whether this occurs in HSCs in response to PI-3kinase/Akt/mTOR activation is unknown. Many gatekeeper tumor suppressors deplete stem cells by limiting self-renewing divisions. These observations raise the question of whether *Pten*-deletion results in HSC depletion through the activation of a tumor suppressor response.

Diverse cellular functions are regulated by FIP200

The PI-3kinase pathway only represents one of many pathways that work in concert to promote the maintenance of HSCs. Understanding the relative contributions of different pathways in the physiologic regulation of HSCs has been aided by the systematic loss-of-function evaluations of important signaling pathways such as Notch (Maillard et al., 2008; Mancini et al., 2005), Wnt/β-catenin (Cobas et al., 2004; Jeannet et al., 2008; Koch et al., 2008), and Hedgehog (Gao et al., 2009; Hofmann et al., 2009). HSCs are likely maintained by signaling nodes that orchestrate a diverse array of cellular functions. FIP200 appears to be such a protein (Gan and Guan, 2008). Focal adhesion

kinase family interacting protein of 200 kD (FIP200) was originally identified as a direct inhibitor of proline-rich tyrosine kinase 2 (Pyk2) and the closely related focal adhesion kinase (FAK) (Ueda et al., 2000). Inhibition of FAK by FIP200 over-expression results in decreased cell spreading, cell migration, and cell cycle progression in human fibroblasts (Abbi et al., 2002).

Other FAK-independent roles for FIP200 have also been identified. Studies in MEFs revealed that FIP200 increases cell size by binding to TSC1 and inhibiting the TSC complex, resulting in increased S6 kinase phosphorylation (Gan et al., 2005). FIP200 also induces RB expression in human leukemic cell lines (Chano et al., 2002a; Kontani et al., 2003), and *FIP200* harbors large truncating deletions in 20% of primary human breast cancers (also known as RB1CC1 for RB1-inducible coiled-coil 1 in these studies) (Chano et al., 2002b). In human breast cancer cell lines, FIP200 promotes p21^{Cip1} expression by binding to and stabilizing p53 (Melkoumian et al., 2005). However, conditional epithelial *FIP200* deletion results in increased keratinocyte proliferation and the development of an inflammatory acanthosis resembling human psoriasis, but not mammary tumorigenesis (Wei et al., 2009). Mice that are completely deficient for FIP200 begin to show signs of apoptosis and gross structural damage to cardiac and hepatic tissues at E13.5 and die shortly thereafter (Gan et al., 2006).

FIP200 and autophagy

Recent studies have linked FIP200 to autophagy through its role as an essential component of the ULK1-mAtg13-FIP200 complex. In this way FIP200 is thought to act as the functional analog of Atg17 in the yeast Atg1-Atg13-Atg17 complex, though

sequence homology is limited (Ganley et al., 2009; Hara and Mizushima, 2009; Hara et al., 2008; Hosokawa et al., 2009; Jung et al., 2009). In yeast, the early steps in autophagosome formation require the full catalytic activity of Atg1, which is facilitated by stable complex formation with Atg13 and Atg17 (Glick et al.; Huang and Klionsky, 2002). In high nutrient conditions, TORC1 phosphorylates Atg13 and prevents its interaction with Atg1 (Huang and Klionsky, 2002). In mammalian cells, an analogous working model is proposed for the regulation and function of the ULK1-mAtg13-FIP200 complex where nutrient rich conditions suppress autophagosome formation through phosphorylation of ULK1 and mAtg13 by mTORC1 (Chan, 2009; Ganley et al., 2009; Hosokawa et al., 2009; Jung et al., 2009). FIP200 is required for complex stability and full catalytic activity of ULK1, as loss of FIP200 results in complete blockage of autophagosome formation (Ganley et al., 2009; Hara et al., 2008). Specific deletion of *FIP200* from the central nervous system results in defective autophagosome formation in cerebellar Purkinje cells, accumulation of damaged mitochondria and protein aggregates, and the progressive death of cerebellar neurons, leading to ataxia and the death of all mice by 8 weeks of age (Liang et al., 2010). Thus, FIP200 is a regulator of autophagy *in vivo*, at least in certain cell types.

In unicellular organisms faced with nutrient starvation, autophagy can temporarily satisfy energy requirements by providing building blocks from the digestion of existing proteins and organelles (Levine and Klionsky, 2004; Lum et al., 2005; Tsukada and Ohsumi, 1993). Autophagy also fulfills similar nutritional roles during the neonatal starvation period between birth and maternal nursing in mice, and even for meeting metabolic demands between meals in mice and humans (Kuma et al., 2004; Mizushima

and Klionsky, 2007). Beyond its originally described role as a response against nutrient deprivation, autophagy is now linked to diverse nutrition-independent cellular processes including cell survival, cell death, immunity, tumor suppression, and development so that too much or too little autophagy is detrimental (Lum et al., 2005; Mizushima et al., 2008). Thus, a carefully regulated basal level of autophagy maintains intracellular homeostasis (Hara et al., 2006; Komatsu et al., 2006). One hypothesized model involves the autophagic clearance of aged or damaged organelles, particularly damaged mitochondria, which increase the production of harmful ROS (Lang-Rollin et al., 2003). A similar model has been proposed to mediate the fatal anemia observed in mice lacking an essential autophagy gene *Atg7*. Erythroid cells from *Atg7*-deleted mice fail to clear mitochondria from cells during the maturation of erythroblasts into mature red blood cells, which results in the accumulation of damaged mitochondria, increased ROS, and death of erythroid cells (Mortensen et al., 2010). Several other autophagy defects in mitochondrial clearance and the development of anemia have also been reported (Kundu et al., 2008; Sandoval et al., 2008).

Stem cell maintenance and autophagy

Given the exquisite sensitivity of HSCs to ROS (Ito et al., 2004; Ito et al., 2006), it is possible that autophagy defects lead to mitochondrial accumulation and elevated ROS levels that deplete HSCs. To date, the role of autophagy in HSC maintenance has never been investigated. In fact, very little is known about whether autophagy plays a role in the maintenance of any stem cell population, though a limited number of studies suggest this possibility. In *Drosophila*, the decline of neuroblasts from larval

development into adulthood is thought to be mediated by a combination of FoxO-induced apoptosis and autophagy, demonstrating that autophagy can negatively regulate these stem cells (Siegrist et al., 2010). In malignant gliomas, autophagy appears to play a cytoprotective role by conferring radioresistant properties (Lomonaco et al., 2009) to a subpopulation of CD133^{+} glioma-initiating cells (Singh et al., 2003; Singh et al., 2004). Similarly, leukemia-initiating cells that maintain chronic myeloid leukemias are resistant to tyrosine kinase inhibition (Copland et al., 2006; Jiang et al., 2007; Oravecz-Wilson et al., 2009), and induction of autophagy appears to be one mechanism by which these cells enhance their survival (Bellodi et al., 2009). Also, human CD34^{+} cord blood cells show increased autophagy in response to heavy metal poisoning, though it is unknown whether this is a cytoprotective response or a mechanism of cell death (Di Gioacchino et al., 2008). Taken together, these results raise the possibility that HSC maintenance is influenced by autophagy.
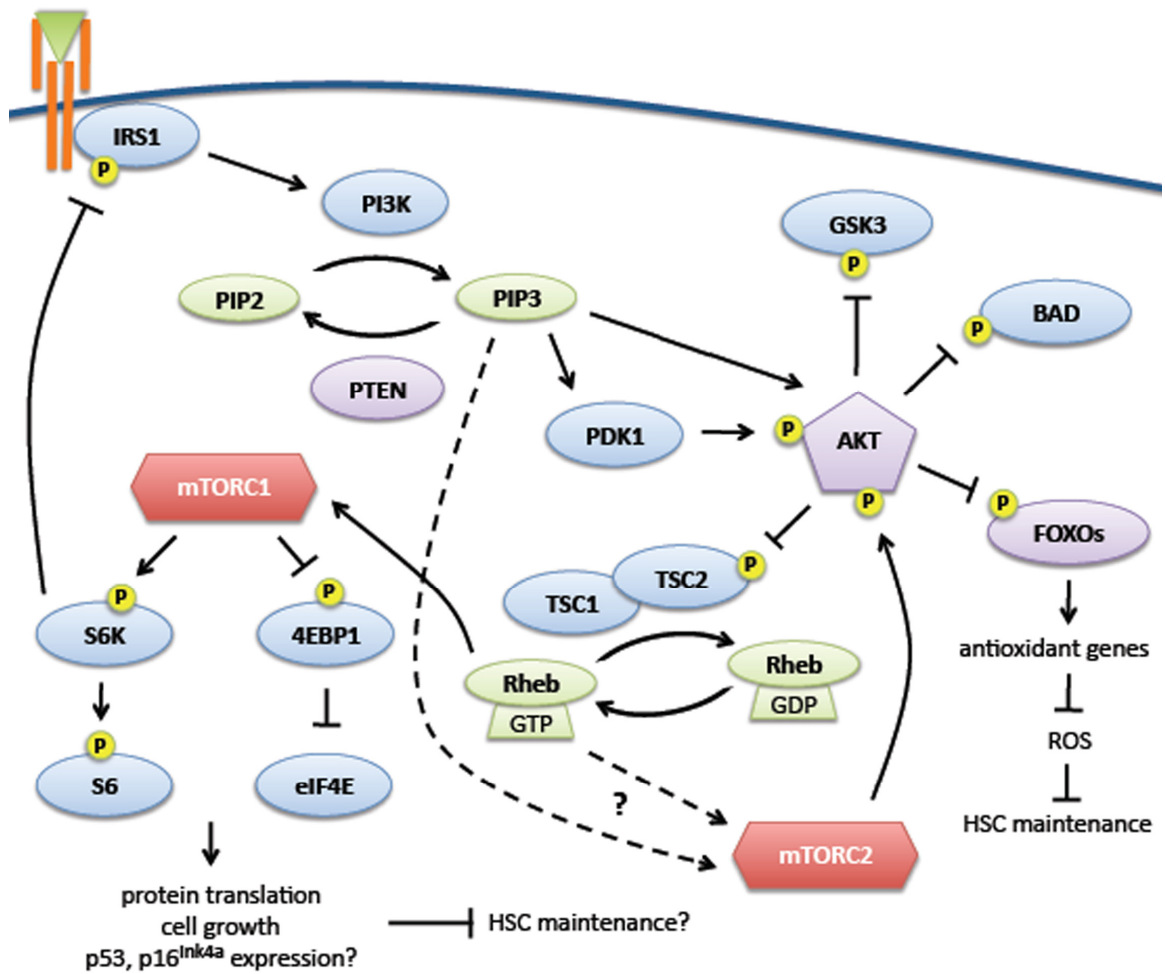
Figure 1.1: A schematic of PI-3kinase pathway signaling adapted from previously published reviews (Laplante and Sabatini, 2009; Soulard and Hall, 2007). See text for details.

BIBLIOGRAPHY

Abbi, S., Ueda, H., Zheng, C., Cooper, L.A., Zhao, J., Christopher, R., and Guan, J.L. (2002). Regulation of focal adhesion kinase by a novel protein inhibitor FIP200. Mol Biol Cell *13*, 3178-3191.

Alimonti, A., Nardella, C., Chen, Z., Clohessy, J.G., Carracedo, A., Trotman, L.C., Cheng, K., Varmeh, S., Kozma, S.C., Thomas, G*., et al.* A novel type of cellular senescence that can be enhanced in mouse models and human tumor xenografts to suppress prostate tumorigenesis. J Clin Invest *120*, 681-693.

Bellodi, C., Lidonnici, M.R., Hamilton, A., Helgason, G.V., Soliera, A.R., Ronchetti, M., Galavotti, S., Young, K.W., Selmi, T., Yacobi, R*., et al.* (2009). Targeting autophagy potentiates tyrosine kinase inhibitor-induced cell death in Philadelphia chromosome-positive cells, including primary CML stem cells. J Clin Invest *119*, 1109-1123.

Bernardi, R., Guernah, I., Jin, D., Grisendi, S., Alimonti, A., Teruya-Feldstein, J., Cordon-Cardo, C., Simon, M.C., Rafii, S., and Pandolfi, P.P. (2006). PML inhibits HIF-1alpha translation and neoangiogenesis through repression of mTOR. Nature *442*, 779-785.

Biggs, W.H., 3rd, Meisenhelder, J., Hunter, T., Cavenee, W.K., and Arden, K.C. (1999). Protein kinase B/Akt-mediated phosphorylation promotes nuclear exclusion of the winged helix transcription factor FKHR1. Proc Natl Acad Sci U S A *96*, 7421-7426.

Braig, M., Lee, S., Loddenkemper, C., Rudolph, C., Peters, A.H., Schlegelberger, B., Stein, H., Dorken, B., Jenuwein, T., and Schmitt, C.A. (2005). Oncogene-induced senescence as an initial barrier in lymphoma development. Nature *436*, 660-665.

Bringold, F., and Serrano, M. (2000). Tumor suppressors and oncogenes in cellular senescence. Exp Gerontol *35*, 317-329.

Brunet, A., Bonni, A., Zigmond, M.J., Lin, M.Z., Juo, P., Hu, L.S., Anderson, M.J., Arden, K.C., Blenis, J., and Greenberg, M.E. (1999). Akt promotes cell survival by phosphorylating and inhibiting a Forkhead transcription factor. Cell *96*, 857-868.

Campbell, T.B., Basu, S., Hangoc, G., Tao, W., and Broxmeyer, H.E. (2009). Overexpression of Rheb2 enhances mouse hematopoietic progenitor cell growth while impairing stem cell repopulation. Blood *114*, 3392-3401.

Carrasco, D.R., Fenton, T., Sukhdeo, K., Protopopova, M., Enos, M., You, M.J., Di Vizio, D., Nogueira, C., Stommel, J., Pinkus, G.S*., et al.* (2006). The PTEN and INK4A/ARF tumor suppressors maintain myelolymphoid homeostasis and cooperate to constrain histiocytic sarcoma development in humans. Cancer Cell *9*, 379-390.

Castilho, R.M., Squarize, C.H., Chodosh, L.A., Williams, B.O., and Gutkind, J.S. (2009). mTOR mediates Wnt-induced epidermal stem cell exhaustion and aging. Cell Stem Cell *5*, 279-289.

Chan, E.Y. (2009). mTORC1 phosphorylates the ULK1-mAtg13-FIP200 autophagy regulatory complex. Sci Signal *2*, pe51.

Chano, T., Ikegawa, S., Kontani, K., Okabe, H., Baldini, N., and Saeki, Y. (2002a). Identification of RB1CC1, a novel human gene that can induce RB1 in various human cells. Oncogene *21*, 1295-1298.

Chano, T., Kontani, K., Teramoto, K., Okabe, H., and Ikegawa, S. (2002b). Truncating mutations of RB1CC1 in human breast cancer. Nat Genet *31*, 285-288.

Chen, C., Liu, Y., Liu, R., Ikenoue, T., Guan, K.L., Liu, Y., and Zheng, P. (2008). TSC-mTOR maintains quiescence and function of hematopoietic stem cells by repressing mitochondrial biogenesis and reactive oxygen species. J Exp Med *205*, 2397-2408.

Chen, Z., Trotman, L.C., Shaffer, D., Lin, H.K., Dotan, Z.A., Niki, M., Koutcher, J.A., Scher, H.I., Ludwig, T., Gerald, W.*, et al.* (2005). Crucial role of p53-dependent cellular senescence in suppression of Pten-deficient tumorigenesis. Nature *436*, 725-730.

Cheng, T., Rodrigues, N., Shen, H., Yang, Y., Dombkowski, D., Sykes, M., and Scadden, D.T. (2000). Hematopoietic stem cell quiescence maintained by p21cip1/waf1. Science *287*, 1804-1808.

Cheshier, S.H., Morrison, S.J., Liao, X., and Weissman, I.L. (1999). In vivo proliferation and cell cycle kinetics of long-term self-renewing hematopoietic stem cells. Proc Natl Acad Sci U S A *96*, 3120-3125.

Cobas, M., Wilson, A., Ernst, B., Mancini, S.J., MacDonald, H.R., Kemler, R., and Radtke, F. (2004). {beta}-Catenin Is Dispensable for Hematopoiesis and Lymphopoiesis. J Exp Med *199*, 221-229.

Codogno, P., and Meijer, A.J. (2005). Autophagy and signaling: their role in cell survival and cell death. Cell Death Differ *12 Suppl 2*, 1509-1518.

Collado, M., Gil, J., Efeyan, A., Guerra, C., Schuhmacher, A.J., Barradas, M., Benguria, A., Zaballos, A., Flores, J.M., Barbacid, M.*, et al.* (2005). Tumour biology: senescence in premalignant tumours. Nature *436*, 642.

Copland, M., Hamilton, A., Elrick, L.J., Baird, J.W., Allan, E.K., Jordanides, N., Barow, M., Mountford, J.C., and Holyoake, T.L. (2006). Dasatinib (BMS-354825) targets an earlier progenitor population than imatinib in primary CML but does not eliminate the quiescent fraction. Blood *107*, 4532-4539.

Courtois-Cox, S., Genther Williams, S.M., Reczek, E.E., Johnson, B.W., McGillicuddy, L.T., Johannessen, C.M., Hollstein, P.E., MacCollin, M., and Cichowski, K. (2006). A negative feedback signaling network underlies oncogene-induced senescence. Cancer Cell *10*, 459-472.

de Stanchina, E., McCurrach, M.E., Zindy, F., Shieh, S.Y., Ferbeyre, G., Samuelson, A.V., Prives, C., Roussel, M.F., Sherr, C.J., and Lowe, S.W. (1998). E1A signaling to p53 involves the p19(ARF) tumor suppressor. Genes Dev *12*, 2434-2442.

Di Cristofano, A., and Pandolfi, P.P. (2000). The multiple roles of PTEN in tumor suppression. Cell *100*, 387-390.

Di Gioacchino, M., Petrarca, C., Perrone, A., Farina, M., Sabbioni, E., Hartung, T., Martino, S., Esposito, D.L., Lotti, L.V., and Mariani-Costantini, R. (2008). Autophagy as an ultrastructural marker of heavy metal toxicity in human cord blood hematopoietic stem cells. Sci Total Environ *392*, 50-58.

Dumble, M., Moore, L., Chambers, S.M., Geiger, H., Van Zant, G., Goodell, M.A., and Donehower, L.A. (2007). The impact of altered p53 dosage on hematopoietic stem cell dynamics during aging. Blood *109*, 1736-1742.

el-Deiry, W.S., Tokino, T., Velculescu, V.E., Levy, D.B., Parsons, R., Trent, J.M., Lin, D., Mercer, W.E., Kinzler, K.W., and Vogelstein, B. (1993). WAF1, a potential mediator of p53 tumor suppression. Cell *19*, 817-825.

Essers, M.A., Offner, S., Blanco-Bose, W.E., Waibler, Z., Kalinke, U., Duchosal, M.A., and Trumpp, A. (2009). IFNalpha activates dormant haematopoietic stem cells in vivo. Nature *458*, 904-908.

Evan, G.I., Wyllie, A.H., Gilbert, C.S., Littlewood, T.D., Land, H., Brooks, M., Waters, C.M., Penn, L.Z., and Hancock, D.C. (1992). Induction of apoptosis in fibroblasts by c-myc protein. Cell *69*, 119-128.

Fingar, D.C., and Blenis, J. (2004). Target of rapamycin (TOR): an integrator of nutrient and growth factor signals and coordinator of cell growth and cell cycle progression. Oncogene *23*, 3151-3171.

Fingar, D.C., Salama, S., Tsou, C., Harlow, E., and Blenis, J. (2002). Mammalian cell size is controlled by mTOR and its downstream targets S6K1 and 4EBP1/eIF4E. Genes Dev *16*, 1472-1487.

Fleming, W.H., Alpern, E.J., Uchida, N., Ikuta, K., Spangrude, G.J., and Weissman, I.L. (1993). Functional heterogeneity is associated with the cell cycle status of murine hematopoietic stem cells. Journal of Cell Biology *122*, 897-902.

Foudi, A., Hochedlinger, K., Van Buren, D., Schindler, J.W., Jaenisch, R., Carey, V., and Hock, H. (2008). Analysis of histone 2B-GFP retention reveals slowly cycling hematopoietic stem cells. Nat Biotechnol.

Fridman, J.S., and Lowe, S.W. (2003). Control of apoptosis by p53. Oncogene *22*, 9030-9040.

Gan, B., and Guan, J.L. (2008). FIP200, a key signaling node to coordinately regulate various cellular processes. Cell Signal *20*, 787-794.

Gan, B., Melkoumian, Z.K., Wu, X., Guan, K.L., and Guan, J.L. (2005). Identification of FIP200 interaction with the TSC1-TSC2 complex and its role in regulation of cell size control. J Cell Biol *170*, 379-389.

Gan, B., Peng, X., Nagy, T., Alcaraz, A., Gu, H., and Guan, J.L. (2006). Role of FIP200 in cardiac and liver development and its regulation of TNFalpha and TSC-mTOR signaling pathways. J Cell Biol *175*, 121-133.

Gan, B., Sahin, E., Jiang, S., Sanchez-Aguilera, A., Scott, K.L., Chin, L., Williams, D.A., Kwiatkowski, D.J., and DePinho, R.A. (2008). mTORC1-dependent and -independent regulation of stem cell renewal, differentiation, and mobilization. Proc Natl Acad Sci U S A *105*, 19384-19389.

Ganley, I.G., Lam du, H., Wang, J., Ding, X., Chen, S., and Jiang, X. (2009). ULK1.ATG13.FIP200 complex mediates mTOR signaling and is essential for autophagy. J Biol Chem *284*, 12297-12305.

Gao, J., Graves, S., Koch, U., Liu, S., Jankovic, V., Buonamici, S., El Andaloussi, A., Nimer, S.D., Kee, B.L., Taichman, R.*, et al.* (2009). Hedgehog signaling is dispensable for adult hematopoietic stem cell function. Cell Stem Cell *4*, 548-558.

Glick, D., Barth, S., and Macleod, K.F. Autophagy: cellular and molecular mechanisms. J Pathol *221*, 3-12.

Guertin, D.A., and Sabatini, D.M. (2007). Defining the role of mTOR in cancer. Cancer Cell *12*, 9-22.

Hara, T., and Mizushima, N. (2009). Role of ULK-FIP200 complex in mammalian autophagy: FIP200, a counterpart of yeast Atg17? Autophagy *5*, 85-87.

Hara, T., Nakamura, K., Matsui, M., Yamamoto, A., Nakahara, Y., Suzuki-Migishima, R., Yokoyama, M., Mishima, K., Saito, I., Okano, H.*, et al.* (2006). Suppression of basal autophagy in neural cells causes neurodegenerative disease in mice. Nature *441*, 885-889.

Hara, T., Takamura, A., Kishi, C., Iemura, S., Natsume, T., Guan, J.L., and Mizushima, N. (2008). FIP200, a ULK-interacting protein, is required for autophagosome formation in mammalian cells. J Cell Biol *181*, 497-510.

Harrison, D.E., and Zhong, R.-K. (1992). The same exhaustible multilineage precursor produces both myeloid and lymphoid cells as early as 3-4 weeks after marrow transplantation. Proceedings of the National Academy of Science USA *89*, 10134-10138.

Hofmann, I., Stover, E.H., Cullen, D.E., Mao, J., Morgan, K.J., Lee, B.H., Kharas, M.G., Miller, P.G., Cornejo, M.G., Okabe, R.*, et al.* (2009). Hedgehog signaling is dispensable

for adult murine hematopoietic stem cell function and hematopoiesis. Cell Stem Cell *4*, 559-567.

Hosokawa, N., Hara, T., Kaizuka, T., Kishi, C., Takamura, A., Miura, Y., Iemura, S., Natsume, T., Takehana, K., Yamada, N.*, et al.* (2009). Nutrient-dependent mTORC1 association with the ULK1-Atg13-FIP200 complex required for autophagy. Mol Biol Cell *20*, 1981-1991.

Huang, W.P., and Klionsky, D.J. (2002). Autophagy in yeast: a review of the molecular machinery. Cell Struct Funct *27*, 409-420.

Inoki, K., Li, Y., Zhu, T., Wu, J., and Guan, K.L. (2002). TSC2 is phosphorylated and inhibited by Akt and suppresses mTOR signalling. Nat Cell Biol *4*, 648-657.

Ito, K., Bernardi, R., Morotti, A., Matsuoka, S., Saglio, G., Ikeda, Y., Rosenblatt, J., Avigan, D.E., Teruya-Feldstein, J., and Pandolfi, P.P. (2008). PML targeting eradicates quiescent leukaemia-initiating cells. Nature *453*, 1072-1078.

Ito, K., Hirao, A., Arai, F., Matsuoka, S., Takubo, K., Hamaguchi, I., Nomiyama, K., Hosokawa, K., Sakurada, K., Nakagata, N.*, et al.* (2004). Regulation of oxidative stress by ATM is required for self-renewal of haematopoietic stem cells. Nature *431*, 997-1002.

Ito, K., Hirao, A., Arai, F., Takubo, K., Matsuoka, S., Miyamoto, K., Ohmura, M., Naka, K., Hosokawa, K., Ikeda, Y.*, et al.* (2006). Reactive oxygen species act through p38 MAPK to limit the lifespan of hematopoietic stem cells. Nat Med *12*, 446-451.

Janzen, V., Forkert, R., Fleming, H.E., Saito, Y., Waring, M.T., Dombkowski, D.M., Cheng, T., DePinho, R.A., Sharpless, N.E., and Scadden, D.T. (2006). Stem-cell ageing modified by the cyclin-dependent kinase inhibitor p16INK4a. Nature *443*, 421-426.

Jeannet, G., Scheller, M., Scarpellino, L., Duboux, S., Gardiol, N., Back, J., Kuttler, F., Malanchi, I., Birchmeier, W., Leutz, A.*, et al.* (2008). Long-term, multilineage hematopoiesis occurs in the combined absence of beta-catenin and gamma-catenin. Blood *111*, 142-149.

Jiang, X., Zhao, Y., Smith, C., Gasparetto, M., Turhan, A., Eaves, A., and Eaves, C. (2007). Chronic myeloid leukemia stem cells possess multiple unique features of resistance to BCR-ABL targeted therapies. Leukemia *21*, 926-935.

Jung, C.H., Jun, C.B., Ro, S.H., Kim, Y.M., Otto, N.M., Cao, J., Kundu, M., and Kim, D.H. (2009). ULK-Atg13-FIP200 complexes mediate mTOR signaling to the autophagy machinery. Mol Biol Cell *20*, 1992-2003.

Kharas, M.G., Okabe, R., Ganis, J.J., Gozo, M., Khandan, T., Paktinat, M., Gilliland, D.G., and Gritsman, K. Constitutively active AKT depletes hematopoietic stem cells and induces leukemia in mice. Blood *115*, 1406-1415.

Kiel, M.J., He, S., Ashkenazi, R., Gentry, S.N., Teta, M., Kushner, J.A., Jackson, T.L., and Morrison, S.J. (2007). Haematopoietic stem cells do not asymmetrically segregate chromosomes or retain BrdU. Nature *449*, 238-242.

Kiel, M.J., Yilmaz, O.H., Iwashita, T., Terhorst, C., and Morrison, S.J. (2005). SLAM Family Receptors Distinguish Hematopoietic Stem and Progenitor Cells and Reveal Endothelial Niches for Stem Cells. Cell *121*, 1109-1121.

Kim, J.S., Lee, C., Bonifant, C.L., Ressom, H., and Waldman, T. (2007). Activation of p53-dependent growth suppression in human cells by mutations in PTEN or PIK3CA. Mol Cell Biol *27*, 662-677.

Kim, W.Y., and Sharpless, N.E. (2006). The regulation of INK4/ARF in cancer and aging. Cell *127*, 265-275.

Koch, U., Wilson, A., Cobas, M., Kemler, R., Macdonald, H.R., and Radtke, F. (2008). Simultaneous loss of beta- and gamma-catenin does not perturb hematopoiesis or lymphopoiesis. Blood *111*, 160-164.

Komatsu, M., Waguri, S., Chiba, T., Murata, S., Iwata, J., Tanida, I., Ueno, T., Koike, M., Uchiyama, Y., Kominami, E.*, et al.* (2006). Loss of autophagy in the central nervous system causes neurodegeneration in mice. Nature *441*, 880-884.

Kontani, K., Chano, T., Ozaki, Y., Tezuka, N., Sawai, S., Fujino, S., Saeki, Y., and Okabe, H. (2003). RB1CC1 suppresses cell cycle progression through RB1 expression in human neoplastic cells. Int J Mol Med *12*, 767-769.

Krishnamurthy, J., Ramsey, M.R., Ligon, K.L., Torrice, C., Koh, A., Bonner-Weir, S., and Sharpless, N.E. (2006). p16INK4a induces an age-dependent decline in islet regenerative potential. Nature *443*, 453-457.

Krishnamurthy, J., Torrice, C., Ramsey, M.R., Kovalev, G.I., Al-Regaiey, K., Su, L., and Sharpless, N.E. (2004). Ink4a/Arf expression is a biomarker of aging. J Clin Invest *114*, 1299-1307.

Kuma, A., Hatano, M., Matsui, M., Yamamoto, A., Nakaya, H., Yoshimori, T., Ohsumi, Y., Tokuhisa, T., and Mizushima, N. (2004). The role of autophagy during the early neonatal starvation period. Nature *432*, 1032-1036.

Kundu, M., Lindsten, T., Yang, C.Y., Wu, J., Zhao, F., Zhang, J., Selak, M.A., Ney, P.A., and Thompson, C.B. (2008). Ulk1 plays a critical role in the autophagic clearance of mitochondria and ribosomes during reticulocyte maturation. Blood *112*, 1493-1502.

Lang-Rollin, I.C., Rideout, H.J., Noticewala, M., and Stefanis, L. (2003). Mechanisms of caspase-independent neuronal death: energy depletion and free radical generation. J Neurosci *23*, 11015-11025.

Laplante, M., and Sabatini, D.M. (2009). mTOR signaling at a glance. J Cell Sci *122*, 3589-3594.

Lee, C.H., Inoki, K., Karbowniczek, M., Petroulakis, E., Sonenberg, N., Henske, E.P., and Guan, K.L. (2007). Constitutive mTOR activation in TSC mutants sensitizes cells to energy starvation and genomic damage via p53. EMBO J *26*, 4812-4823.

Lessard, J., and Sauvageau, G. (2003). Bmi-1 determines the proliferative capacity of normal and leukaemic stem cells. Nature *423*, 255-260.

Levine, B., and Klionsky, D.J. (2004). Development by self-digestion: molecular mechanisms and biological functions of autophagy. Dev Cell *6*, 463-477.

Liang, C.C., Wang, C., Peng, X., Gan, B., and Guan, J.L. Neural-specific deletion of FIP200 leads to cerebellar degeneration caused by increased neuronal death and axon degeneration. J Biol Chem *285*, 3499-3509.

Liu, J., Cao, L., Chen, J., Song, S., Lee, I.H., Quijano, C., Liu, H., Keyvanfar, K., Chen, H., Cao, L.Y.*, et al.* (2009a). Bmi1 regulates mitochondrial function and the DNA damage response pathway. Nature *459*, 387-392.

Liu, Y., Elf, S.E., Miyata, Y., Sashida, G., Huang, G., Di Giandomenico, S., Lee, J.M., Deblasio, A., Menendez, S., Antipin, J.*, et al.* (2009b). p53 Regulates Hematopoietic Stem Cell Quiescence. Cell Stem Cell *4*, 37-48.

Lomonaco, S.L., Finniss, S., Xiang, C., Decarvalho, A., Umansky, F., Kalkanis, S.N., Mikkelsen, T., and Brodie, C. (2009). The induction of autophagy by gamma-radiation contributes to the radioresistance of glioma stem cells. Int J Cancer *125*, 717-722.

Lowe, S.W., Cepero, E., and Evan, G. (2004). Intrinsic tumour suppression. Nature *432*, 307-315.

Lum, J.J., DeBerardinis, R.J., and Thompson, C.B. (2005). Autophagy in metazoans: cell survival in the land of plenty. Nat Rev Mol Cell Biol *6*, 439-448.

MacKey, M.C. (2001). Cell kinetic status of haematopoietic stem cells. Cell Prolif *34*, 71-83.

Maehama, T., and Dixon, J.E. (1998). The tumor suppressor, PTEN/MMAC1, dephosphorylates the lipid second messenger, phosphatidylinositol 3,4,5-trisphosphate. J Biol Chem *273*, 13375-13378.

Maillard, I., Koch, U., Dumortier, A., Shestova, O., Xu, L., Sai, H., Pross, S.E., Aster, J.C., Bhandoola, A., Radtke, F.*, et al.* (2008). Canonical notch signaling is dispensable for the maintenance of adult hematopoietic stem cells. Cell Stem Cell *2*, 356-366.

Mancini, S.J., Mantei, N., Dumortier, A., Suter, U., Macdonald, H.R., and Radtke, F. (2005). Jagged1-dependent Notch signaling is dispensable for hematopoietic stem cell self-renewal and differentiation. Blood *105*, 2340-2342.

Manning, B.D., and Cantley, L.C. (2007). AKT/PKB signaling: navigating downstream. Cell *129*, 1261-1274.

Matsuoka, S., Oike, Y., Onoyama, I., Iwama, A., Arai, F., Takubo, K., Mashimo, Y., Oguro, H., Nitta, E., Ito, K.*, et al.* (2008). Fbxw7 acts as a critical fail-safe against premature loss of hematopoietic stem cells and development of T-ALL. Genes Dev *22*, 986-991.

Melkoumian, Z.K., Peng, X., Gan, B., Wu, X., and Guan, J.L. (2005). Mechanism of cell cycle regulation by FIP200 in human breast cancer cells. Cancer Res *65*, 6676-6684.

Meng, A., Wang, Y., Van Zant, G., and Zhou, D. (2003). Ionizing radiation and busulfan induce premature senescence in murine bone marrow hematopoietic cells. Cancer Res *63*, 5414-5419.

Michaloglou, C., Vredeveld, L.C., Soengas, M.S., Denoyelle, C., Kuilman, T., van der Horst, C.M., Majoor, D.M., Shay, J.W., Mooi, W.J., and Peeper, D.S. (2005). BRAFE600-associated senescence-like cell cycle arrest of human naevi. Nature *436*, 720-724.

Minella, A.C., and Clurman, B.E. (2005). Mechanisms of tumor suppression by the SCF(Fbw7). Cell Cycle *4*, 1356-1359.

Miyamoto, K., Araki, K.Y., Naka, K., Arai, F., Takubo, K., Yamazaki, S., Matsuoka, S., Miyamoto, T., Ito, K., Ohmura, M.*, et al.* (2007). Foxo3a is essential for maintenance of the hematopoietic stem cell pool. Cell Stem Cell *1*, 101-112.

Mizushima, N., and Klionsky, D.J. (2007). Protein turnover via autophagy: implications for metabolism. Annu Rev Nutr *27*, 19-40.

Mizushima, N., Levine, B., Cuervo, A.M., and Klionsky, D.J. (2008). Autophagy fights disease through cellular self-digestion. Nature *451*, 1069-1075.

Molofsky, A.V., He, S., Bydon, M., Morrison, S.J., and Pardal, R. (2005). Bmi-1 promotes neural stem cell self-renewal and neural development but not mouse growth and survival by repressing the p16Ink4a and p19Arf senescence pathways. Genes Dev *19*, 1432-1437.

Molofsky, A.V., Pardal, R., Iwashita, T., Park, I.K., Clarke, M.F., and Morrison, S.J. (2003). Bmi-1 dependence distinguishes neural stem cell self-renewal from progenitor proliferation. Nature *425*, 962-967.

Molofsky, A.V., Slutsky, S.G., Joseph, N.M., He, S., Pardal, R., Krishnamurthy, J., Sharpless, N.E., and Morrison, S.J. (2006). Increasing p16INK4a expression decreases forebrain progenitors and neurogenesis during ageing. Nature *443*, 448-452.

Mortensen, M., Ferguson, D.J., Edelmann, M., Kessler, B., Morten, K.J., Komatsu, M., and Simon, A.K. Loss of autophagy in erythroid cells leads to defective removal of mitochondria and severe anemia in vivo. Proc Natl Acad Sci U S A *107*, 832-837.

Nishino, J., Kim, I., Chada, K., and Morrison, S.J. (2008). Hmga2 promotes neural stem cell self-renewal in young but not old mice by reducing p16Ink4a and p19Arf Expression. Cell *135*, 227-239.

Oguro, H., Iwama, A., Morita, Y., Kamijo, T., van Lohuizen, M., and Nakauchi, H. (2006). Differential impact of Ink4a and Arf on hematopoietic stem cells and their bone marrow microenvironment in Bmi1-deficient mice. J Exp Med *203*, 2247-2253.

Oravecz-Wilson, K.I., Philips, S.T., Yilmaz, O.H., Ames, H.M., Li, L., Crawford, B.D., Gauvin, A.M., Lucas, P.C., Sitwala, K., Downing, J.R*., et al.* (2009). Persistence of leukemia-initiating cells in a conditional knockin model of an imatinib-responsive myeloproliferative disorder. Cancer Cell *16*, 137-148.

Orford, K.W., and Scadden, D.T. (2008). Deconstructing stem cell self-renewal: genetic insights into cell-cycle regulation. Nat Rev Genet *9*, 115-128.

Pardal, R., Molofsky, A.V., He, S., and Morrison, S.J. (2005). Stem cell self-renewal and cancer cell proliferation are regulated by common networks that balance the activation of proto-oncogenes and tumor suppressors. Cold Spring Harb Symp Quant Biol *70*, 177-185.

Park, I.K., Qian, D., Kiel, M., Becker, M.W., Pihalja, M., Weissman, I.L., Morrison, S.J., and Clarke, M.F. (2003). Bmi-1 is required for maintenance of adult self-renewing haematopoietic stem cells. Nature *423*, 302-305.

Puzio-Kuter, A.M., Castillo-Martin, M., Kinkade, C.W., Wang, X., Shen, T.H., Matos, T., Shen, M.M., Cordon-Cardo, C., and Abate-Shen, C. (2009). Inactivation of p53 and Pten promotes invasive bladder cancer. Genes Dev *23*, 675-680.

Ruas, M., and Peters, G. (1998). The p16INK4a/CDKN2A tumor suppressor and its relatives. Biochim Biophys Acta *1378*, F115-177.

Sandoval, H., Thiagarajan, P., Dasgupta, S.K., Schumacher, A., Prchal, J.T., Chen, M., and Wang, J. (2008). Essential role for Nix in autophagic maturation of erythroid cells. Nature *454*, 232-235.

Sarbassov, D.D., Ali, S.M., Sengupta, S., Sheen, J.H., Hsu, P.P., Bagley, A.F., Markhard, A.L., and Sabatini, D.M. (2006). Prolonged rapamycin treatment inhibits mTORC2 assembly and Akt/PKB. Molecular cell *22*, 159-168.

Sarbassov, D.D., Guertin, D.A., Ali, S.M., and Sabatini, D.M. (2005). Phosphorylation and regulation of Akt/PKB by the rictor-mTOR complex. Science *307*, 1098-1101.

Schlessinger, J. (2000). Cell signaling by receptor tyrosine kinases. Cell *103*, 211-225.

Serrano, M., Lin, A.W., McCurrach, M.E., Beach, D., and Lowe, S.W. (1997). Oncogenic ras provokes premature cell senescence associated with accumulation of p53 and p16INK4a. Cell *88*, 593-602.

Sharpless, N.E., and DePinho, R.A. (2007). How stem cells age and why this makes us grow old. Nat Rev Mol Cell Biol *8*, 703-713.

Sherr, C.J. (2004). Principles of tumor suppression. Cell *116*, 235-246.

Sherr, C.J. (2006). Divorcing ARF and p53: an unsettled case. Nat Rev Cancer *6*, 663-673.

Sherr, C.J., and Roberts, J.M. (1999). CDK inhibitors: positive and negative regulators of G1-phase progression. Genes Dev *13*, 1501-1512.

Siegrist, S.E., Haque, N.S., Chen, C.H., Hay, B.A., and Hariharan, I.K. Inactivation of both foxo and reaper promotes long-term adult neurogenesis in Drosophila. Curr Biol *20*, 643-648.

Singh, S.K., Clarke, I.D., Terasaki, M., Bonn, V.E., Hawkins, C., Squire, J., and Dirks, P.B. (2003). Identification of a cancer stem cell in human brain tumors. Cancer Res *63*, 5821-5828.

Singh, S.K., Hawkins, C., Clarke, I.D., Squire, J.A., Bayani, J., Hide, T., Henkelman, R.M., Cusimano, M.D., and Dirks, P.B. (2004). Identification of human brain tumour initiating cells. Nature *432*, 396-401.

Soulard, A., and Hall, M.N. (2007). SnapShot: mTOR signaling. Cell *129*, 434.

Stepanova, L., and Sorrentino, B.P. (2005). A limited role for p16Ink4a and p19Arf in the loss of hematopoietic stem cells during proliferative stress. Blood *106*, 827-832.

Sun, H., Lesche, R., Li, D.-M., Liliental, J., Zhang, H., Gao, J., Gavrilova, N., Mueller, B., Liu, X., and Wu, H. (1999). PTEN modulates cell cycle progression and cell survival by regulating phosphatidylinositol 3,4,5-triphosphate and Akt/protein kinase B signaling pathway. Proc Natl Acad Sci USA *96*, 6199-6204.

Tang, E.D., Nunez, G., Barr, F.G., and Guan, K.L. (1999). Negative regulation of the forkhead transcription factor FKHR by Akt. The Journal of biological chemistry *274*, 16741-16746.

TeKippe, M., Harrison, D.E., and Chen, J. (2003). Expansion of hematopoietic stem cell phenotype and activity in Trp53-null mice. Exp Hematol *31*, 521-527.

Tothova, Z., and Gilliland, D.G. (2007). FoxO transcription factors and stem cell homeostasis: insights from the hematopoietic system. Cell Stem Cell *1*, 140-152.

Tothova, Z., Kollipara, R., Huntly, B.J., Lee, B.H., Castrillon, D.H., Cullen, D.E., McDowell, E.P., Lazo-Kallanian, S., Williams, I.R., Sears, C.*, et al.* (2007). FoxOs are critical mediators of hematopoietic stem cell resistance to physiologic oxidative stress. Cell *128*, 325-339.

Tsukada, M., and Ohsumi, Y. (1993). Isolation and characterization of autophagy-defective mutants of Saccharomyces cerevisiae. FEBS Lett *333*, 169-174.

Ueda, H., Abbi, S., Zheng, C., and Guan, J.L. (2000). Suppression of Pyk2 kinase and cellular activities by FIP200. J Cell Biol *149*, 423-430.

van Os, R., Kamminga, L.M., Ausema, A., Bystrykh, L.V., Draijer, D.P., van Pelt, K., Dontje, B., and de Haan, G. (2007). A Limited role for p21Cip1/Waf1 in maintaining normal hematopoietic stem cell functioning. Stem Cells *25*, 836-843.

Ventura, A., Kirsch, D.G., McLaughlin, M.E., Tuveson, D.A., Grimm, J., Lintault, L., Newman, J., Reczek, E.E., Weissleder, R., and Jacks, T. (2007). Restoration of p53 function leads to tumour regression in vivo. Nature *445*, 661-665.

Viatour, P., Somervaille, T.C., Venkatasubrahmanyam, S., Kogan, S., McLaughlin, M.E., Weissman, I.L., Butte, A.J., Passegue, E., and Sage, J. (2008). Hematopoietic stem cell quiescence is maintained by compound contributions of the retinoblastoma gene family. Cell Stem Cell *3*, 416-428.

Vogelstein, B., Lane, D., and Levine, A.J. (2000). Surfing the p53 network. Nature *408*, 307-310.

Wang, Y., Schulte, B.A., LaRue, A.C., Ogawa, M., and Zhou, D. (2006). Total body irradiation selectively induces murine hematopoietic stem cell senescence. Blood *107*, 358-366.

Wei, H., Gan, B., Wu, X., and Guan, J.L. (2009). Inactivation of FIP200 leads to inflammatory skin disorder, but not tumorigenesis, in conditional knock-out mouse models. J Biol Chem *284*, 6004-6013.

Wilson, A., Laurenti, E., Oser, G., van der Wath, R.C., Blanco-Bose, W., Jaworski, M., Offner, S., Dunant, C.F., Eshkind, L., Bockamp, E.*, et al.* (2008). Hematopoietic Stem Cells Reversibly Switch from Dormancy to Self-Renewal during Homeostasis and Repair. Cell.

Wlodarski, P., Wasik, M., Ratajczak, M.Z., Sevignani, C., Hoser, G., Kawiak, J., Gewirtz, A.M., Calabretta, B., and Skorski, T. (1998). Role of p53 in hematopoietic recovery after cytotoxic treatment. Blood *91*, 2998-3006.

Xue, W., Zender, L., Miething, C., Dickins, R.A., Hernando, E., Krizhanovsky, V., Cordon-Cardo, C., and Lowe, S.W. (2007). Senescence and tumour clearance is triggered by p53 restoration in murine liver carcinomas. Nature *445*, 656-660.

Yalcin, S., Zhang, X., Luciano, J.P., Mungamuri, S.K., Marinkovic, D., Vercherat, C., Sarkar, A., Grisotto, M., Taneja, R., and Ghaffari, S. (2008). Foxo3 is essential for the regulation of ataxia telangiectasia mutated and oxidative stress-mediated homeostasis of hematopoietic stem cells. J Biol Chem *283*, 25692-25705.

Yilmaz, O.H., Valdez, R., Theisen, B.K., Guo, W., Ferguson, D.O., Wu, H., and Morrison, S.J. (2006). Pten dependence distinguishes haematopoietic stem cells from leukaemia-initiating cells. Nature *441*, 475-482.

You, M.J., Castrillon, D.H., Bastian, B.C., O'Hagan, R.C., Bosenberg, M.W., Parsons, R., Chin, L., and DePinho, R.A. (2002). Genetic analysis of Pten and Ink4a/Arf interactions in the suppression of tumorigenesis in mice. Proc Natl Acad Sci U S A *99*, 1455-1460.

Yu, H., Yuan, Y., Shen, H., and Cheng, T. (2006). Hematopoietic stem cell exhaustion impacted by p18 INK4C and p21 Cip1/Waf1 in opposite manners. Blood *107*, 1200-1206.

Yuan, T.L., and Cantley, L.C. (2008). PI3K pathway alterations in cancer: variations on a theme. Oncogene *27*, 5497-5510.

Yuan, Y., Shen, H., Franklin, D.S., Scadden, D.T., and Cheng, T. (2004). In vivo self-renewing divisions of haematopoietic stem cells are increased in the absence of the early G1-phase inhibitor, p18INK4C. Nat Cell Biol *6*, 436-442.

Zhang, J., Grindley, J.C., Yin, T., Jayasinghe, S., He, X.C., Ross, J.T., Haug, J.S., Rupp, D., Porter-Westpfahl, K.S., Wiedemann, L.M*., et al.* (2006). PTEN maintains haematopoietic stem cells and acts in lineage choice and leukaemia prevention. Nature *441*, 518-522.

Zheng, H., Ying, H., Yan, H., Kimmelman, A.C., Hiller, D.J., Chen, A.J., Perry, S.R., Tonon, G., Chu, G.C., Ding, Z*., et al.* (2008). p53 and Pten control neural and glioma stem/progenitor cell renewal and differentiation. Nature *455*, 1129-1133.

Zick, Y. (2005). Ser/Thr phosphorylation of IRS proteins: a molecular basis for insulin resistance. Sci STKE *2005*, pe4.

Zindy, F., Eischen, C.M., Randle, D.H., Kamijo, T., Cleveland, J.L., Sherr, C.J., and Roussel, M.F. (1998). Myc signaling via the ARF tumor suppressor regulates p53-dependent apoptosis and immortalization. Genes Dev *12*, 2424-2433.

Zindy, F., Quelle, D.E., Roussel, M.F., and Sherr, C.J. (1997). Expression of the p16(INK4a) tumor suppressor versus other INK4 family members during mouse development and aging. Oncogene *15*, 203-211.

CHAPTER 2

MTOR ACTIVATION INDUCES TUMOR SUPPRESSORS THAT INHIBIT LEUKEMOGENESIS AND DEPLETE HEMATOPOIETIC STEM CELLS AFTER PTEN DELETION[1]

SUMMARY

Pten deficiency depletes hematopoietic stem cells (HSCs) but expands leukemia-initiating cells. Understanding this mechanistic difference could lead to anti-leukemia therapies with less toxicity to HSCs. Indeed, the mTOR inhibitor, rapamycin, blocks HSC depletion and leukemogenesis after *Pten* deletion, raising the question of how mTOR activation depletes HSCs. In contrast to what occurs after *FoxO1/3/4* deletion, we found that the depletion of *Pten*-deficient HSCs was not caused by oxidative stress and could not be blocked by N-acetyl-cysteine. Instead, *Pten* deletion induced the expression of p16^{Ink4a} and p53 in HSCs, and p19^{Arf} and p53 in other hematopoietic cells. Rapamycin treatment attenuated the increased expression of these tumor suppressors. Analysis of compound mutant mice indicated that p53 suppressed leukemogenesis and promoted HSC depletion after *Pten* deletion. p16^{Ink4a} also promoted HSC depletion but had a limited role suppressing leukemogenesis. p19^{Arf} strongly suppressed leukemogenesis but did not deplete HSCs. *Pten* deficiency and *FoxO* deficiency therefore deplete HSCs by

different mechanisms. These results provide functional evidence that mTOR activation depletes stem cells by inducing a tumor suppressor response.

INTRODUCTION

Phosphatidylinositol 3-kinase (PI-3kinase) pathway signaling promotes cell growth, proliferation, and survival through a variety of downstream mechanisms (Wullschleger et al., 2006; Yuan and Cantley, 2008). Tyrosine kinase receptors and other signaling pathways activate PI-3kinase, which generates phosphatidylinositol-3,4,5-trisphosphate (PIP3) (Yuan and Cantley, 2008). PIP3 activates Akt, which promotes cell growth, proliferation, and survival by phosphorylating diverse substrates (Manning and Cantley, 2007), including the Tuberous Sclerosis Complex (TSC) (Inoki et al., 2002; Tang et al., 1999). Phosphorylation by Akt negatively regulates TSC, leading to the activation of the mammalian target of rapamycin (mTOR) kinase (Inoki et al., 2002). mTOR functions in two distinct complexes, mTORC1, which is directly inhibited by rapamycin, and mTORC2, which can be indirectly inhibited by rapamycin (Guertin and Sabatini, 2007; Sarbassov et al., 2006). mTORC1 promotes cell growth and proliferation by activating S6 kinase and inactivating 4EBP1, promoting protein synthesis (Inoki et al., 2002). mTORC2 regulates Akt activation (Guertin and Sabatini, 2007). PI-3kinase pathway signaling is attenuated by Pten, which dephosphorylates PIP3 (Maehama and Dixon, 1998), reducing the activation of Akt, mTORC1, and S6 kinase. As a result, Pten deficiency increases the growth, proliferation, and survival of many cells (Sun et al., 1999) and *Pten* is commonly deleted in diverse cancers (Di Cristofano and Pandolfi, 2000).

PI-3kinase pathway signaling has divergent effects on stem cells. Conditional deletion of *Pten* from embryonic stem cells and neural stem cells increases PI-3kinase pathway activation, cell cycle entry, self-renewal, and survival (Gregorian et al., 2009; Groszer et al., 2006; Groszer et al., 2001; Sun et al., 1999). In contrast, *Pten* deletion from adult HSCs increases PI-3kinase pathway signaling and cell cycle entry, but this leads to rapid HSC depletion (Yilmaz et al., 2006; Zhang et al., 2006). We showed that this depletion was mediated by mTOR activation as rapamycin blocked the depletion of *Pten*-deficient HSCs (Yilmaz et al., 2006). Subsequent studies of *Tsc1*-deficient HSCs confirmed that increased PI-3kinase pathway signaling can drive HSCs into cycle but that this is deleterious for HSC maintenance and leads to mTOR-mediated HSC depletion (Chen et al., 2008; Gan et al., 2008). Similar results were obtained as a result of *Pml* deletion, which also leads to increased HSC cycling and mTOR-mediated HSC depletion (Ito et al., 2008). Activation of mTOR by Wnt signaling in the epidermis also leads to stem cell depletion (Castilho et al., 2009). mTOR is thus a critical modulator of stem cell maintenance in multiple tissues, raising the question of how mTOR activation leads to stem cell depletion.

This question gains added importance from the observation that mTOR activation can have opposite effects on cancer cells as compared to normal stem cells. While *Pten* deletion and mTOR activation lead to the depletion of normal HSCs, this leads to the generation and expansion of leukemia-initiating cells (Yilmaz et al., 2006). This makes it possible to deplete leukemia-initiating cells while rescuing normal HSC function using rapamycin in *Pten* mutant mice (Yilmaz et al., 2006). A sophisticated understanding of

stem cell self-renewal mechanisms, and PI-3kinase pathway signaling in particular, can lead to therapies that eliminate cancer cells without toxicity to normal stem cells.

One mechanism by which *Pten* deletion and PI-3kinase pathway activation could deplete stem cells involves the activation of a tumor suppressor response. Sustained oncogenic signaling can induce tumor suppressors in the p53 and Rb pathways that cause cellular senescence (Lin et al., 1998; Serrano et al., 1997). $p16^{Ink4a}/p19^{Arf}$ deficiency increases the incidence of tumors in *Pten* heterozygous mice, implying that p16[Ink4a] and p19[Arf] suppress the neoplastic proliferation of *Pten* mutant cells in certain tissues (You et al., 2002). Conditional inactivation of *Pten* in prostate leads to the induction of p53-mediated senescence, impeding the development of prostate cancer (Chen et al., 2005). These studies raise the question of whether a similar tumor suppressor response occurs after *Pten* deletion in the hematopoietic system, and whether this could suppress leukemogenesis or deplete HSCs.

Another mechanism by which *Pten* deletion could deplete HSCs involves the inactivation of FoxO family transcription factors. When localized to the nucleus, FoxO transcription factors promote the expression of enzymes that eliminate reactive oxygen species (ROS). However, activated Akt phosphorylates FoxO proteins, leading to their retention in the cytoplasm (Biggs et al., 1999; Brunet et al., 1999), reducing the expression of these enzymes and increasing ROS levels. HSCs are particularly sensitive to the toxic effects of ROS (Ito et al., 2004; Ito et al., 2006). Indeed, deletion of *FoxO1/3/4* from adult HSCs leads to increased ROS levels and HSC depletion (Tothova et al., 2007). The depletion of *FoxO1/3/4*-deficient HSCs can be at least partially rescued by the antioxidant N-Acetyl-cysteine (NAC), proving that oxidative stress contributes to

the depletion of these HSCs (Tothova et al., 2007). FoxO3a is particularly important for stem cell maintenance as deletion of *FoxO3a* alone leads to increased ROS levels and HSC depletion (Miyamoto et al., 2007; Yalcin et al., 2008). FoxO transcription factors are also important for the maintenance of neural stem cells (Paik et al., 2009; Renault et al., 2009).

These results raise the possibility that *Pten* deletion depletes HSCs by increasing Akt activation, which reduces FoxO function and increases oxidative stress. Consistent with this possibility, the depletion of *Tsc1*-deficient HSCs is mediated partly by oxidative stress and rescued by NAC treatment (Chen et al., 2008). On the other hand, constitutively active Akt did not increase ROS levels in HSCs and the depletion of these HSCs could not be rescued by NAC treatment (Kharas et al., 2010). It would appear that activation of PI-3kinase pathway intermediates sometimes leads to HSC depletion as a consequence of oxidative stress but in other cases HSCs are depleted by other, unknown, mechanisms.

These results raise the question of whether *Pten* deficiency and *FoxO* deficiency deplete HSCs by similar mechanisms. We were unable to detect FoxO3a inactivation or a significant increase in ROS levels in HSCs after *Pten* deletion. We were not able to rescue the depletion of *Pten*-deficient HSCs by treating with NAC. *Pten* deficiency and *FoxO1/3/4* deficiency therefore lead to HSC depletion by different mechanisms. Indeed, *Pten* deletion induced the expression of p16^{Ink4a} and p53 in HSCs, and p19^{Arf} and p53 in other hematopoietic cells. Analysis of compound mutant mice revealed that deficiency for *p19^{Arf}*, or *p16^{Ink4a}/p19^{Arf}*, or *p53* (but not *p16^{Ink4a}*) accelerated leukemogenesis after *Pten* deletion. Moreover, deficiency for *p16^{Ink4a}*, or *p16^{Ink4a}/p19^{Arf}*, or *p53* (but not *p19^{Arf}*)

autonomously prolonged the reconstituting capacity of HSCs after *Pten* deletion. Our results demonstrate there are multiple distinct mechanisms by which increased PI-3kinase pathway signaling can lead to stem cell depletion, including an mTOR-mediated tumor suppressor response that occurs in HSCs after *Pten* deletion.

MATERIALS AND METHODS

Mice

C57BL/Ka-Thy-1.1 (CD45.2) and C57BL/Ka-Thy-1.2 (CD45.1) mice were used in hematopoietic reconstitution experiments. *Mx-1-Cre*[+] mice (Kuhn et al., 1995), *Pten*^{fl/fl} mice (Groszer et al., 2001), *Ink4a*^{+/-} mice (Sharpless et al., 2001), *Arf*^{+/-} mice (Kamijo et al., 1997), *Ink4a/Arf*^{+/-} mice (Serrano et al., 1996), and *p53*^{+/-} mice (Jacks et al., 1994) were backcrossed for at least ten generations onto a C57BL/Ka background. All mice were housed in the Unit for Laboratory Animal Medicine at the University of Michigan in accordance with the National Research Council's guide for the care and use of laboratory animals.

pIpC, rapamycin, and *N*-Acetyl-L-cysteine administration

For experiments involving *Pten* deletion, polyinosine-polycytidine (pIpC) and rapamycin were administered as previously described (Yilmaz et al., 2006). Briefly, pIpC from Sigma (St. Louis, MO) or from Amersham (Piscataway, NJ) was resuspended in Dulbecco's phosphate-buffered saline (D-PBS) at 2 mg/ml (for Sigma) or 50 µg/ml (for Amersham), and mice were injected intraperitoneally (IP) with 25 µg/gram (for Sigma) or 0.5 µg/gram (for Amersham) of body mass every other day for 6-14 days. Rapamycin (LC Laboratories, Woburn, MA) was dissolved in absolute ethanol at 10 mg/ml and diluted in 5% Tween-80 (Sigma) and 5% PEG-400 (Hampton Research, Aliso Viejo, CA) before being administered daily by IP injection at a dose of 4 mg/kg. N-Acetyl-L-cysteine (NAC; Sigma) was administered daily by subcutaneous injection at 100 mg/kg (pH 7.0) starting one day after the final dose of pIpC.

Flow cytometry and HSC isolation

Bone marrow cells were obtained by crushing the long bones (tibias and femurs), pelvic bones, and vertebrae in a mortar and pestle with Hank's buffered salt solution without calcium or magnesium, supplemented with 2% heat-inactivated calf serum (GIBCO, Grand Island, NY; HBSS+). Cells were triturated and filtered through nylon screen (45 μm, Sefar America, Kansas City, MO) to obtain a single-cell suspension. For isolation of c-Kit$^+$Flk2$^-$Lin$^-$Sca-1$^+$CD48$^-$ cells, whole bone marrow cells were incubated with FITC-conjugated monoclonal antibodies to lineage markers including B220 (6B2), CD3 (KT31.1), CD4 (GK1.5), CD5 (53-7.3), CD8 (53-6.7), Gr-1 (8C5), Mac-1 (M1/70), and Ter119 (TER-119) in addition to APC-conjugated anti-Sca-1 (Ly6A/E; E13-6.7) and biotin-conjugated anti-c-Kit (2B8). A PE/Cy5-conjugated antibody against Flk-2 (A2F10.1) was used to isolate Flk-2$^-$ progenitors. Biotin-conjugated c-Kit staining was visualized using streptavidin APC-Cy7.

For isolation of CD150$^+$CD48$^-$CD41$^-$Lin$^-$Sca-1$^+$c-kit$^+$ HSCs, bone marrow cells were incubated with PE-conjugated anti-CD150 (TC15-12F12.2; BioLegend, San Diego, CA), FITC-conjugated anti-CD48 (HM48-1; BioLegend), FITC-conjugated anti-CD41 (MWReg30; BD PharMingen, San Diego, CA), APC-conjugated anti-Sca-1 (Ly6A/E; E13-6.7), and biotin-conjugated anti-c-Kit (2B8) antibody, in addition to antibodies against the following FITC-conjugated lineage markers: CD2 (RM2-5), B220 (6B2), CD3 (KT31.1), CD5 (53-7.3), CD8 (53-6.7), Gr-1 (8C5), and Ter119 (TER-119). Biotin-conjugated c-Kit was visualized using streptavidin-conjugated APC-Cy7. HSCs were sometimes pre-enriched by selecting c-Kit$^+$ cells using paramagnetic anti-biotin

microbeads and autoMACS (Miltenyi Biotec, Auburn, CA). Dead cells were excluded using the viability dye 4',6-diamidino-2-phenylindole (DAPI) (1 µg/ml).

To measure ROS levels, bone marrow cells were isolated and stained as above except that the HSC stain was modified to make the FITC channel available for DCFDA (2'-7'-dichlorofluorescein diacetate, Molecular Probes, Eugene, OR) staining. Antibodies for HSC isolation were as described above except for the following antibodies: PE/Cy5-conjugated anti-CD150 (TC15-12F12.2; BioLegend), PE-conjugated anti-CD48 (HM48-1; BioLegend), PE-conjugated anti-CD41 (MWReg30; BD PharMingen), and PE-conjugated antibodies against lineage markers. After antibody staining, thymus cells, whole bone marrow cells, or c-Kit$^+$ enriched cells were incubated with 5 µM DCFDA for 15 min at 37°C followed by flow cytometry.

Competitive repopulation and leukemogenesis assays

Wild-type adult recipient mice (CD45.1) were irradiated using a Cesium137 GammaCell40 Exactor Irradiator (MDS Nordia, Kanata, ON) delivering 110 rad/min in two equal doses of 570 rad, delivered at least 2 hr apart. Cells were injected into the retro-orbital venous sinus of anesthetized recipients. Each recipient mouse received 10 CD150$^+$CD48$^-$CD41$^-$Lin$^-$Sca-1$^+$c-kit$^+$ HSCs from CD45.2 donor mice (after pIpC treatment) along with 300,000 CD45.1 bone marrow cells for radioprotection. NAC treatment, when tested, started one day after transplantation. Beginning four weeks after transplantation and continuing for at least 16 weeks, blood from the tail veins of recipient mice, was subjected to ammonium-chloride potassium red cell lysis and stained with directly conjugated antibodies to CD45.2 (104), B220 (6B2), Mac-1 (M1/70),

CD3(KT31.1), and Gr-1(8C5) to quantitate donor cell engraftment. For leukemogenesis assays, 1×10^6 unexcised donor bone marrow cells were co-injected with 500,000 recipient bone marrow cells into irradiated wild-type recipient mice. Six weeks after transplantation, recipient mice were treated with seven injections of pIpC over 14 days and their survival was monitored over time. NAC treatment, when tested, was started after the final dose of pIpC.

Immunofluorescence assay

Immunofluorescence assays on sorted cells were performed as previously described (Ema et al., 2006). Cells were sorted into drops of PBS on poly-D-lysine coated slides and fixed with 2% paraformaldehyde for 10 minutes. In some experiments, cells were sorted into medium (IMDM + 10% fetal bovine serum) with or without SCF (20 ng/ml) and TPO (50 ng/ml), then incubated for 24 hours at 37°C and fixed. After washing, cells were permeabilized with PBS containing 0.3 % Triton X-100 and blocked with PBS containing 10% goat serum. Slides were stained with anti-FoxO3a (#2497) and anti-phospho-S6 (#2215) antibodies (Cell Signaling Technology, dilution 1:200) at 4°C overnight. After washing, slides were incubated with secondary antibodies conjugated with AlexaFluor 488 or 555 (Invitrogen) together with DAPI and analyzed with an FV-500 confocal microscope (Olympus).

Immunoprecipitation

Two million Lineage⁻c-Kit⁺ progenitor cells were sorted and proteins were extracted by incubating on ice in lysis buffer (50 mM Tris-HCl, pH7.5, 150 mM NaCl,

1% Triton-X 100, 1mM EDTA) supplemented with complete EDTA-free protease inhibitor cocktail (Roche), 1mM PMSF and Halt phosphatase inhibitor cocktail (Pierce) with brief sonication. All extracts were precleared with Protein-L agarose (Santa Cruz Biotechnology) and incubated with Protein-L agarose bound with antibodies against p53 (#2524, Cell Signaling Technology), p19^{Arf} (ab26696, Abcam) and p16^{Ink4a} (sc-1207, Santa Cruz Biotechnology) or control IgG from mouse, rat, and rabbit for 12 hours at 4°C. Immunoprecipitates were washed four times with lysis buffer and heated to 70°C for 10 minutes in 1X LDS sample buffer (Invitrogen). The eluted proteins were separated on a Bis-Tris gel (Invitrogen) and immunoblotted with the antibodies indicated above. To detect p53, secondary antibodies against mouse IgG light chain (Jackson Immunoresearch) were used to prevent the IgG heavy chain from obscuring p53 detection.

Western blotting

The same number (25,000-50,000 depending on the experiment) of c-Kit^{+}Flk2^{-}Lin^{-}Sca-1^{+}CD48^{-} HSCs or whole bone marrow cells were sorted into microcentrifuge tubes with PBS and then protein was extracted by adding TCA to a final concentration of 10%. Extracts were incubated on ice for 15 minutes and spun down for 10 minutes at 16.1 rcf at 4°C. The supernatant was removed and the pellets were washed with acetone twice then dried. The protein pellets were solubilized with Solubilization buffer (9M Urea, 2% Triton X-100, 1% DTT) before adding LDS loading buffer (Invitrogen, Carlsbad, CA). For spleen samples, equivalent numbers of cells were pelleted, then lysed in RIPA buffer (50mM Tris, 150mM NaCl, 0.1% SDS, 0.5% Na

43

deoxycholate, 1% Triton X-100) supplemented with complete EDTA-free protease inhibitors (Roche Applied Science, Indianapolis, IN), 1mM DTT, Halt phosphatase inhibitor cocktail (Thermo Fisher Scientific, Rockford, IL), and 1□M PMSF, spun down for 10 minutes at 16.1 rcf at 4°C. LDS loading buffer (Invitrogen) was added to the cleared supernatant. Proteins were separated on a Bis-Tris polyacrylamide gel (Invitrogen) and transferred to a PVDF membrane (Millipore, Billerica, MA). Antibodies used for Western blotting were anti-phospho Akt T308 (#4056), anti-Akt (#9272), anti-phospho-S6 (#2215), anti-S6 (#2217), anti-phospho-4E-BP1 (Thr37/46) (#2855), anti-4E-BP1 (#9452), anti-FoxO3a (#2497), and anti-p53 (#2524) (all from Cell Signaling Technology, Danvers, MA), and anti-p16[Ink4a] (sc-1207, Santa Cruz, Santa Cruz, CA), anti-p19[Arf] (ab26696, Abcam), anti-p21[Cip1] (sc-6246, Santa Cruz), and anti-ß-actin (A1978, Sigma).

Quantitative (real-time) reverse-transcriptase PCR

A total of 2000 HSCs or 20,000 unfractionated bone marrow cells were sorted into Trizol (Invitrogen) and RNA was isolated using chloroform extraction and isopropanol precipitation. cDNA was made with random primers and SuperScript III reverse transcriptase (Invitrogen). Quantitative PCR was performed with cDNA from 200 cell equivalents using a SYBR Green Kit and a LightCycler 480 (Roche Applied Science). Each sample was normalized to -actin. Primer sequences were as follows:

 -actin F, CGTCGACAACGGCTCCGGCATG;

 -actin R, GGGCCTCGTCACCCACATAGGAG;

Nfe2 F, TGGCCATGAAGATTCCTTTC; Nfe2 R, TAGCGGATACTGTGCCAACA;

Nrf1 F, GTCACCATGGCCCTCAAC; Nrf1 R, GGACTATCTGTCTCCCACCTTG;

Nrf2 F, CATGATGGACTTGGAGTTGC; Nrf2 R, CCTCCAAAGGATGTCAATCAA;

catalase F, CCTTCAAGTTGGTTAATGCAGA;

catalase R, CAAGTTTTTGATGCCCTGGT;

SOD1 F, GTGACTGCTGGAAAGAACG; SOD1 R, TCTCGTGGACCACCATTGTA;

SOD2 F, GGCTTGGCTTCAATAAGGAG;

SOD2 R, ATACTGAAGGTAGTAAGCGTG;

Ink4a F, CGAACTCTTTCGGTCGTACCC;

Ink4a R, CGAATCTGCACCGTAGTTGAGC;

Arf F, GTTCTTGGTCACTGTGAGGATTCAG;

Arf R, CCATCATCATCACCTGGTCCAG;

Cip1 F, TCCACAGCGATATCCAGACA; Cip1 R, AGACAACGGCACACTTTGCT;

Trp53 F, AAAGGATGCCCATGCTACAG;

Trp53 R, TATGGCGGGAAGTAGACTGG.

Annexin V, BrdU, and senescence-associated -galactosidase staining

Annexin V was detected by flow-cytometry using Annexin V APC (BD PharMingen) and Annexin V Binding Buffer (BD PharMingen) as described by the manufacturer. BrdU incorporation was measured by flow-cytometry (BD PharMingen). As described previously (Cheshier et al., 1999), mice were given an intraperitoneal injection of 0.1 mg of BrdU/g of body mass in Dulbecco's phosphate buffered saline (D-PBS, Gibco). For senescence-associated -galactosidase staining, cells were sorted into

45

drops of PBS on a poly-lysine coated slide and stained using the senescence-associated β-gal Staining Kit (#9860, Cell Signaling Technology).

Histopathology

Spleen, liver, and thymus samples were fixed in 10% neutral buffered formalin and paraffin embedded. Thin sections (5 μm) were cut on a microtome and stained with hematoxylin and eosin using standard protocols. The slides were then analyzed with a hematopathologist and classified according to the Bethesda protocols for the classification of hematopoietic neoplasms in mice (Kogan et al., 2002; Morse et al., 2002).

RESULTS

Akt activation after *Pten* deletion activates mTORC1 but does not inactivate FoxO3a

We conditionally deleted *Pten* from HSCs and other hematopoietic cells in young adult *Pten^{fl/fl}Mx-1-Cre^+* mice and *Pten^{+/fl}Mx-1-Cre^+* littermate controls by administering seven doses of polyinosine-polycytidine (pIpC) over 14 days (Yilmaz et al., 2006). *Pten*-deleted mice and littermate controls were then treated for a week with daily injections of rapamycin or vehicle to assess the effects of *Pten* deletion and rapamycin treatment on the activation of signaling molecules in the PI-3kinase pathway. The analyses were performed by western blotting of protein from bone marrow cells or c-kit^+Flk-2^-Lin^-Sca-1^+CD48^- cells, a population highly enriched for HSCs (Christensen and Weissman, 2001; Kiel et al., 2005). Rapamycin treatment and *Pten* deletion both appeared to increase Akt activation based on T308 phosphorylation in bone marrow cells and in HSCs (Fig. 2.1A, B). The increase in Akt phosphorylation after rapamycin treatment is consistent with the attenuation of a negative feedback loop from S6 kinase to IRS-1 as a result of reduced mTORC1 activation (Harrington et al., 2004). Rapamycin does not, therefore, rescue the reconstituting activity of *Pten*-deficient HSCs by normalizing Akt activation.

Since rapamycin failed to normalize Akt activation, our data suggested that effects of Akt activation on FoxO function were unlikely to mediate HSC depletion after *Pten* deletion. Consistent with this, neither *Pten* deletion nor rapamycin treatment appeared to significantly affect total FoxO3a levels in c-kit^+Flk-2^-Lin^-Sca-1^+CD48^- cells (Fig. 2.1B). Neither *Pten* deletion nor rapamycin treatment appeared to affect phospho-Foxo3a levels, total FoxO1 levels, or phospho-H2AX levels in c-kit^+Lin^-Sca-1^+ cells

47

either (Fig. 2.8). Since FoxO3a is excluded from the nucleus upon phosphorylation by Akt, we also analyzed its subcellular localization by immunohistochemistry in $CD150^+CD48^-CD41^-Lin^-c-Kit^+Sca-1^+$ cells, which are very highly purified HSCs (Kiel et al., 2005). To validate this assay, HSCs were sorted from control and *Pten*-deleted mice and stimulated with high levels of SCF and TPO in culture for 24 hours before staining. Under these conditions, HSCs from control and *Pten*-deleted mice showed an overall decrease in FoxO3a staining as well as strongly decreased nuclear staining and increased cytoplasmic staining (Fig. 2.9). In contrast, when HSCs were stained immediately after isolation from mice rather than after stimulation with growth factors in culture, we detected no change in FoxO3a expression levels or subcellular localization (Fig. 2.1F-H). FoxO3a continued to localize to the nucleus in uncultured HSCs after *Pten* deletion. These results suggest that *Pten* deletion is unlikely to significantly reduce FoxO3a function in HSCs.

In contrast to our failure to detect clear effects of *Pten* deletion on FoxO3a, mTORC1 activity was clearly elevated after *Pten* deletion based on the increased phospho-S6 levels in freshly isolated bone marrow cells and HSCs (Fig. 2.1A, 1B, 1D, 1E, 1H). This increase in phospho-S6 levels was attenuated by rapamycin treatment (Fig. 2.1A, 1B). These changes were further confirmed by the observation of increased phospho-4EBP1 levels in bone marrow cells after *Pten* deletion (Fig. 2.1A). This increase in phospho-4EBP1 levels was also attenuated by rapamycin treatment (Fig. 2.1A). Thus, *Pten* deletion increased mTORC1 and S6 kinase activation in a manner that was reversed by rapamycin, suggesting that the changes that lead to HSC depletion after *Pten* deletion are mediated by this branch of the PI-3kinase pathway.

Pten deletion increases ROS levels in the thymus but not in HSCs or bone marrow cells

Although FoxO3a did not appear to have been inactivated after _Pten_ deletion, we examined ROS levels to assess whether changes in ROS might contribute to HSC depletion. We assessed the intracellular levels of ROS in CD150$^+$CD48$^-$CD41$^-$Lin$^-$c-kit$^+$Sca-1$^+$ HSCs, CD150$^-$CD48$^-$CD41$^-$Lin$^-$c-Kit$^+$Sca-1$^+$ transiently reconstituting multipotent progenitors (MPPs) (Kiel et al., 2008), bone marrow cells, and thymus cells from _Pten_-deleted mice and littermate controls one week after finishing pIpC treatment. ROS levels were quantitated by flow-cytometry using 2'-7'-dichlorofluorescein diacetate (DCFDA) staining (Fig. 2.2). After _Pten_ deletion, we detected a significant increase in ROS levels in thymocytes (Fig. 2.2C, D; 2.8-fold, p<0.05) but we did not consistently detect changes in ROS levels within unfractionated bone marrow cells, HSCs, or MPPs (Fig. 2.2B, D). We also did not detect an increase in ROS levels within unfractionated bone marrow cells, HSCs, or MPPs three weeks after finishing pIpC treatment (Fig. 2.2E, F). Only mice showing no signs of neoplasms were used in these experiments.

The increase in ROS levels in the thymus after _Pten_ deletion was attenuated by daily subcutaneous injection of the anti-oxidant NAC, but NAC did not affect ROS levels in bone marrow cells, HSCs, or MPPs (Fig. 2.2F). We do not know why _Pten_ deletion increased ROS levels in thymocytes but not in HSCs or WBM cells, but ROS regulation is known to differ among hematopoietic cells (Ito et al., 2004; Ito et al., 2006; Tothova et al., 2007). These data demonstrate that _Pten_ deletion had a limited effect on ROS levels in HSCs, consistent with our failure to detect any effect of _Pten_ deletion on FoxO1 or

FoxO3a expression or localization. We were also unable to detect significant effects of *Pten* deletion on the expression of known FoxO target genes (Tothova et al., 2007) or antioxidant response genes (Nguyen et al., 2009) in bone marrow cells, HSCs, or MPPs (Fig. 2.10). Tested genes included *Nfe2* (*nuclear factor, erythroid derived 2*), *Nrf1* (*nuclear respiratory factor 1*), *Nrf2*, *catalase*, *Sod1* (*superoxide dismutase 1*), and *Sod2*.

NAC does not rescue major hematopoietic defects after *Pten* deletion

Although we did not detect an increase in ROS levels in HSCs using DCDFA staining, HSCs might still experience oxidative stress after *Pten* deletion. To directly assess whether HSC depletion could be rescued by attenuating oxidative stress, we treated mice with daily subcutaneous injections of NAC beginning the day after pIpC treatment ended. Three weeks after finishing pIpC treatment, splenic mass (normalized to body mass) was 3-fold higher (p<0.005), and thymic mass (normalized to body mass) was 2-fold higher (p<0.005) in *Pten*-deleted mice as compared to littermate controls (Fig. 2.3A). Consistent with this, the number of cells in spleen and thymus were also significantly greater in *Pten*-deleted mice as compared to littermate controls (Fig. 2.3B). Daily treatment with NAC for 3 weeks after pIpC treatment did not rescue these changes in spleen or thymus size or cellularity in *Pten*-deleted mice (Fig. 2.3A, B).

In contrast to the increase in spleen and thymus cellularity, bone marrow cellularity declined significantly three weeks after *Pten* deletion (Fig. 2.3B, p<0.005). NAC treatment also did not rescue this change after *Pten* deletion. The failure of NAC treatment to rescue changes in the cellularity of hematopoietic organs after *Pten* deletion

contrasts with the ability of rapamycin treatment to rescue all of these phenotypes (Yilmaz et al., 2006).

Three weeks after pIpC treatment, HSC frequency and number in the bone marrow were significantly reduced in *Pten*-deleted mice as compared to littermate controls (Fig. 2.3C, F), as we reported previously (Yilmaz et al., 2006). NAC did not rescue the depletion of bone marrow HSCs (Fig. 2.3C, F). MPP frequency and number in the bone marrow was not significantly affected by *Pten* deletion or NAC treatment (Fig. 2.3D, G). The frequency and absolute number of HSCs and MPPs increased significantly in the spleen three weeks after pIpC treatment (Fig. 2.3E, H), consistent with the extramedullary hematopoiesis that arises after *Pten* deletion (Yilmaz et al., 2006). NAC attenuated the increase in splenic HSCs, though HSC frequency and number still increased significantly in the spleen (Fig. 2.3E, H). NAC did not significantly affect MPP frequency or number in the spleen after *Pten* deletion (Fig. 2.3E, H). NAC also had little effect on other changes in hematopoiesis after *Pten* deletion (Fig. 2.11). These results indicate that NAC treatment had little effect on the changes in HSC frequency and localization after *Pten* deletion, in contrast to rapamycin which rescues all of these phenotypes (Yilmaz et al., 2006).

NAC does not prevent the loss of HSCs or leukemogenesis after *Pten* deletion

To formally test whether NAC rescues the function of *Pten*-deleted HSCs, we treated *Pten*$^{fl/fl}$*Mx-1-Cre*$^{+}$ and *Pten*$^{+/fl}$*Mx-1-Cre*$^{+}$ mice with 7 doses of pIpC over 14 days, then transplanted 10 donor CD150^{+}CD48^{-}CD41^{-}Lin^{-}c-Kit^{+}Sca-1^{+} HSCs along with a radioprotective dose of recipient bone marrow cells into lethally irradiated recipients.

Half of the recipients then received daily subcutaneous injections of NAC, while the other half received daily saline injections, starting on the day of transplantation. In three independent experiments, all recipients of control HSCs, whether they were treated with NAC or vehicle, were long-term multilineage-reconstituted by donor cells (Fig. 2.4A-E). All of the recipients of *Pten*-deleted HSCs showed transient multilineage reconstitution, irrespective of whether they were treated with NAC (Fig. 2.4A-E). Daily treatment of transplanted mice with NAC therefore did not significantly affect the loss of HSC reconstituting capacity after *Pten* deletion. The inability of NAC treatment to rescue changes in HSC frequency or function after *Pten* deletion suggests that oxidative stress is unlikely to be the primary determinant of HSC depletion after *Pten* deletion in contrast to what has been observed after *FoxO1/3/4* deletion (Tothova et al., 2007).

To assess whether NAC treatment reduces leukemogenesis after *Pten* deletion, we transplanted 1×10^6 bone marrow cells from untreated *Pten$^{fl/fl}$Mx-1-Cre$^+$* mice or *Pten$^{+/fl}$Mx-1-Cre$^+$* controls along with 500,000 recipient bone marrow cells into irradiated recipients. Six weeks later, we treated the recipients with seven doses of pIpC over 14 days. The recipients were then treated with NAC or vehicle daily. In two independent experiments, recipients of control cells became long-term multilineage reconstituted by donor cells. All survived for 120 days and showed no signs of leukemogenesis (n=20, Fig. 2.4F). In contrast, all 20 recipients of *Pten*-deleted bone marrow died with myeloproliferative disease (MPD) and/or T-cell acute lymphoblastic leukemia (T-ALL) 33 to 112 days after pIpC treatment, irrespective of whether they were treated with NAC (Fig. 2.4F; Fig. 2.12). NAC treatment did not significantly affect the lifespan of mice

after *Pten* deletion (Fig. 2.4F) in contrast to rapamycin, which prevents leukemogenesis and extends the lifespan of *Pten*-deleted mice (Yilmaz et al., 2006).

***Pten* deletion leads to a tumor suppressor response in HSCs**

Since oxidative stress did not explain the major changes in hematopoiesis after *Pten* deletion we tested whether *Pten* deletion induced a tumor suppressor response. We first assessed the expression of p16^{Ink4a}, p19^{Arf}, p53, and p21^{Cip1} tumor suppressors in splenocytes. We did not detect p16^{Ink4a} protein expression in splenocytes with or without *Pten* deletion (Fig. 2.5A). We did detect very low levels of *p16^{Ink4a}* transcript in splenocytes, but transcript levels were not significantly affected by *Pten* deletion or rapamycin treatment (Fig. 2.13A). In contrast, we observed clear increases in p19^{Arf}, p53 and p21^{Cip1} protein after *Pten* deletion (Fig. 2.5A). These increases in p19^{Arf}, p53 and p21^{Cip1} were attenuated or eliminated by rapamycin treatment, suggesting that the expression of these tumor suppressors was elevated as a consequence of mTOR activation (Fig. 2.5A). At the RNA level we confirmed significantly increased expression of *p19^{Arf}* (Fig. 2.5B) and *p21^{Cip1}* (Fig. 2.13B) by qPCR in *Pten*-deficient splenocytes, and that these increases were eliminated by rapamycin treatment. We observed no effect of *Pten* deletion or rapamycin treatment on *p53* transcript levels (Fig. 2.13C), consistent with the observation that p53 expression is mainly regulated post-transcriptionally (Jimenez et al., 1999; Lee et al., 2007; Takagi et al., 2005). Increased mTOR activation as a result of *Pten* deletion induces a tumor suppressor response in hematopoietic cells.

We hypothesized that this response suppressed leukemogenesis but promoted the depletion of HSCs after *Pten* deletion, and that rapamycin rescued HSC depletion by

attenuating the tumor suppressor response in HSCs. p16[Ink4a] and p19[Arf] are expressed at extraordinarily low levels in non-transformed primary somatic cells and are notoriously difficult to detect, even in circumstances in which genetic analysis demonstrates that they are functionally important (Bertwistle and Sherr, 2006; Krishnamurthy et al., 2004; Molofsky et al., 2003; Molofsky et al., 2006; Zindy et al., 1997; Zindy et al., 2003). This problem is compounded in rare HSCs, from which only limited amounts of protein are available. Therefore, to test this we sorted 2×10^6 Lineage[-]c-kit[+] hematopoietic stem/progenitor cells, immunoprecipitated p16[Ink4a], p19[Arf], and p53, then performed Western blots to assess the levels of p16[Ink4a], p19[Arf], and p53 in the protein extract from Lineage[-]c-kit^{+} cells. We used wild type and *p16[Ink4a]/p19[Arf]*–deficient mouse embryonic fibroblasts for positive and negative controls. We observed p16[Ink4a] and p53 expression in the *Pten*-deficient Lineage[-]c-kit^{+} cells but not in wild-type cells or cells treated with rapamycin, but did not detect p19[Arf] expression in wild-type or *Pten*-deficient Lineage[-]c-kit^{+} cells (Fig. 2.5C).

To independently verify the increases in p16[Ink4a] and p53 expression within HSCs we performed qPCR or immunohistochemistry on highly purified HSCs. We confirmed that *p16[Ink4a]* transcript levels increased in CD150^{+}CD48^{-}CD41^{-}Lin[-]c-Kit^{+}Sca-1^{+} HSCs after *Pten* deletion and that this increase was attenuated by rapamycin treatment (Fig. 2.5D). *p16[Ink4a]* transcript could only be amplified from 2 of 10 samples of wild-type CD150^{+}CD48^{-}CD41^{-}Lin[-]c-Kit^{+}Sca-1^{+} HSCs (with or without rapamycin treatment) but was detected in 5 of 5 samples of *Pten* deficient CD150^{+}CD48^{-}CD41^{-}Lin[-]c-Kit^{+}Sca-1^{+} HSCs and in 2 of 5 *Pten* deficient CD150^{+}CD48^{-}CD41^{-}Lin[-]c-Kit^{+}Sca-1^{+} HSCs treated with rapamycin (Fig. 2.5D). We were able to amplify *p19[Arf]* transcript from only 4 of 10

54

wild-type and 6 of 10 *Pten* deficient CD150$^+$CD48$^-$CD41$^-$Lin$^-$c-Kit$^+$Sca-1$^+$ HSCs (Fig. 2.5D). We also stained CD150$^+$CD48$^-$CD41$^-$Lin$^-$c-Kit$^+$Sca-1$^+$ HSCs with anti-p53 antibody on slides to assess the level of p53 expression on a cell-by-cell basis. *Pten* deficient HSCs that had not been treated with rapamycin exhibited significantly increased p53 staining (Fig. 2.5E, F), consistent with what we had observed by western blot (Fig. 2.5C). Together, our results suggest that p16^{Ink4a} and p53, but not p19^{Arf}, are induced in HSCs after *Pten* deletion. To definitively test whether these tumor suppressors contributed to HSC depletion or leukemia suppression after *Pten* deletion we functionally tested whether they modulated these phenotypes (see below).

Deficiency for p19^{Arf} or p53, but not p16^{Ink4a}, accelerates leukemogenesis

To test if p16^{Ink4a}, p19^{Arf}, or p53 suppressed the development of leukemia after *Pten*-deletion we generated compound mutant mice from which we could conditionally delete *Pten* in backgrounds that lacked *p16^{Ink4a}*, *p19^{Arf}*, *p16^{Ink4a}/p19^{Arf}* or *p53*. In initial experiments, we found that conditional deletion of *Pten* from *p16^{Ink4a}/p19^{Arf}*-deficient or *p53*-deficient backgrounds led to leukemogenesis (T-ALL, MPD, and/or histiocytic sarcoma) and to the death of mice within 14 days after the start of pIpC treatment (data not shown). This indicated that elimination of these tumor suppressors accelerated leukemogenesis because conditional deletion of *Pten* from mice with wild-type tumor suppressors caused the mice to die with leukemia (T-ALL, MPD) 30 to 46 days after the start of pIpC treatment (data not shown).

To avoid the rapid death of compound mutant mice and to compare the rates of leukemogenesis from limited numbers of mutant cells in wild-type mice, we transplanted

1×10^6 unexcised donor (CD45.2$^+$) bone marrow cells from wild-type, $p16^{Ink4a}/p19^{Arf-/-}$, $Pten^{fl/fl}Mx\text{-}1\text{-}Cre^+$, and $Pten^{fl/fl}Mx\text{-}1\text{-}Cre^+p16^{Ink4a}/p19^{Arf-/-}$ mice into irradiated wild-type recipient mice along with 500,000 recipient (CD45.1$^+$) bone marrow cells. Six weeks after transplantation, when the donor cells had stably engrafted, all recipients were treated with 7 injections of pIpC over 14 days to induce *Pten*-deletion. Recipients of wild-type and $p16^{Ink4a}/p19^{Arf-/-}$ bone marrow cells almost all survived for the duration of the experiment (165 days) with no signs of leukemogenesis (Fig. 2.6A). In contrast, recipients of $Pten^{fl/fl}Mx\text{-}1\text{-}Cre^+$ cells died 49 to 162 days after ending pIpC treatment (Fig. 2.6A). Recipients of $Pten^{fl/fl}Mx\text{-}1\text{-}Cre^+p16^{Ink4a}/p19^{Arf-/-}$ cells died significantly ($p<0.02$) more quickly, 27 to 65 days after ending pIpC treatment (Fig. 2.6A). Histology confirmed that the mice had MPD and/or histiocytic sarcoma and/or T-ALL when they died. These data indicate that deficiency for $p16^{Ink4a}$ and $p19^{Arf}$ accelerates leukemogenesis after *Pten* deletion.

To better understand the relative contributions of p16^{Ink4a} and p19^{Arf} to the suppression of leukemogenesis after *Pten* deletion we performed the same experiment using mice that were compound mutants for *Pten* and $p16^{Ink4a}$ (Fig. 2.6C) or *Pten* and $p19^{Arf}$ (Fig. 2.6B). $p16^{Ink4a}$ deficiency did not significantly affect the rate at which mice died after treatment with pIpC. Moreover, the spectrum of hematopoietic neoplasms did not differ between recipients of $Pten^{fl/fl}Mx\text{-}1\text{-}Cre^+$ cells versus $Pten^{fl/fl}Mx\text{-}1\text{-}Cre^+p16^{Ink4a-/-}$ cells (Fig. 2.6C). In contrast, $p19^{Arf}$ deficiency did significantly ($p<0.02$) increase the rate at which mice died after pIpC treatment (Fig. 2.6B). These results suggest that p19^{Arf} suppresses leukemogenesis after *Pten* deletion, consistent with the increase in p19^{Arf} expression in splenocytes after *Pten* deletion (Fig. 2.5A).

We observed no histiocytic sarcomas from $Pten^{fl/fl}Mx\text{-}1\text{-}Cre^{+}p16^{Ink4a\text{-}/\text{-}}$ cells (Fig. 2.6C; 0% of mice) and few from $Pten^{fl/fl}Mx\text{-}1\text{-}Cre^{+}p19^{Arf\text{-}/\text{-}}$ cells (Fig. 2.6B; 7% of mice), but abundant histiocytic sarcomas from $Pten^{fl/fl}Mx\text{-}1\text{-}Cre^{+}p16^{Ink4a}/p19^{Arf\text{-}/\text{-}}$ cells (Fig. 2.6A; 59% of mice). This is consistent with prior reports in suggesting that the development of histiocytic sarcomas requires loss of $p16^{Ink4a}$ and $p19^{Arf}$ in addition to *Pten* (Carrasco et al., 2006; You et al., 2002).

To assess the role of p53 in suppressing leukemogenesis after *Pten* deletion we performed the same experiment using mice that were compound mutant for *Pten* and *p53* (Fig. 2.6D). Recipients of $Pten^{fl/fl}Mx\text{-}1\text{-}Cre^{+}p53^{-/-}$ cells died much more quickly after pIpC treatment as compared to recipients of $Pten^{fl/fl}Mx\text{-}1\text{-}Cre^{+}$ cells (p<0.0001; Fig. 2.6D). All mice were confirmed to have MPD, AML, and/or T-ALL (but not histiocytic sarcoma) when they died (Fig. 2.6D). These results are consistent with our observation of an increase in p53 expression after *Pten* deletion (Fig. 2.5A) in suggesting that p53 suppresses leukemogenesis after *Pten* deletion.

p16^{Ink4a} and p53 promote the depletion of HSCs after *Pten* deletion

We wondered whether the tumor suppressors that suppress leukemogenesis after *Pten* deletion also contribute to the depletion of HSCs. To definitively test whether these tumor suppressors act cell-autonomously within HSCs to promote their depletion after *Pten* deletion, we transplanted 10 donor CD150^{+}CD48^{-}CD41^{-}Lin^{-}c-Kit^{+}Sca-1^{+} HSCs from mice with each of the genetic backgrounds depicted in Figure 6 into irradiated wild-type recipient mice, along with a radioprotective dose of 300,000 recipient bone marrow cells. The HSCs were isolated from the donor mice after they had been treated with 3

injections of pIpC over 6 days. The low dose of donor HSCs was designed to reconstitute the recipient mice while minimizing the incidence of leukemias. We monitored the reconstitution of recipient mice by donor HSCs for 16 weeks after transplantation to test whether deficiency for $p16^{Ink4a}$, $p19^{Arf}$, $p16^{Ink4a}/p19^{Arf}$ or $p53$ could prolong the reconstituting capacity of *Pten*-deficient HSCs.

$p16^{Ink4a}$ deficiency prolonged the reconstituting capacity of *Pten*-deficient HSCs. Wild-type and $p16^{Ink4a}$-deficient HSCs gave long-term multilineage reconstitution by donor cells in all recipient mice (Fig. 2.7A). In contrast, *Pten*-deleted (*Pten^{fl/fl}Mx-1-Cre^+*) HSCs only gave transient multilineage reconstitution for 6 to 8 weeks after transplantation, consistent with our prior study (Yilmaz et al., 2006). Surprisingly, compound mutant *Pten^{fl/fl}Mx-1-Cre^+p16^{Ink4a-/-}* HSCs gave multilineage reconstitution for at least 8 to 16 weeks, significantly longer than observed from *Pten^{fl/fl}Mx-1-Cre^+* HSCs (p<0.002; Fig. 2.7A). Moreover, the levels of donor cell reconstitution from *Pten^{fl/fl}Mx-1-Cre^+p16^{Ink4a-/-}* HSCs were significantly higher than the levels of reconstitution from *Pten^{fl/fl}Mx-1-Cre^+* HSCs (Fig. 2.7A). Sixteen weeks after transplantation 4 recipients of *Pten^{fl/fl}Mx-1-Cre^+p16^{Ink4a-/-}* HSCs remained alive and 2 of these mice remained multilineage reconstituted by donor cells. In a separate experiment, we confirmed that $CD150^+CD48^-CD41^-Lin^-c-Kit^+Sca-1^+$ donor HSCs (Fig. 2.7E) and $CD150^-CD48^-CD41^-Lin^-c-Kit^+Sca-1^+$ donor MPPs (Fig. 2.7G) could be recovered 8 weeks after transplantation from mice transplanted with 10 *Pten^{fl/fl}Mx-1-Cre^+p16^{Ink4a-/-}* HSCs but not with 10 *Pten^{fl/fl}Mx-1-Cre^+* HSCs. These data indicate that $p16^{Ink4a}$ promotes the depletion of *Pten*-deficient HSCs, consistent with our observation of $p16^{Ink4a}$ expression in HSCs after *Pten* deletion (Fig. 2.5C, D).

Recipient mice that were transplanted with $Pten^{fl/fl}Mx\text{-}1\text{-}Cre^+p16^{Ink4a\text{-}/\text{-}}$ HSCs did begin to die with MPD and/or T-ALL 12 to 16 weeks after transplantation whereas recipients of $Pten^{fl/fl}Mx\text{-}1\text{-}Cre^+$ HSCs did not develop neoplasms (Fig. 2.7A). This difference partly reflects the fact that $Pten^{fl/fl}Mx\text{-}1\text{-}Cre^+$ HSCs no longer had any donor cell chimerism by 12 weeks after transplantation and therefore were unable to develop donor cell leukemias (Fig. 2.7A). Therefore, $p16^{Ink4a}$ deficiency increased the opportunity for leukemogenesis by prolonging the reconstituting capacity of *Pten*-deleted HSCs, leading to donor cell reconstitution by compound mutant cells at late time points after *Pten*-deficient hematopoietic cells had already been depleted. Nonetheless, these data might also reflect a limited role for p16[Ink4a] in the suppression of leukemogenesis after *Pten* deletion.

$p19^{Arf}$ deficiency did not rescue the depletion of *Pten*-deficient HSCs. Wild-type and $p19^{Arf}$-deficient HSCs gave long-term multilineage reconstitution by donor cells in all recipient mice (Fig. 2.7B). In contrast, *Pten*-deleted ($Pten^{fl/fl}Mx\text{-}1\text{-}Cre^+$) HSCs only gave transient multilineage reconstitution for 6 to 8 weeks after transplantation. Compound mutant $Pten^{fl/fl}Mx\text{-}1\text{-}Cre^+p19^{Arf\text{-}/\text{-}}$ HSCs also gave multilineage reconstitution for only 4 to 8 weeks and at levels that were not significantly different from those observed from $Pten^{fl/fl}Mx\text{-}1\text{-}Cre^+$ HSCs (Fig. 2.7B). This indicates that $p19^{Arf}$ is not required for the depletion of HSCs after *Pten* deletion (Fig. 2.6B), consistent with our failure to detect $p19^{Arf}$ expression in *Pten* deficient HSCs (Fig. 2.5C, D). Only a minority of recipients of $Pten^{fl/fl}Mx\text{-}1\text{-}Cre^+p19^{Arf\text{-}/\text{-}}$ HSCs died with leukemia (beginning 8 weeks after transplantation), reflecting the transient reconstitution by these cells (Fig. 2.7B). Our data suggest that p16[Ink4a] contributes more than p19[Arf] to HSC depletion after *Pten* deletion.

Consistent with the partial rescue of HSC depletion by $p16^{Ink4a}$ deficiency, we also observed a partial rescue of HSC depletion by $p16^{Ink4a}/p19^{Arf}$ deficiency. Wild-type and $p16^{Ink4a}/p19^{Arf}$-deficient HSCs gave long-term multilineage reconstitution by donor cells in almost all recipient mice (Fig. 2.7C). In contrast, *Pten*-deleted (*Pten*$^{fl/fl}$*Mx-1-Cre*$^+$) HSCs only gave transient multilineage reconstitution for 4 to 8 weeks after transplantation. Compound mutant *Pten*$^{fl/fl}$*Mx-1-Cre*$^+$*p16*$^{Ink4a}/p19^{Arf-/-}$ HSCs gave multilineage reconstitution for up to 14 weeks after transplantation, significantly longer than observed from *Pten*$^{fl/fl}$*Mx-1-Cre*$^+$ HSCs (p<0.01; Fig. 2.7C). The levels of donor cell reconstitution from *Pten*$^{fl/fl}$*Mx-1-Cre*$^+$*p16*$^{Ink4a}/p19^{Arf-/-}$ HSCs were also significantly higher than levels of reconstitution from *Pten*$^{fl/fl}$*Mx-1-Cre*$^+$ HSCs (Fig. 2.7C). Most of the recipients of *Pten*$^{fl/fl}$*Mx-1-Cre*$^+$*p16*$^{Ink4a}/p19^{Arf-/-}$ HSCs died with MPD, T-ALL, and/or histiocytic sarcoma between 12 and 16 weeks after transplantation. These results are consistent with the data above in suggesting that p16^{Ink4a} depletes HSCs after *Pten* deletion.

p53 deficiency also prolonged the reconstituting capacity of *Pten*-deficient HSCs. Wild-type and *p53*-deficient HSCs gave long-term multilineage reconstitution by donor cells in all recipient mice for at least 16 weeks while *Pten*-deleted (*Pten*$^{fl/fl}$*Mx-1-Cre*$^+$) HSCs gave transient multilineage reconstitution for 4 to 6 weeks after transplantation (Fig. 2.7D). Compound mutant *Pten*$^{fl/fl}$*Mx-1-Cre*$^+$*p53*$^{-/-}$ HSCs gave multilineage reconstitution for up to 12 weeks, significantly longer than observed from *Pten*$^{fl/fl}$*Mx-1-Cre*$^+$ HSCs (p<0.002; Fig. 2.7D). The levels of donor cell reconstitution from *Pten*$^{fl/fl}$*Mx-1-Cre*$^+$*p53*$^{-/-}$ HSCs were also significantly higher than the levels of reconstitution from *Pten*$^{fl/fl}$*Mx-1-Cre*$^+$ HSCs (Fig. 2.7D). Most of the recipients of *Pten*$^{fl/fl}$*Mx-1-Cre*$^+$*p53*$^{-/-}$

HSCs died with MPD, AML and/or T-ALL 8 to 12 weeks after transplantation. In a separate experiment, we confirmed that $CD150^+CD48^-CD41^-Lin^-c$-$Kit^+Sca$-$1^+$ donor HSCs (Fig. 2.7F) and $CD150^-CD48^-CD41^-Lin^-c$-$Kit^+Sca$-$1^+$ donor MPPs (Fig. 2.7H) could be recovered 8 weeks after transplantation from mice transplanted with 10 $Pten^{fl/fl}Mx$-1-$Cre^+p53^{-/-}$ HSCs but not with 10 $Pten^{fl/fl}Mx$-1-Cre^+ HSCs. These data indicate that p53 contributes to the depletion of *Pten*-deficient HSCs in addition to suppressing leukemogenesis, consistent with its increased expression after *Pten* deletion in splenocytes and HSCs (Fig. 2.5).

The mechanisms by which $p16^{Ink4a}$ and p53 promote the depletion of HSCs after *Pten* deletion are uncertain. We did not detect any effect of *Pten* deletion or rapamycin treatment on the frequency of whole bone marrow cells or HSCs undergoing cell death (Fig. 2.14A). We also did not detect any effect of *Pten* deletion or rapamycin treatment on the frequency of senescence-associated ß-galactosidase$^+$ whole bone marrow cells or HSCs (Fig. 2.14C-E). This contrasts with results from prostate in which *Pten* deletion induces p53-mediated senescence marked by ß-galactosidase expression (Chen et al., 2005) and suggests that *Pten* deletion promotes HSC depletion by mechanisms that are different than those observed in prostate. Indeed, we observe an increase in the frequency of dividing HSCs after *Pten* deletion (rather than a decrease as would be expected if senescence were occurring), and this increase is rescued by rapamycin treatment (Fig. 2.14B). These results suggest that increased $p16^{Ink4a}$ and p53 expression in dividing HSCs is incompatible with HSC maintenance, perhaps because these tumor suppressors promote exit from the stem cell pool in dividing HSCs. Consistent with this possibility, cycling HSCs have less reconstituting capacity (Fleming et al., 1993) and compound

deficiency for $p16^{Ink4a}$, $p19^{Arf}$, and $p53$ leads to a dramatic expansion of HSCs and the maintenance of long-term self-renewal potential among CD150$^-$CD48$^-$CD41$^-$Lin$^-$c-Kit$^+$Sca-1$^+$ MPPs, which would otherwise only be capable of transient multilineage reconstitution (Akala et al., 2008; Kiel et al., 2008). These published results demonstrate that p16^{Ink4a} and p53 promote the maturation of HSCs into MPPs, raising the possibility that elevated expression of p16^{Ink4a} and p53 in *Pten*-deficient HSCs leads to premature maturation and HSC depletion.

DISCUSSION

Pten deletion increased Akt, mTORC1, and S6 kinase activation in HSCs (Fig. 2.1B, D, E) but we could find no evidence for reduced FoxO1 or FoxO3a expression or cytoplasmic sequestration (Fig. 2.1B, F-H; Fig. 2.8). We observed a clear increase in ROS levels within thymocytes after *Pten* deletion but not in HSCs (Fig. 2.2). Consistent with this, NAC treatment attenuated the increase in ROS levels in thymocytes but did not rescue the changes in hematopoiesis, HSC frequency (Fig. 2.3), or HSC reconstituting capacity (Fig. 2.4A) after *Pten* deletion. This contrasted with results from *FoxO1/3/4-* deficient mice in which ROS levels clearly increased within HSCs and NAC treatment at least partially rescued HSC depletion (Tothova et al., 2007). *Pten* deletion and *FoxO1/3/4* deletion thus lead to the depletion of HSCs by different mechanisms. HSC depletion after *Pten* deletion is mediated largely by mTOR activation with no evidence so far for an important contribution by oxidative stress. In contrast, HSC depletion after *FoxO1/3/4* deletion is mediated largely by oxidative stress (Tothova et al., 2007).

Pten deletion induces a tumor suppressor response in hematopoietic cells, characterized by increased expression of p19^{Arf} and p53 in splenocytes (Fig. 2.5A, B) and increased expression of p16^{Ink4a} and p53 in HSCs (Fig. 2.5C-F). Although the increase in p16^{Ink4a} expression in HSCs was barely detectable by western blot, it was confirmed by qPCR and by the cell-autonomous function of p16^{Ink4a} in HSCs (Fig. 2.7). The increased tumor suppressor expression appeared to arise as a result of increased mTOR activation, as these increases were attenuated by rapamycin treatment in both splenocytes (Fig. 2.5A, B), and HSCs (Fig. 2.5C, D, F). In functional studies, we found that *p16^{Ink4a}/p19^{Arf}* deficiency, *p19^{Arf}* deficiency, or *p53* deficiency significantly accelerated leukemogenesis

after *Pten* deletion (Fig. 2.6A, B, D). $p16^{Ink4a}$ deficiency did not significantly affect the rate of leukemogenesis after *Pten* deletion, though it did appear to suppress the generation of histiocytic sarcomas (Fig. 2.6C). This suggests that hematopoietic cells mainly rely upon tumor suppressors in the p53 pathway to suppress leukemogenesis after *Pten* deletion. This is consistent with results from mouse prostate in which *Pten* deletion induces p53-dependent senescence (Chen et al., 2005). Interestingly, this senescence response is $p19^{Arf}$-independent in prostate (Chen et al., 2009) but $p19^{Arf}$ did suppress leukemogenesis after *Pten* deletion, indicating tissue-specific functions for $p19^{Arf}$ in tumor suppression.

To directly test whether these tumor suppressors acted autonomously within HSCs to regulate their depletion we transplanted 10 highly purified $CD150^+CD48^-CD41^-$ $Lin^-c-Kit^+Sca-1^+$ HSCs from each genetic background to test whether deficiency for *$p16^{Ink4a}$*, *$p19^{Arf}$*, *$p16^{Ink4a}$/$p19^{Arf}$*, or *p53* could prolong the reconstituting capacity of HSCs after *Pten* deletion. *$p16^{Ink4a}$* deficiency, *$p16^{Ink4a}$/$p19^{Arf}$* deficiency, or *p53* deficiency all significantly prolonged the ability of *Pten*-deficient HSCs to give multilineage reconstitution in irradiated mice (Fig. 2.7). Interestingly, *$p19^{Arf}$* deficiency did not prolong the reconstituting capacity of *Pten*-deficient HSCs (Fig. 2.7B). Thus *$p19^{Arf}$* is critical for the suppression of leukemogenesis but not for HSC depletion after *Pten* deletion. In contrast, *$p16^{Ink4a}$* is critical for HSC depletion but plays a more limited role in the suppression of leukemogenesis. The functions of tumor suppressors in the suppression of leukemogenesis are somewhat distinct from their functions in HSC depletion.

Our results thus indicate that *Pten* deletion induces an mTOR mediated tumor suppressor response in hematopoietic cells, suppressing leukemogenesis and depleting HSCs. This suggests that leukemias likely arise from rare clones of *Pten*-deficient hematopoietic cells that acquire secondary mutations that inactivate the tumor suppressor response before they are depleted. However, we do not know which hematopoietic cells are transformed after *Pten* deletion. Therefore, it remains uncertain whether the tumor suppressors act in HSCs themselves to suppress leukemogenesis or whether they act in HSCs to promote their depletion while primarily acting in downstream cells to suppress leukemogenesis.

Although *p16^{Ink4a}* and *p19^{Arf}* are both encoded at the *Cdkn2a* locus, they are regulated by different promoters, encoded by a combination of different exons and alternative reading frames, have no sequence homology, and different molecular functions (Lowe and Sherr, 2003; Sherr, 2001). p16^{Ink4a} is a cyclin-dependent kinase inhibitor that negatively regulates proliferation by inhibiting the interaction of CDK4/6 with D-type cyclins, thus maintaining Rb in its hypophosphorylated (active) form. p19^{Arf} negatively regulates proliferation by inhibiting the Mdm2-mediated degradation of p53 and through poorly understood p53-independent functions (Sherr, 2006). Our conclusion that p16^{Ink4a} and p19^{Arf} have different expression patterns and functions after *Pten* deletion is consistent with other examples of situations in which the proteins have different expression patterns or functions (Baker et al., 2008; Bruggeman et al., 2005; Lowe and Sherr, 2003; Molofsky et al., 2005; Sherr, 2001).

We did not detect any evidence that hematopoietic cells underwent senescence or cell death after *Pten* deletion. For example, we did not detect senescence-associated ß-

galactosidase activity in HSCs after *Pten* deletion (Fig. 2.14). We were also unable to detect a significant increase in cell death within HSCs after *Pten* deletion (Fig. 2.14). However, HSCs are depleted over a 4 to 8 week period after *Pten* deletion (Fig. 2.7), suggesting that they are asynchronously lost over time. This raises the formal possibility that HSCs asynchronously undergo cell death or senescence over a period of 4 to 8 weeks, such that very few HSCs express markers of cell death or senescence at any single time point, rendering it undetectable. Nonetheless, we are able to clearly see increased proliferation among HSCs after Pten deletion and this phenotype is rescued by rapamycin treatment. Therefore, the simplest interpretation of the available data is that p16^{Ink4a} and p53 expression in dividing HSCs cause these cells to prematurely exist the stem cell pool, perhaps by maturing in to transit amplifying MPPs. As this also would occur asynchronously over time, the number of HSCs that prematurely exit the stem cell pool at any single time point would be imperceptibly small but the cumulative effect of premature maturation over a period of weeks would lead to HSC depletion.

Consistent with this model, cycling HSCs have less reconstituting capacity (Fleming et al., 1993) and less self-renewal potential (Foudi et al., 2009; Wilson et al., 2008). Deficiency for *p16^{Ink4a}*, *p19^{Arf}*, and *p53* dramatically expands HSC frequency and confers long-term self-renewal potential to CD150$^-$CD48$^-$CD41$^-$Lin$^-$c-Kit$^+$Sca-1$^+$ MPPs, which are normally only capable of transient multilineage reconstitution (Akala et al., 2008; Kiel et al., 2008). These tumor suppressors thus play a physiological role promoting the transition from HSCs to MPPs and negatively regulating the self-renewal potential of multipotent cells. Increased expression of p16^{Ink4a} and p53 in dividing HSCs

after *Pten* deletion may accelerate the normal maturation of cells out of the HSC pool, leading to HSC depletion.

p16^{Ink4a}, p19^{Arf}, and p53 may not be entirely responsible for HSC depletion after *Pten* deletion. Although we were able to completely rescue HSC depletion by treating with rapamycin (Yilmaz et al., 2006), we were not able to completely rescue HSC depletion by deleting any of the individual tumor suppressors we studied (Fig. 2.7). The best rescue we observed came from the deletion of *p16^{Ink4a}*; however, only half of the recipients of *Pten$^{fl/fl}$Mx-1-Cre$^+$p16$^{Ink4a-/-}$* HSCs remained multilineage reconstituted 16 weeks after transplantation, in contrast to recipients of control HSCs which were all multilineage reconstituted at the same time point (Fig. 2.7A). One possibility is that deficiency for both *p16^{Ink4a}* and *p53* would completely rescue HSC depletion after *Pten* deletion. Another possibility is that there are mechanisms independent of these tumor suppressors downstream of mTOR, which contribute to HSC depletion.

The induction of *p16^{Ink4a}* and *p53* in *Pten*-deficient HSCs may also be influenced by non-autonomous factors. *Pten*-deficient HSCs may be more sensitive to stresses associated with transplantation into irradiated mice and more likely to induce tumor suppressor expression than wild-type HSCs. Leukemogenesis in *Pten*-deficient mice might also create hematopoietic stresses that contribute to the induction of tumor suppressors in HSCs. However, neither leukemogenesis nor transplantation are necessary for the depletion of *Pten*-deficient HSCs. Recipients of 10 *Pten*-deficient HSCs consistently reconstituted recipient mice for less than 8 weeks after transplantation even though all of these mice survived for the duration of the experiment (16 weeks) with no

signs of leukemia (Fig. 2.7A-D). *Pten*-deficient HSCs are also depleted over time in mice even if they are not transplanted (Fig. 2.3F) (Yilmaz et al., 2006).

The ability to rescue the hematopoietic phenotypes in *Pten*-deficient mice with rapamycin suggests that these phenotypes are primarily driven by increased mTORC1 activation. However, rapamycin can also indirectly inhibit mTORC2 function (Sarbassov et al., 2006) and mTORC2 is required for the development of prostate cancer after *Pten* deletion (Guertin et al., 2009). This suggests that mTORC2 may mediate some of the effects of *Pten* deletion on HSCs and other hematopoietic cells.

The depletion of HSCs (and other hematopoietic progenitors) after *Pten* deletion may explain why few leukemias exhibit *Pten* deletion (Aggerholm et al., 2000; Chang et al., 2006; Sakai et al., 1998). Rare clones of *Pten*-deficient hematopoietic progenitors would be unlikely to have the opportunity to acquire secondary mutations before being depleted and therefore would be unlikely to progress to leukemia. Leukemias may be more likely to hyper-active the PI-3kinase pathway by other types of mutations that are better tolerated by hematopoietic cells than *Pten* deletion. Additional studies of the PI-3kinase pathway in stem cells will provide additional insights into stem cell regulation and the development of cancer.

10 CD150$^+$CD48$^-$CD41$^-$Lin$^-$c-Kit$^+$Sca-1$^+$ cells transplanted			
Donor	**Total number of recipients**	**Recipients engrafted at 2 weeks**	**Recipients that developed leukemia**
A	35	22	7
B	14	10	5
C	10	4	1
D	10	3	1
50 CD150$^+$CD48$^-$CD41$^-$Lin$^-$c-Kit$^+$Sca-1$^+$ cells transplanted			
Donor	**Total number of recipients**	**Recipients engrafted at 2 weeks**	**Recipients that developed leukemia**
E	15	10	10
F	20	18	18

Table 2.1: Transplanting increasing numbers of CD150$^+$CD48$^-$CD41$^-$Lin$^-$c-Kit$^+$Sca-1$^+$ cells from *Pten*-deleted mice with leukemia increased the percentage of recipient mice that developed leukemia.
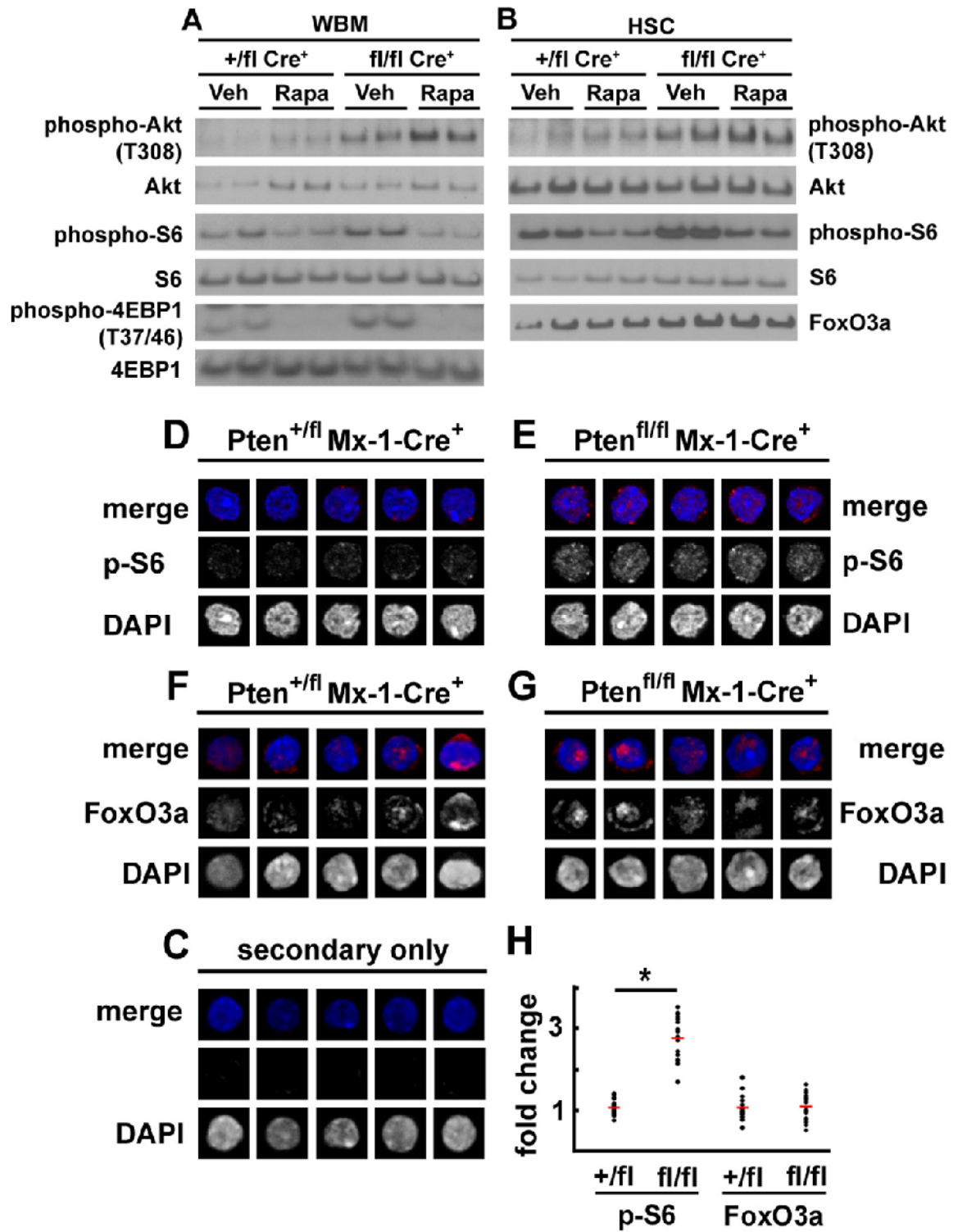
Figure 2.1

Figure 2.1: *Pten* deletion activated Akt and mTORC1 signaling in HSCs but FoxO3a was not inactivated.

(A, B) *Pten* deletion increased phospho-Akt (T308), phospho-S6, and phospho-4EBP1 (T37/46) levels in whole bone marrow cells (A) as well as in c-Kit$^+$Flk-2$^-$Lin$^-$Sca-1$^+$CD48$^-$ HSCs (B) as expected. Rapamycin treatment tended to further increase phospho-Akt levels, but decreased phospho-S6, and phospho-4EBP1 (T37/46) levels, as expected. Quantification demonstrated that *Pten* deletion increased phospho-Akt levels by 2.6-fold and phospho-S6 levels by 1.5-fold by in HSCs. Rapamycin treatment further increased phospho-Akt levels by 1.7-fold in HSCs and decreased phospho-S6 levels by 40% in HSCs. Total protein levels of FoxO3a did not decrease with *Pten* deletion and were unaffected by rapamycin treatment (B). Each lane contained protein extracted from 40,000 sorted cells. (C-H) Staining of sorted CD150$^+$CD48$^-$CD41$^-$Lin$^-$c-Kit$^+$Sca-1$^+$ HSCs with secondary antibody alone (C), or primary and secondary antibody against phospho-S6 (D-E) or FoxO3a (F-G). Phospho-S6 staining was significantly elevated in *Pten$^{fl/fl}$Mx-1-Cre$^+$* HSCs as compared to *Pten$^{+/fl}$Mx-1-Cre$^+$* control HSCs, as expected (D-E, H; *, p<0.0001 by Student's t-test), but the level and subcellular localization of FoxO3a staining did not differ between *Pten$^{fl/fl}$Mx-1-Cre$^+$* and control HSCs (F-H). We analyzed 10-30 HSCs from 1-2 mice/genotype in each of 3 independent experiments. In a similar assay, culture of HSCs in medium containing SCF (20 ng/ml) and TPO (50 ng/ml) for 24 hours did lead to decreased total FoxO3a levels and cytoplasmic localization (Fig. 2.9).
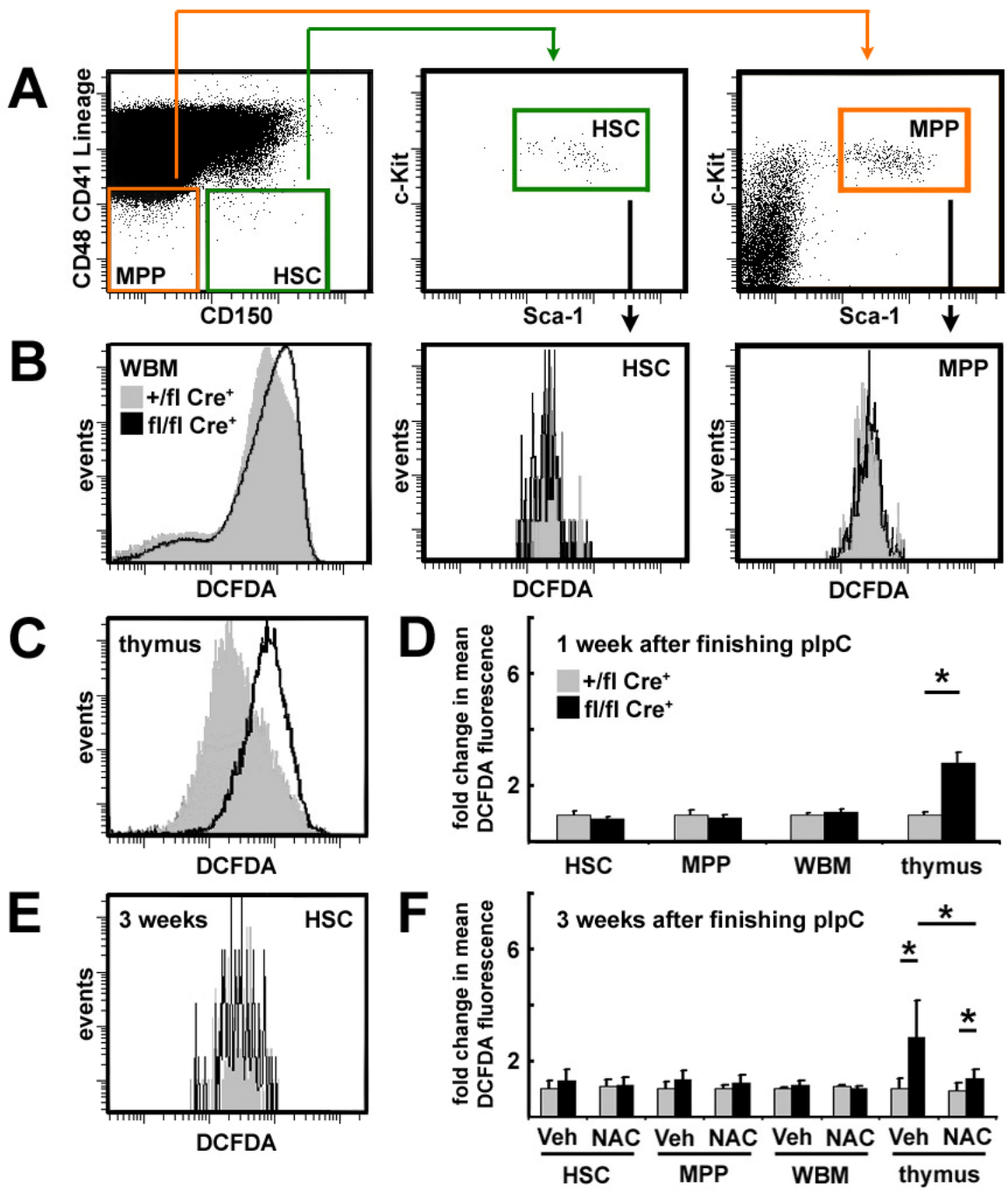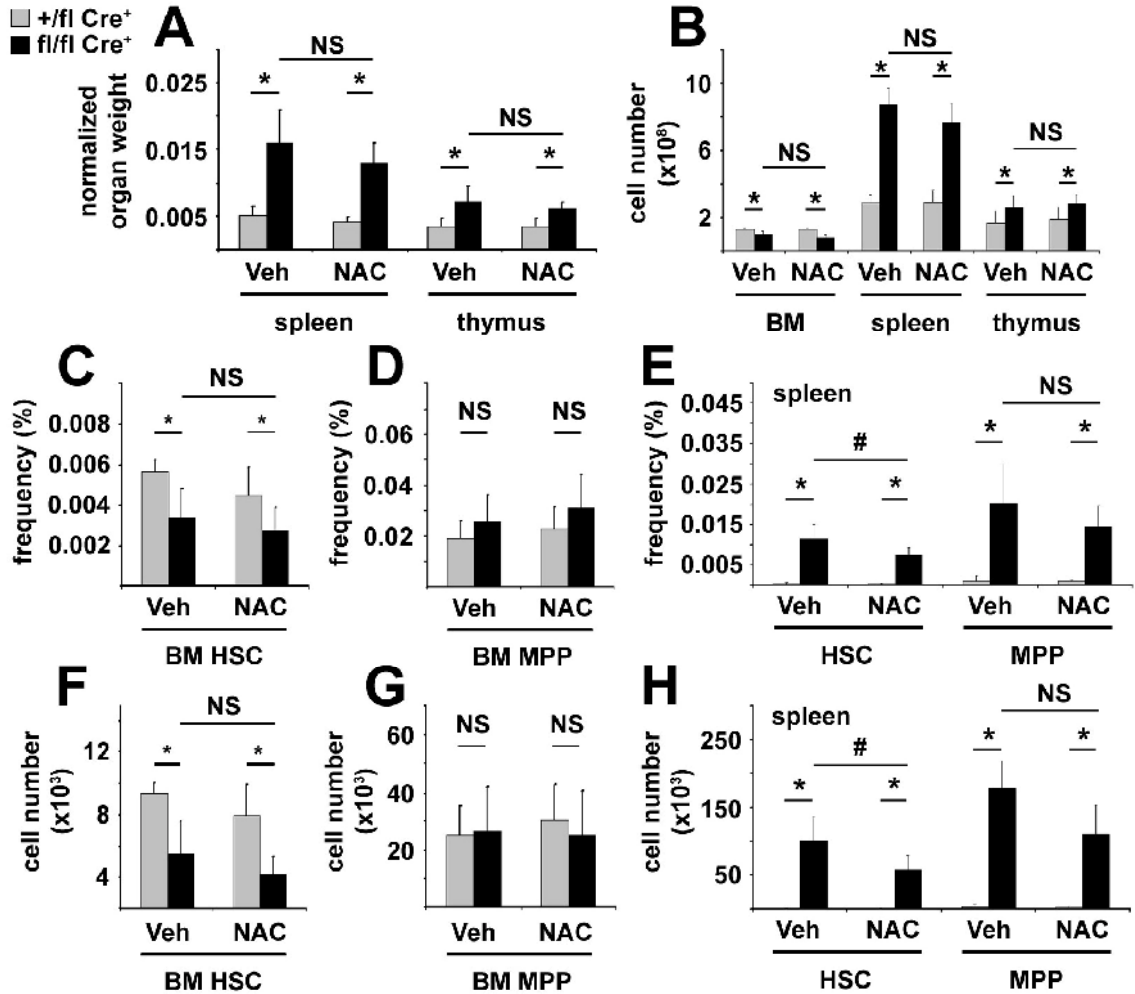
Figure 2.2

Figure 2.2: *Pten* deletion significantly increased ROS levels in thymocytes but not in HSCs, MPPs, or whole bone marrow cells.

(A) Gating scheme used to assess intracellular ROS levels in $CD150^+CD48^-CD41^-Lin^-c$-$Kit^+Sca$-$1^+$ HSCs and $CD150^-CD48^-CD41^-Lin^-c$-$Kit^+Sca$-$1^+$ MPPs. (B) 7 days after finishing pIpC treatment (7 doses of pIpC over 14 days), DCFDA staining of whole bone marrow cells, HSCs, and MPPs did not significantly differ between *Pten$^{fl/fl}$Mx-1-Cre$^+$* and *Pten$^{+/fl}$Mx-1-Cre$^+$* control mice. (C) In contrast, thymocytes from *Pten$^{fl/fl}$Mx-1-Cre$^+$* mice did exhibit significantly greater DCFDA staining than thymocytes from *Pten$^{+/fl}$Mx-1-Cre$^+$* controls. (D) Mean DCFDA fluorescence levels showed no evidence of increased ROS levels in HSCs, MPPs, or bone marrow cells, but a significant (*, $p<0.05$ by Student's t-test) increase in ROS levels within thymocytes. Similar experiments performed 21 days after finishing pIpC treatment yielded similar results (E, F). Daily subcutaneous injections of NAC after pIpC treatment did not significantly affect DCFDA staining of HSCs, MPPs, or bone marrow cells, but did significantly reduce DCFDA staining of thymocytes (F). Data (mean±standard deviation) are from 4 independent experiments with 1-2 mice/genotype/treatment.

Figure 2.3: Treatment with N-Acetyl-cysteine (NAC) did not rescue the major effects of *Pten* deletion on the hematopoietic system.

All mice were injected with seven doses of pIpC over 14 days then daily subcutaneous injections of NAC or vehicle for 21 days. *Pten* deletion significantly (*, $p<0.005$ by Student's t-test) increased the mass (normalized to body mass; A) and cellularity (B) of the spleen and thymus but these changes were not affected by NAC treatment. Bone marrow cellularity significantly declined after *Pten* deletion but this change also was not affected by NAC (B). The frequency (C) and absolute number (F) of $CD150^+CD48^-$ $CD41^-Lin^-c-Kit^+Sca-1^+$ HSCs in the bone marrow declined significantly after *Pten* deletion but was not affected by NAC. The frequency (D) and absolute number (G) of $CD150^-CD48^-CD41^-Lin^-c-Kit^+Sca-1^+$ MPPs in the bone marrow were not affected by *Pten* deletion or NAC. The frequency (E) and absolute number (H) of HSCs and MPPs in the spleen significantly increased after *Pten* deletion. The increase in HSCs was slightly but significantly (#, $p<0.05$) attenuated by NAC treatment but the increase in MPPs was not significantly affected (E, H). All data represent mean±standard deviation from 4 independent experiments with 1-2 mice/genotype/treatment.
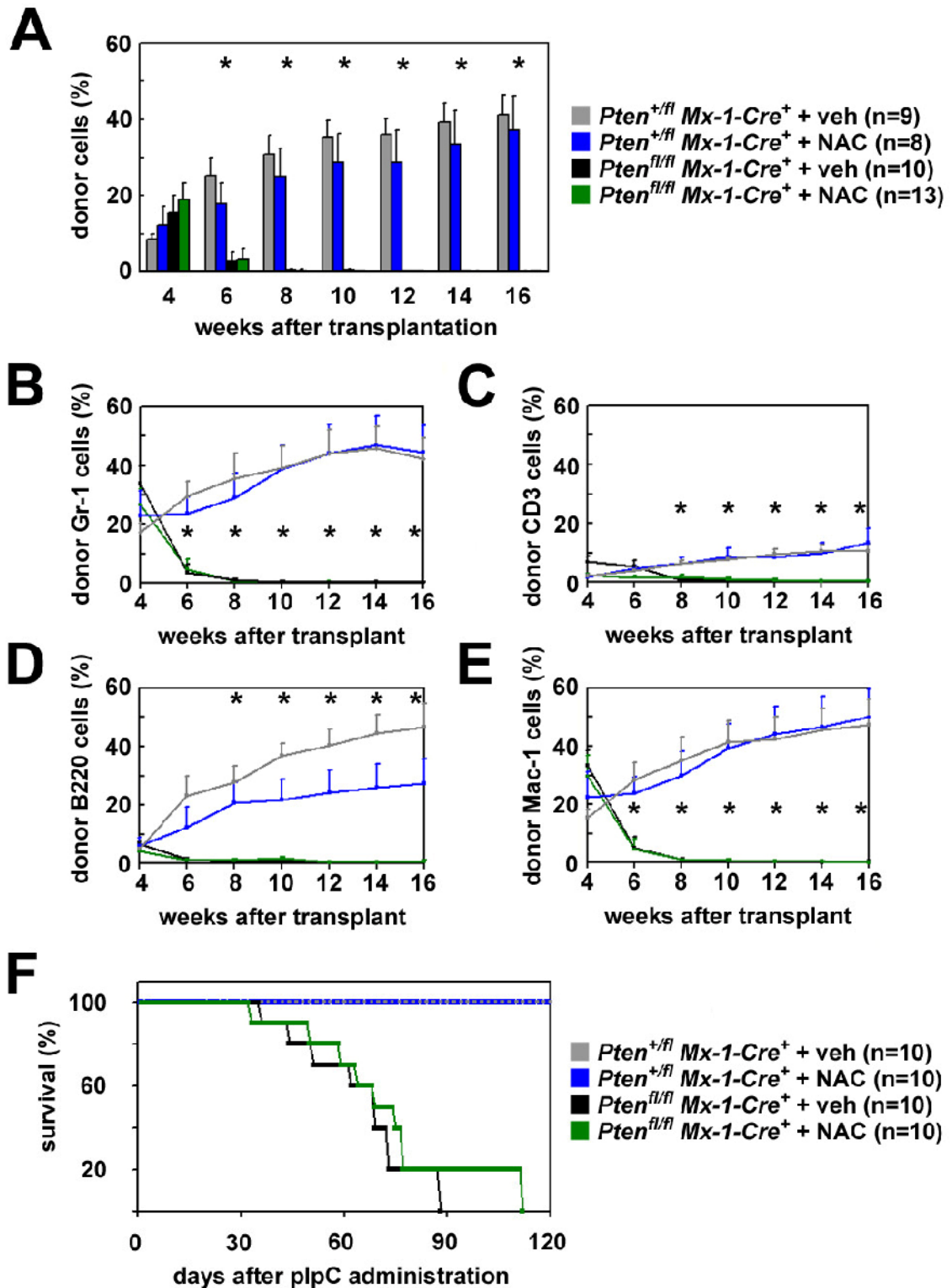
74

Figure 2.4

Figure 2.4: NAC treatment did not restore the reconstituting capacity of HSCs or block leukemogenesis after *Pten*-deletion.

(A-E) After pIpC treatment, 10 donor CD150$^+$CD48$^-$CD41$^-$Lin$^-$c-Kit$^+$Sca-1$^+$ HSCs were transplanted into lethally irradiated recipients along with 300,000 recipient bone marrow cells, and recipients were maintained on daily injections of NAC or vehicle beginning the day after transplantation. Control (*Pten$^{+/fl}$Mx-1-Cre$^+$*) HSCs gave high levels of long-term multilineage reconstitution by donor Gr-1+ myeloid (B), CD3+ T (C), B220+ B (D), and Mac-1+ myeloid cells (E) in all recipients, irrespective of NAC treatment. *Pten*-deleted (*Pten$^{fl/fl}$Mx-1-Cre$^+$*) HSCs gave transient multilineage reconstitution in all recipients, and significantly (*, p<0.05 by Student's t-test) lower levels of donor Gr-1+ myeloid cells (B), CD3+ T cells (C), B220+ B cells (D), and Mac-1+ myeloid cells (E), irrespective of NAC treatment. NAC treatment did not significantly affect reconstitution levels from either *Pten*-deleted or control HSCs. Data represent mean±SEM from 3 independent experiments. (F) In 2 independent experiments, 1x10^6 unexcised donor cells from *Pten$^{fl/fl}$Mx-1-Cre$^+$* or *Pten$^{+/fl}$Mx-1-Cre$^+$* mice were transplanted into irradiated recipient mice. Six weeks later *Pten* was deleted by pIpC treatment, then recipients were given daily injections of NAC or vehicle. NAC treatment did not prolong the survival of mice or delay the onset of leukemia after *Pten* deletion. None of the recipients of control cells developed neoplasms but all mice with *Pten*-deficient cells had MPD and/or T-ALL when they died, irrespective of NAC treatment.
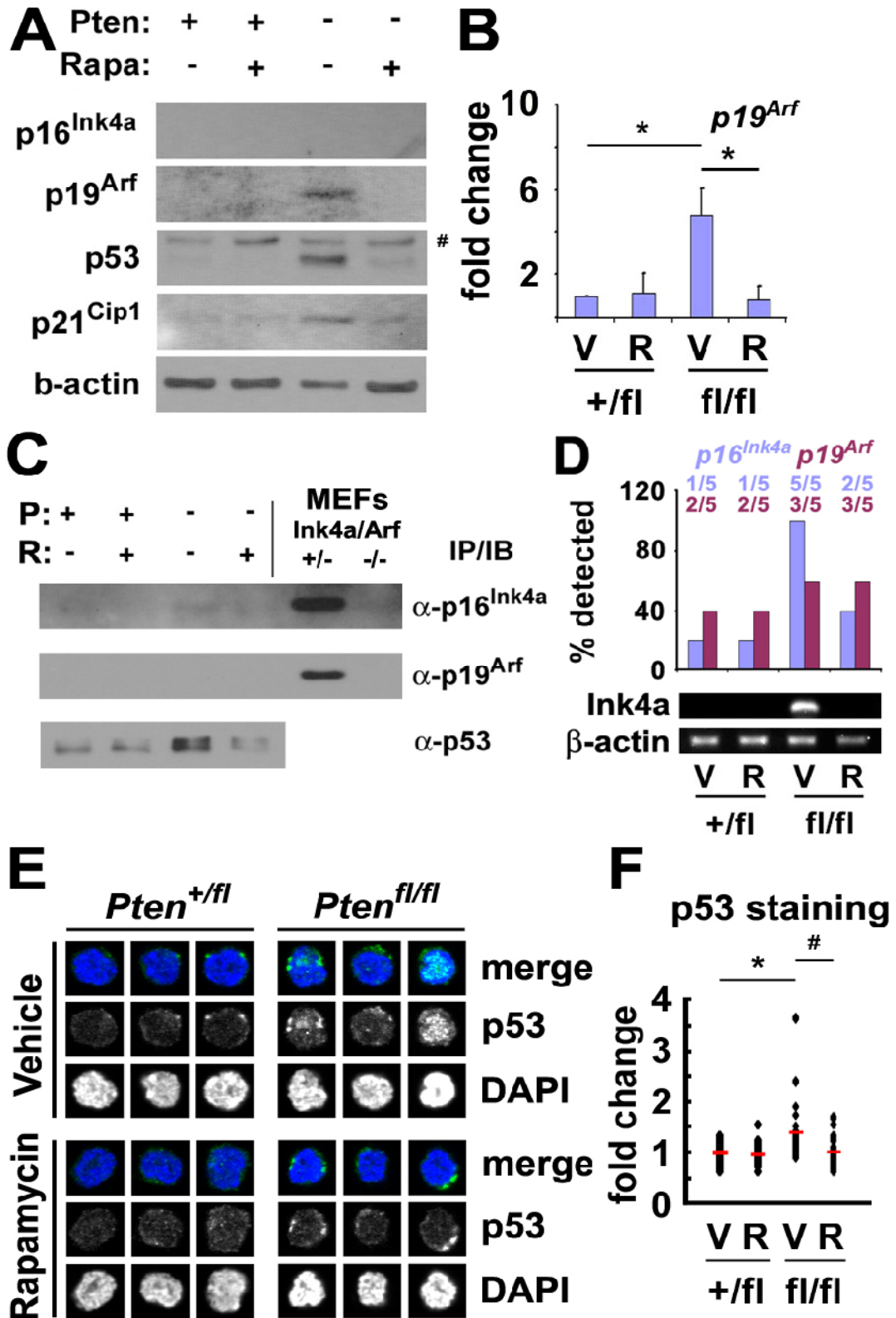
Figure 2.5

Figure 2.5: *Pten* deletion increased p19^{Arf}, p21^{Cip1}, and p53 expression in splenocytes, and p16^{Ink4a} and p53 in HSCs, and rapamycin attenuated these increases.

(A) Levels of p16^{Ink4a}, p19^{Arf}, p21^{Cip1}, and p53 were assessed by Western blot in unfractionated spleen cells from *Pten$^{fl/fl}$Mx-1-Cre^{+}* mice and *Pten$^{+/fl}$Mx-1-Cre^{+}* controls 14 days after pIpC treatment. Mice were given daily injections of rapamycin or vehicle after pIpC treatment ended. Analysis of *p53*-deficient MEFs (data not shown) indicated that the upper band (#) was not specific for p53 but the lower band was. This blot is representative of 3 independent experiments. (B) We also observed increased *p19^{Arf}* transcript levels by qPCR in splenocytes after *Pten* deletion and this effect was attenuated by rapamycin treatment (mean±SD from 3 independent experiments). (C) 4 weeks after pIpC treatment ended, 2,000,000 Lineage$^-$c-Kit$^+$ stem/progenitor cells were sorted from control and *Pten*-deleted mice and cell lysates were immunoprecipitated using antibodies against p16^{Ink4a}, p19^{Arf}, and p53 before Western blotting. p16^{Ink4a} and p53 levels increased in *Pten*-deleted cells, but we detected no increase in p19^{Arf}. MEFs that were deficient or heterozygous for *p16^{Ink4a}/p19^{Arf}* were used as negative and positive controls. (D) *p16^{Ink4a}* transcript could always be amplified from *Pten* deficient CD150$^+$CD48$^-$CD41$^-$Lin$^-$c-Kit$^+$Sca-1$^+$ HSCs (5 of 5 samples) but usually not from control (1 of 5) or rapamycin-treated samples (2 or 5) 4 weeks after *Pten* deletion. *p19^{Arf}* transcripts could only be amplified from about half of the samples, irrespective of *Pten* deletion or rapamycin treatment (data are from 5 independent experiments). (E, F) 4 weeks after pIpC treatment ended, CD150$^+$CD48$^-$CD41$^-$Lin$^-$c-Kit$^+$Sca-1$^+$ HSCs from *Pten*-deleted mice exhibited higher levels of immunofluorescence for p53 than control HSCs or *Pten* deleted HSCs treated with rapamycin. (F) The average staining intensity for p53 increased 1.4-fold (*, $p<0.008$ by Student's t-test) in *Pten*-deleted HSCs as compared to control HSCs. Rapamycin treatment rescued this effect (#, $p<0.003$ by Student's t-test; data are from 30 HSCs per group compiled from 2 independent experiments). None of the mice studied in this figure showed any signs of hematopoietic neoplasms.
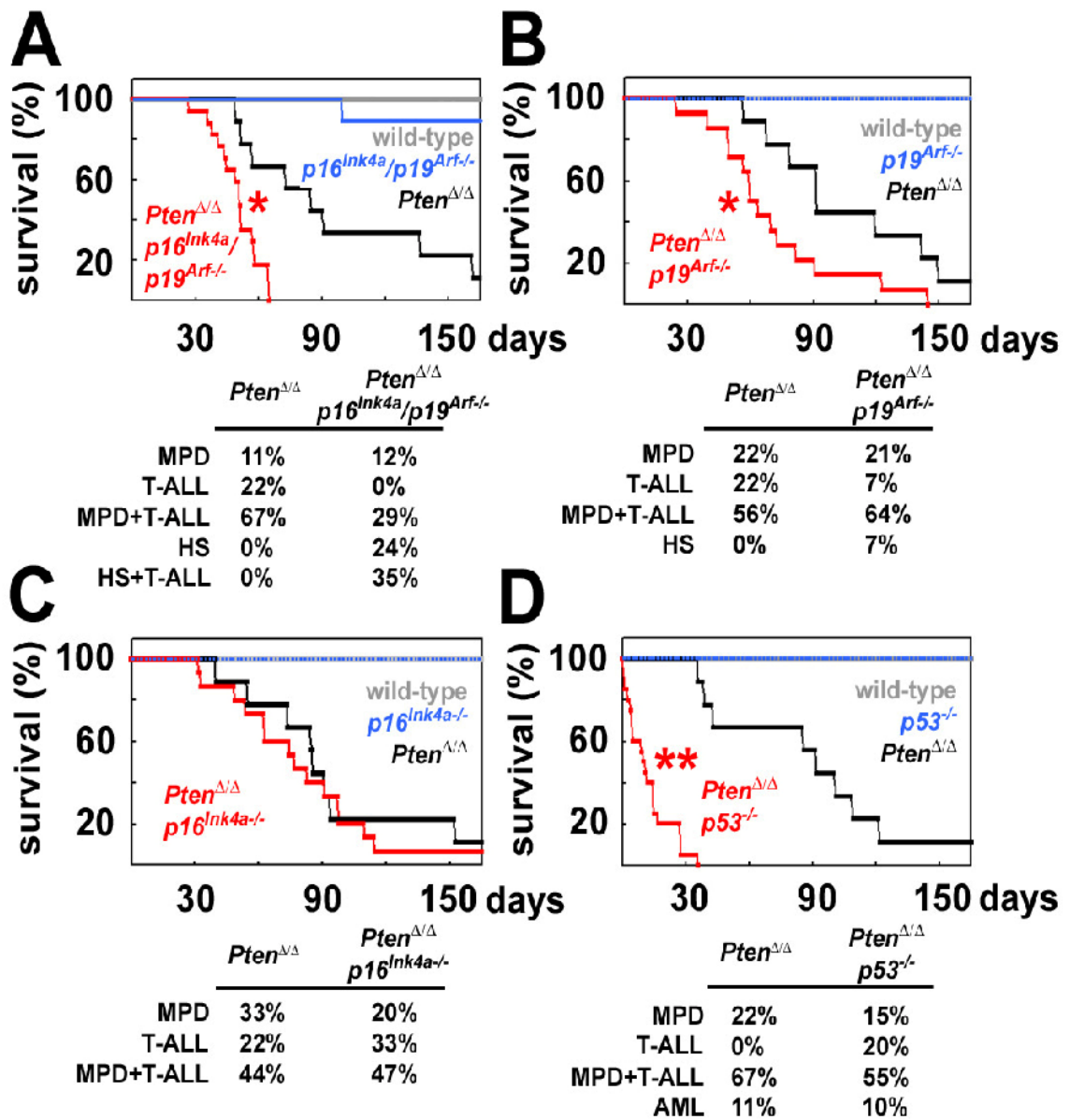
Figure 2.6

Figure 2.6: Deficiency for *p19^Arf* or *p53*, but not *p16^Ink4a*, accelerated leukemogenesis after *Pten*-deletion.

1×10^6 donor bone marrow cells from mice with the indicated genotypes were transplanted into irradiated recipient mice along with 500,000 recipient bone marrow cells. Six weeks after transplantation, all recipients were treated with pIpC and their survival was monitored over time (up to 165 days after pIpC treatment ended). (A) Recipients of *Pten^{fl/fl}Mx-1-Cre^+p16^{Ink4a}/p19^{Arf-/-}* cells (displayed as *Pten^{Δ/Δ}p16^{Ink4a}/p19^{Arf-/-}*) exhibited significantly (*, $p<0.02$ by Student's t-test) accelerated death as compared to recipients of *Pten^{fl/fl}Mx-1-Cre^+* cells (*Pten^{Δ/Δ}*). Mice were sacrificed when moribund and their hematopoietic tissues analyzed. The neoplasms observed in each mouse at the time of sacrifice included myeloproliferative disease (MPD), T-ALL, MPD+T-ALL, histiocytic sarcoma (HS), and HS+T-ALL. (B) Recipients of *Pten^{fl/fl}Mx-1-Cre^+p19^{Arf-/-}* cells (*Pten^{Δ/Δ}p19^{Arf-/-}*) exhibited significantly (*, $p<0.02$ by log-rank test) accelerated death from leukemogenesis as compared to recipients of *Pten^{fl/fl}Mx-1-Cre^+* cells (*Pten^{Δ/Δ}*). (C) Recipients of *Pten^{fl/fl}Mx-1-Cre^+p16^{Ink4a}* (*Pten^{Δ/Δ}p16^{Ink4a}*) cells died at a similar rate and with similar neoplasms as recipients of *Pten^{fl/fl}Mx-1-Cre^+* cells (*Pten^{Δ/Δ}*). (D) Recipients of *Pten^{fl/fl}Mx-1-Cre^+p53^{-/-}* cells (*Pten^{Δ/Δ}p53^{-/-}*) exhibited significantly (**, $p<0.0001$ by log-rank test) accelerated death from leukemogenesis as compared to recipients of *Pten^{fl/fl}Mx-1-Cre^+* cells (*Pten^{Δ/Δ}*). Data are from 3 independent experiments with a total of 9 mice/genotype except for compound mutant mice, which had 14-20 mice/genotype.

Figure 2.7

Figure 2.7: Deficiency for *p16^Ink4a^* or *p53* prolonged the reconstituting capacity of *Pten*-deficient HSCs.
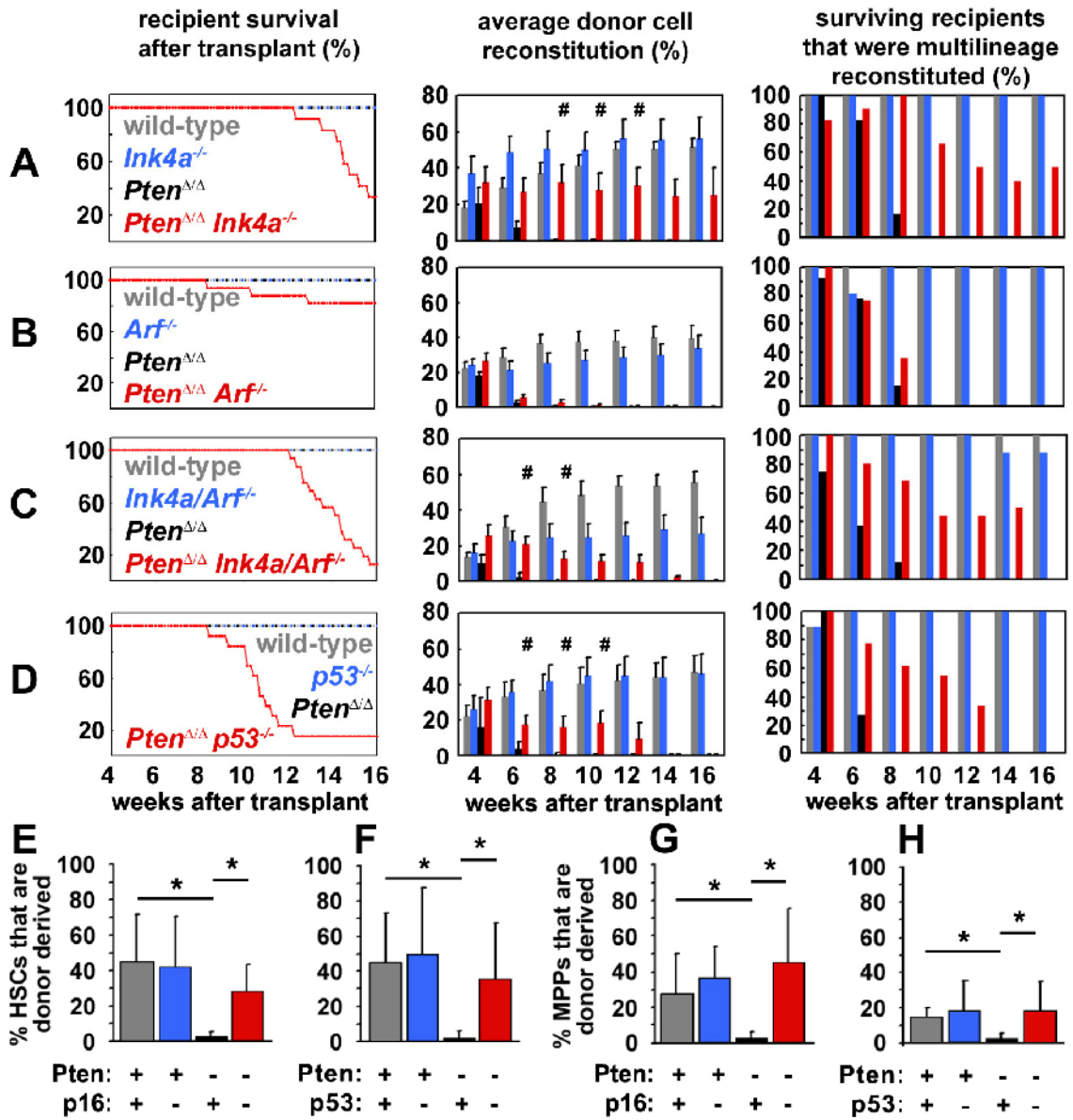
(A) 10 CD150$^+$CD48$^-$CD41$^-$Lin$^-$c-Kit$^+$Sca-1$^+$ cells were sorted from mice with each of the indicated genotypes after pIpC treatment and co-injected with 300,000 recipient bone marrow cells into irradiated recipient mice. The survival, donor cell reconstitution levels (mean±SEM), and percentage of surviving recipients with multilineage reconstitution by donor cells were monitored for 16 weeks after transplantation. In all experiments, recipients of wild-type cells (A-D) and recipients of *p16^Ink4a^*-deficient cells (A), *p19^Arf^*-deficient cells (B), *p16^Ink4a^*/*p19^Arf^*-deficient cells (C) or *p53*-deficient cells (D) survived for the duration of the experiment and showed high levels of long-term multilineage reconstitution by donor cells. In contrast, recipients of *Pten*-deficient cells showed only transient multilineage reconstitution for 4 to 8 weeks in each experiment (A-D). HSCs that were compound mutant for *Pten* in addition to *p16^Ink4a^* (A), *p16^Ink4a^*/*p19^Arf^* (C) or *p53* (D) gave significantly (#, p<0.05 by Student's t-test) higher levels of donor cell reconstitution and multilineage reconstitution for a significantly longer period of time as compared to HSCs that were deficient only for *Pten*. *p19^Arf^* deficiency did not significantly affect the duration or level of reconstitution by *Pten*-deficient HSCs (B). Compound mutant mice that died had MPD, T-ALL, and/or histiocytic sarcoma at the time of death. All data are from 3 independent experiments with a total of 7-17 recipients per treatment. (E-H) Mice were transplanted with mutant HSCs as described above then sacrificed 8 weeks later to assess the frequency of donor CD150$^+$CD48$^-$CD41$^-$Lin$^-$c-Kit$^+$Sca-1$^+$ HSCs and CD150$^-$CD48$^-$CD41$^-$Lin$^-$c-Kit$^+$Sca-1$^+$ MPPs. Donor HSCs and MPPs were not detectable by this time point in the absence of *Pten* but depletion was rescued by either *p16^Ink4a^* deficiency (E,G) or *p53* deficiency (F,H; *, p<0.05 by Student's t-test). These data are from 3 independent experiments with a total of 3-8 recipients per treatment. Transplantation of higher doses of *Pten*-deficient CD150$^+$CD48$^-$CD41$^-$Lin$^-$c-Kit$^+$Sca-1$^+$ cells from leukemic donors into irradiated wild-type mice led to the development of leukemia in a higher proportion of the recipient mice (Table 2.1).
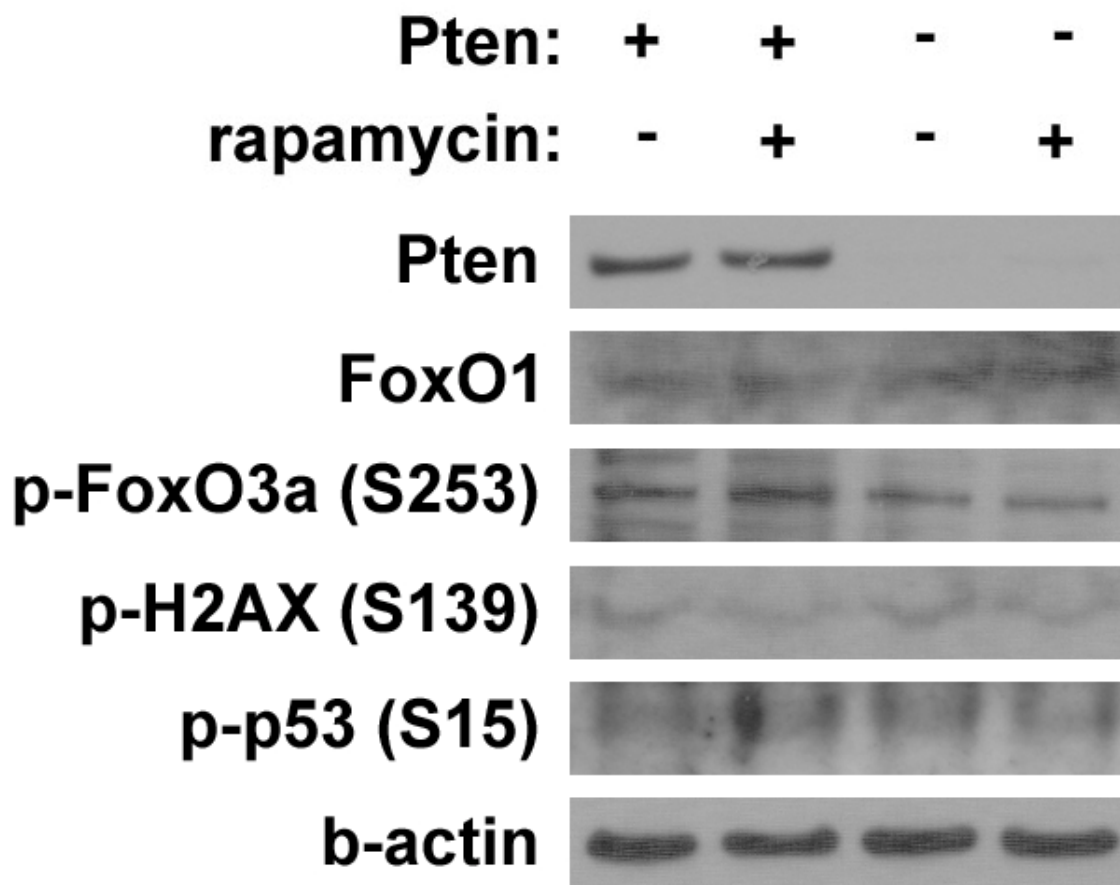
Figure 2.8: FoxO1, phospho-FoxO3a, and phospho-H2AX levels did not significantly change in hematopoietic stem/progenitor cells after *Pten* deletion.

Control mice and *Pten*-deleted mice were treated with either vehicle or rapamycin for 1 week after pIpC treatment ended, then 200,000 Lin$^-$c-Kit$^+$Sca-1$^+$ cells were sorted from each treatment and subjected to Western blotting. The levels of FoxO1 did not decrease and the levels of phospho-FoxO3a (S253) did not increase after *Pten* deletion. We were not able to detect FoxO4 expression in these cells (data not shown). The extent of DNA damage was estimated by blotting for phospho-H2AX (S139), which was detectable at very low levels in both control and *Pten*-deleted cells. We did not detect any change in phospho-p53 levels in Lin$^-$c-Kit$^+$Sca-1$^+$ cells after *Pten* deletion. These blots are representative of 2 independent experiments.
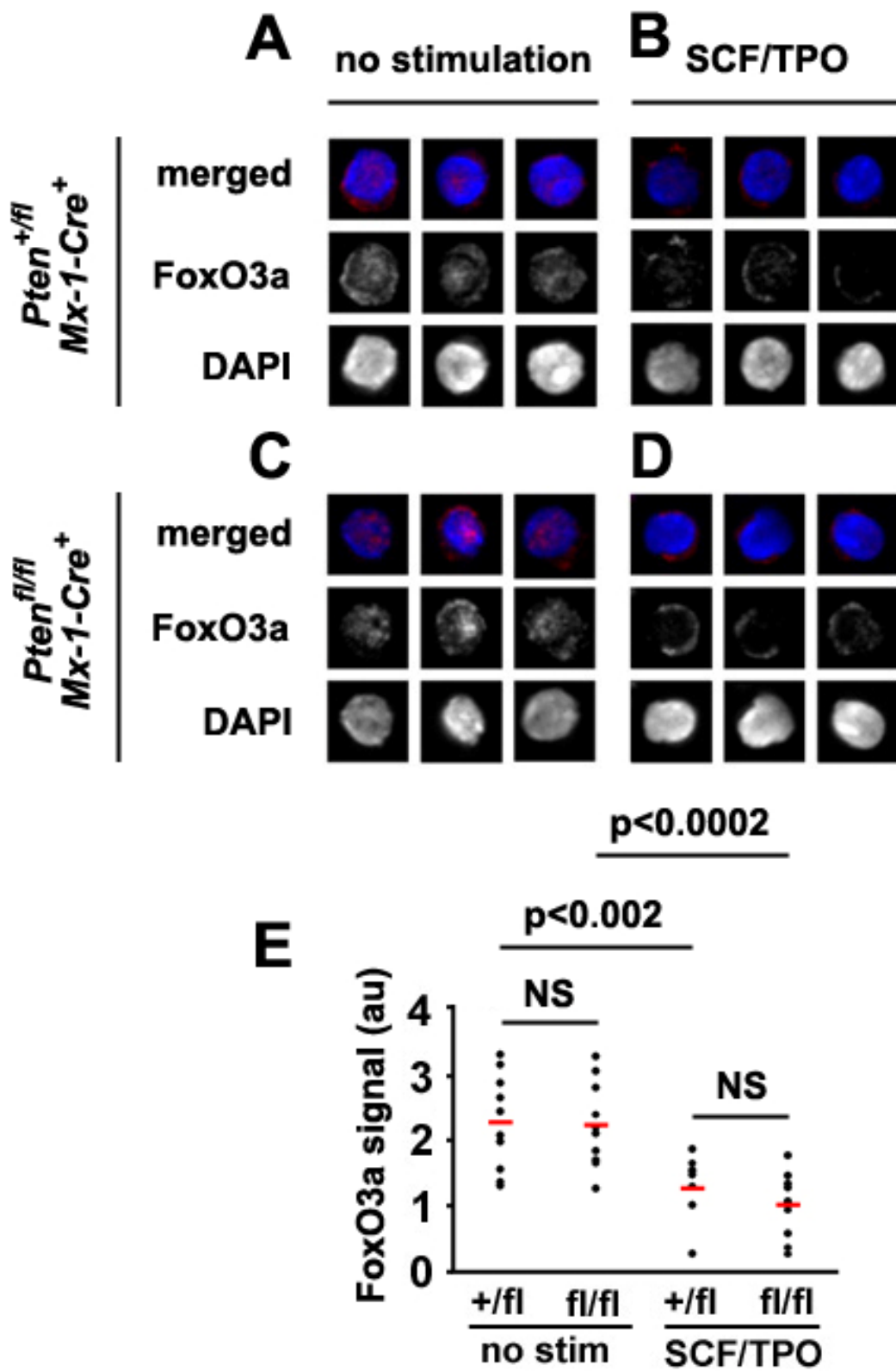
Figure 2.9

Figure 2.9: Stimulation of HSCs in culture with SCF and TPO reduced the levels of nuclear FoxO3a staining.

CD150$^+$CD48$^-$CD41$^-$Lin$^-$c-Kit$^+$Sca-1$^+$ HSCs from two control (A, B; *Pten$^{+/fl}$Mx-1-Cre$^+$*) and two *Pten*-deficient (C, D; *Pten$^{fl/fl}$Mx-1-Cre$^+$*) mice were incubated at 37°C in IMDM medium (+10% fetal bovine serum) with (B, D) or without (A, C) 20ng/ml SCF and 50ng/ml TPO. 24 hours later the cells were fixed, permeabilized, and stained for FoxO3a. Prominent nuclear FoxO3a staining was evident in both control (A) and *Pten*-deficient HSCs (C), similar to the staining observed in freshly isolated HSCs (Fig. 2.1F-G), but the total level of FoxO3a staining, and nuclear FoxO3a staining in particular, declined significantly ($p<0.002$ by Student's t-test; E) in HSCs of both genotypes that were stimulated with SCF and TPO (B, D). A total of 10 HSCs per treatment were imaged and quantified.
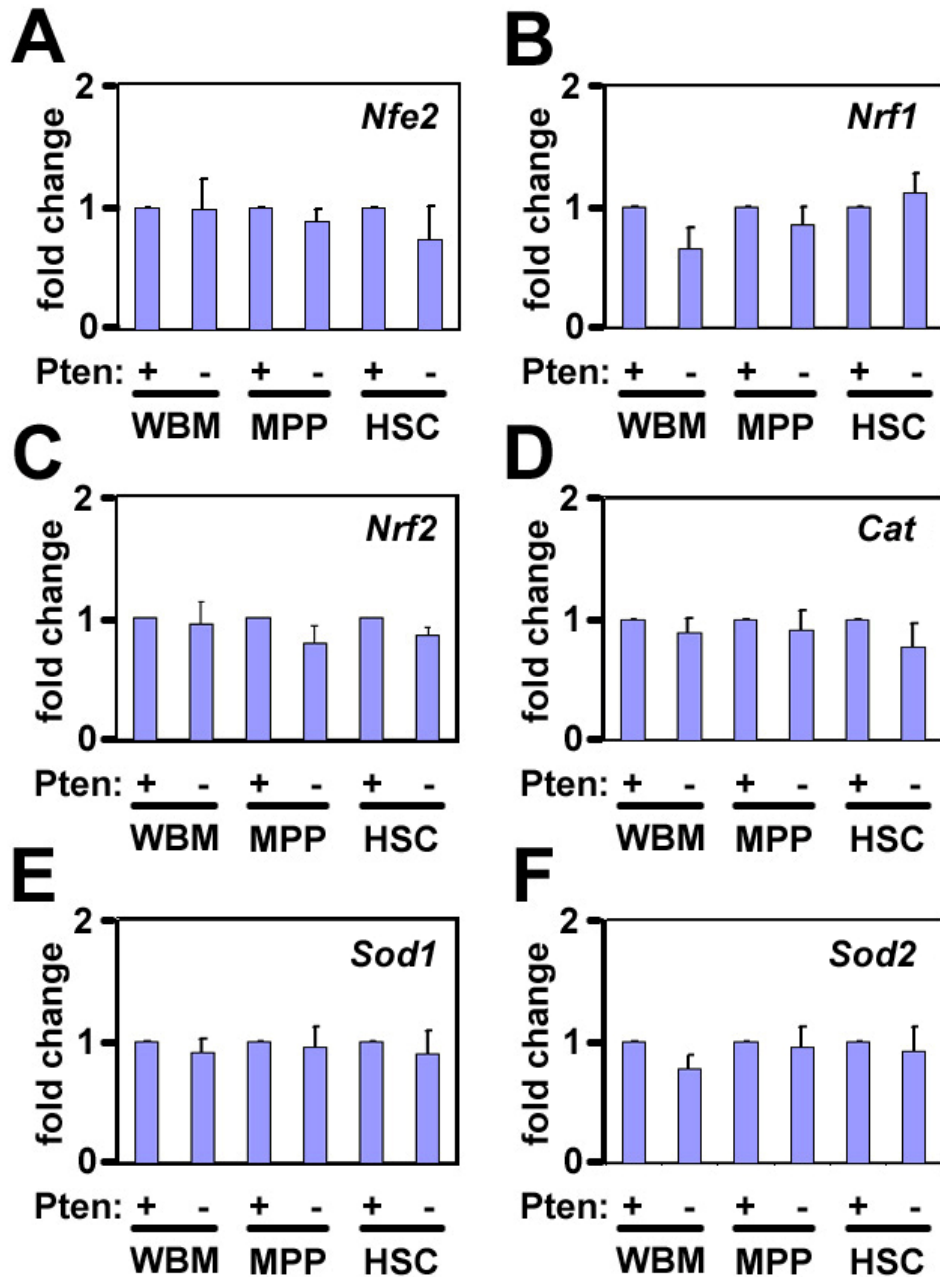
Figure 2.10: The expression levels of genes involved in the antioxidant response did not significantly change one week after *Pten* deletion.

Expression levels of *Nfe2* (A), *Nrf1* (B), *Nrf2* (C), *catalase* (D), *Sod1* (E), and *Sod2* (F) were assessed by quantitative PCR in whole bone marrow (WBM) cells, CD150$^+$CD48$^-$CD41$^-$Lin$^-$c-Kit$^+$Sca-1$^+$ HSCs, and CD150$^-$CD48$^-$CD41$^-$Lin$^-$c-Kit$^+$Sca-1$^+$ MPPs. The RNA content of samples was normalized based on -actin and fold-change comparisons were made between *Pten*-deficient and control cells (control cells were set to 1 for purposes of the comparison). Data represent mean±SD from 2 independent experiments.
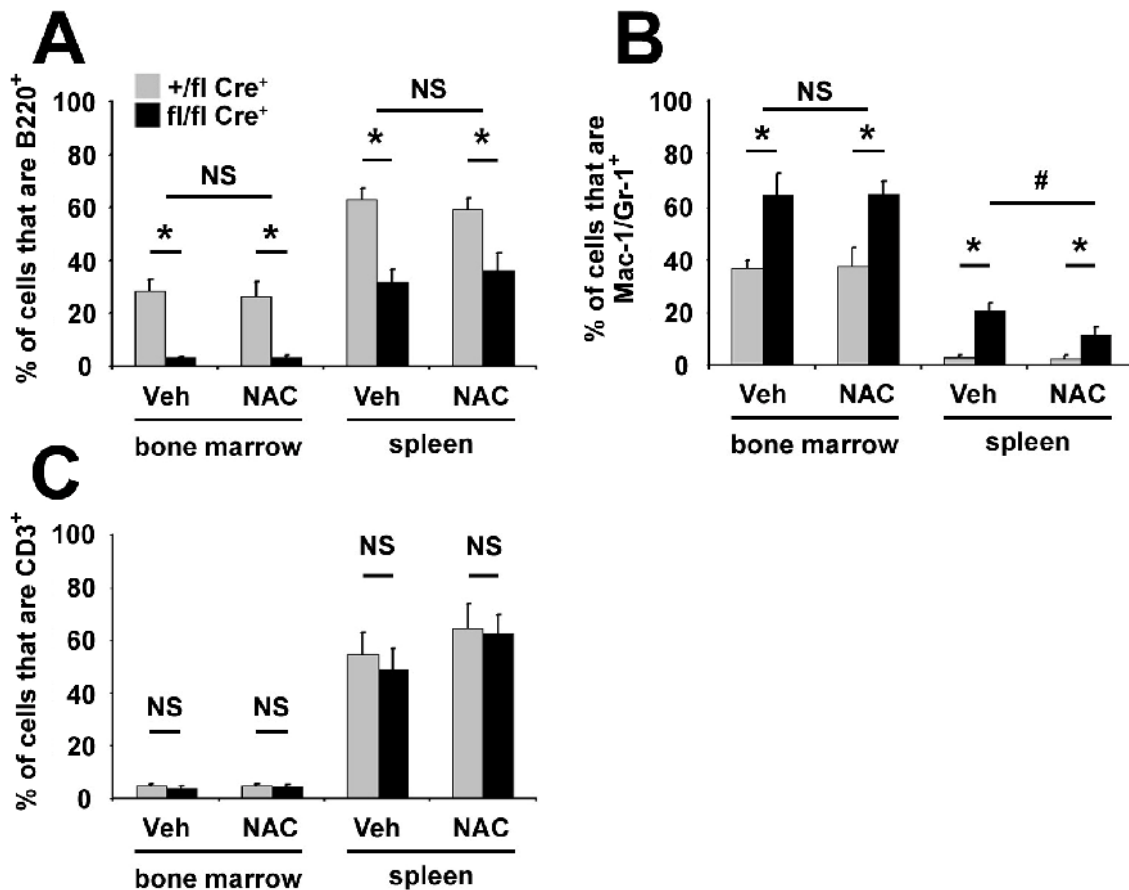
Figure 2.11: Changes in hematopoiesis after *Pten* deletion were not rescued by treatment with NAC.

NAC treatment did not affect the frequency of B220+ B cells (A), Mac-1+Gr-1+ myeloid cells (B), or CD3+ T cells (C) in the bone marrow or spleen of *Pten*-deleted (*Pten$^{fl/fl}$Mx-1-Cre$^+$*) or control (*Pten$^{+/fl}$Mx-1-Cre$^+$*) mice. (A) *Pten* deletion significantly (*, p<0.0001 by Student's t-test) reduced the frequency of B220$^+$ B cells in the bone marrow and spleen, but these decreases were not rescued by NAC treatment. All subpopulations of B-cells including B220$^+$sIgM$^-$CD43$^-$ pre-B cells, B220$^+$sIgM$^-$CD43^{low} pro-B cells, and mature B220$^+$sIgM$^+$ cells were depleted by *Pten* deletion and were not rescued by NAC treatment (data not shown). (B) *Pten* deletion significantly increased the frequency of Mac-1$^+$Gr-1$^+$ myeloid cells in the bone marrow and spleen. NAC did not affect the increase in myeloid cells within the bone marrow but did attenuate the increase in the spleen (#, p<0.001 by Student's t-test). (C) Neither *Pten* deletion nor NAC treatment significantly affected the frequency of CD3$^+$ T cells in the bone marrow or spleen. All data represent mean±standard deviation from 4 independent experiments with 1-2 mice/genotype/treatment.
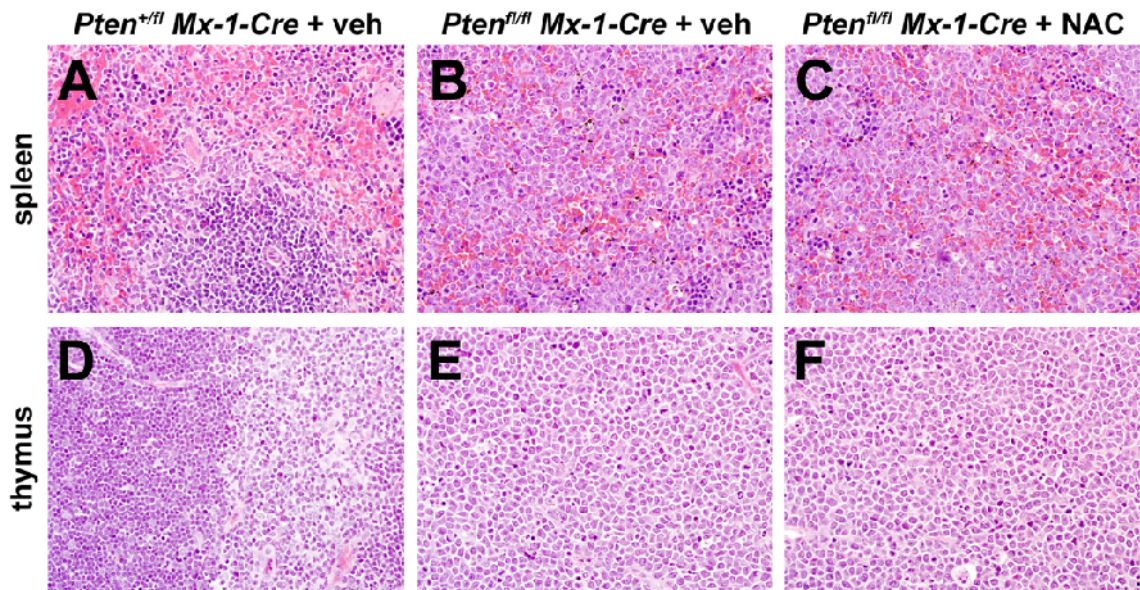
Figure 2.12: NAC treatment did not prevent the development of T-ALL in recipients of *Pten*-deficient cells.

The mice described in Figure 4F that had been transplanted with *Pten*-deficient or control bone marrow cells were examined for evidence of hematopoietic neoplasms. (A) Splenic architecture was normal in recipients of control bone marrow cells with clear boundaries between red and white pulp. (B) In recipients of *Pten*-deleted bone marrow cells the spleen was filled with lymphoid blasts and splenic architecture was completely effaced. (C) This was not affected by NAC treatment. (D) Thymic architecture was normal, with distinct cortex and medulla, in recipients of control cells. (E). In recipients of *Pten*-deleted bone marrow cells the thymus was filled with lymphoid blasts and thymic architecture was completely effaced. (F) This was not affected by NAC treatment.
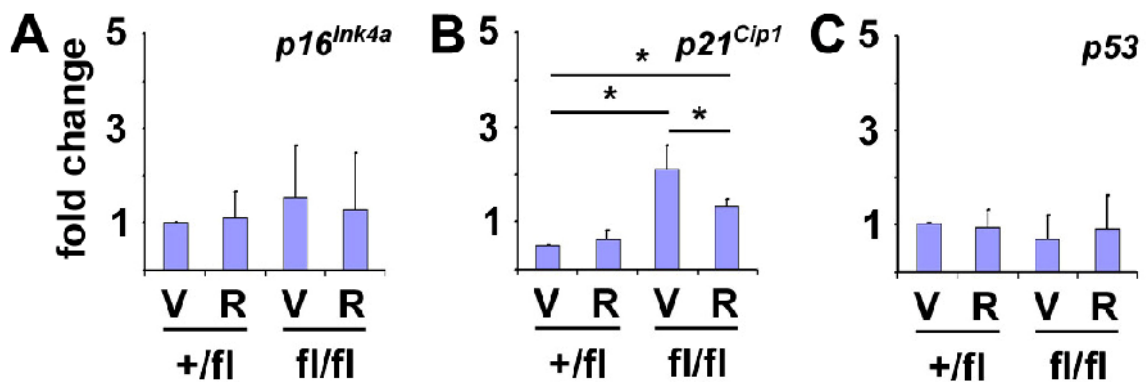
Figure 2.13: *Pten* deletion increased the levels of *p21*^{Cip1} but not *p16*^{Ink4a} or *p53* transcript in splenocytes.

Splenocytes from mice described in Figure 5A were also tested for the induction of *p16*^{Ink4a}, *p21*^{Cip1}, and *p53* by quantitative (real-time) PCR. *p16*^{Ink4a} and *p53* transcript levels were not significantly affected by *Pten* deletion or rapamycin treatment, but *p21*^{Cip1} transcript levels were significantly (*, $p<0.05$ by Student's t-test) increased by *Pten* deletion and significantly reduced by rapamycin treatment. Data represent mean±standard deviation from 3 independent experiments.
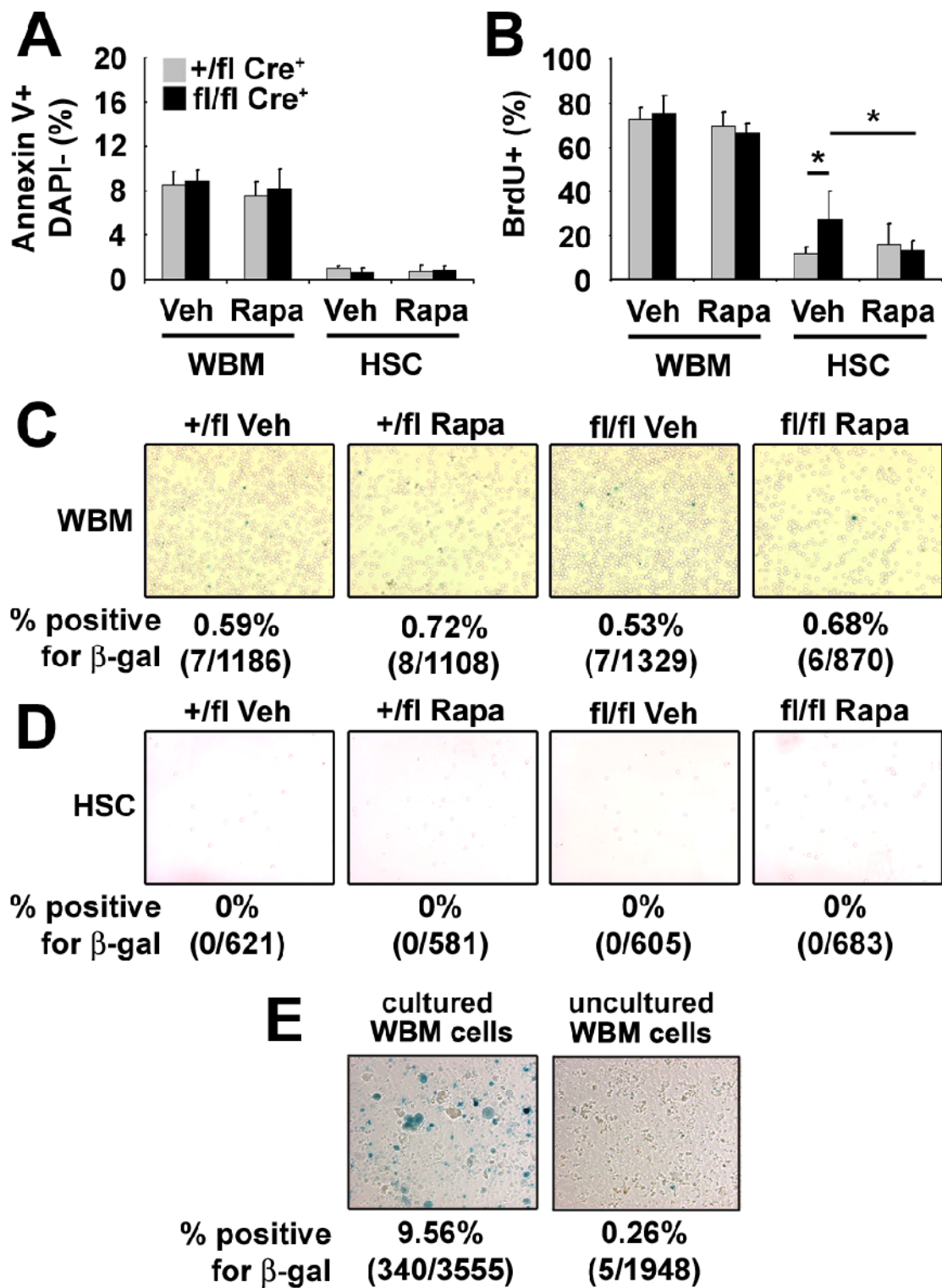
Figure 2.14

Figure 2.14: *Pten* deletion drove HSCs into cycle but did not detectably increase cell death or senescence in HSCs.

(A) 3 weeks after *Pten* deletion, the frequency of whole bone marrow (WBM) cells or $CD150^+CD48^-CD41^-Lin^-c\text{-}Kit^+Sca\text{-}1^+$ HSCs that were Annexin V^+ DAPI$^-$ was not affected by *Pten* deletion or rapamycin treatment (mean±standard deviation from 3 independent experiments). (B) The rate of cell cycle entry was estimated by assessing the percentage of cells that incorporated BrdU over a 24 hour pulse administered 3 weeks after ending pIpC treatment. The frequency of BrdU$^+$ cells was significantly increased by *Pten* deletion and normalized by rapamycin treatment in HSCs but not significantly affected in WBM (*, $p<0.05$ by Student's t-test; data are mean±SD from 3 independent experiments). (C-E) Neither *Pten* deletion nor rapamycin treatment affected the frequency of ß-galactosidase expressing WBM cells (C; 870 to 1186 cells counted/treatment) or HSCs (D; 581 to 683 cells counted/treatment) obtained from mice 4 weeks after pIpC treatment ended. In each treatment, uncultured cells were sorted onto slides, then stained with X-gal, and counted. Rare X-gal stained cells (blue) were observed in WBM but not among HSCs. Culturing WBM cells increased the frequency of X-gal stained cells.

ACKNOWLEDGEMENTS

AUTHOR CONTRIBUTIONS

J.Y.L. and D.N. performed all experiments involving *Pten*$^{fl/fl}$ mice and participated in the design and interpretation of experiments. O.H.Y. initiated the project and generated the compound mutant mice involving *Pten*. M.S.L. analyzed mouse pathology with help from J.Y.L. Z.T. and D.G.G. participated in the conception and interpretation of these experiments. S.J.M. participated in the design and interpretation of *Pten* experiments and wrote the paper with J.Y.L.

BIBLIOGRAPHY

Aggerholm, A., Gronbaek, K., Guldberg, P., and Hokland, P. (2000). Mutational analysis of the tumour suppressor gene MMAC1/PTEN in malignant myeloid disorders. European journal of haematology *65*, 109-113.

Akala, O.O., Park, I.K., Qian, D., Pihalja, M., Becker, M.W., and Clarke, M.F. (2008). Long-term haematopoietic reconstitution by Trp53-/-p16Ink4a-/-p19Arf-/- multipotent progenitors. Nature *453*, 228-232.

Baker, D.J., Perez-Terzic, C., Jin, F., Pitel, K., Niederlander, N.J., Jeganathan, K., Yamada, S., Reyes, S., Rowe, L., Hiddinga, H.J.*, et al.* (2008). Opposing roles for p16Ink4a and p19Arf in senescence and ageing caused by BubR1 insufficiency. Nature cell biology *10*, 825-836.

Bertwistle, D., and Sherr, C.J. (2006). Regulation of the Arf tumor suppressor in E{micro}-Myc transgenic mice: longitudinal study of Myc-induced lymphomagenesis. Blood.

Biggs, W.H., 3rd, Meisenhelder, J., Hunter, T., Cavenee, W.K., and Arden, K.C. (1999). Protein kinase B/Akt-mediated phosphorylation promotes nuclear exclusion of the winged helix transcription factor FKHR1. Proceedings of the National Academy of Sciences of the United States of America *96*, 7421-7426.

Bruggeman, S.W., Valk-Lingbeek, M.E., van der Stoop, P.P., Jacobs, J.J., Kieboom, K., Tanger, E., Hulsman, D., Leung, C., Arsenijevic, Y., Marino, S.*, et al.* (2005). Ink4a and Arf differentially affect cell proliferation and neural stem cell self-renewal in Bmi1-deficient mice. Genes & development *19*, 1438-1443.

Brunet, A., Bonni, A., Zigmond, M.J., Lin, M.Z., Juo, P., Hu, L.S., Anderson, M.J., Arden, K.C., Blenis, J., and Greenberg, M.E. (1999). Akt promotes cell survival by phosphorylating and inhibiting a Forkhead transcription factor. Cell *96*, 857-868.

Carrasco, D.R., Fenton, T., Sukhdeo, K., Protopopova, M., Enos, M., You, M.J., Di Vizio, D., Nogueira, C., Stommel, J., Pinkus, G.S.*, et al.* (2006). The PTEN and INK4A/ARF tumor suppressors maintain myelolymphoid homeostasis and cooperate to constrain histiocytic sarcoma development in humans. Cancer Cell *9*, 379-390.

Castilho, R.M., Squarize, C.H., Chodosh, L.A., Williams, B.O., and Gutkind, J.S. (2009). mTOR mediates Wnt-induced epidermal stem cell exhaustion and aging. Cell stem cell *5*, 279-289.

Chang, H., Qi, X.Y., Claudio, J., Zhuang, L., Patterson, B., and Stewart, A.K. (2006). Analysis of PTEN deletions and mutations in multiple myeloma. Leukemia research *30*, 262-265.

Chen, C., Liu, Y., Liu, R., Ikenoue, T., Guan, K.L., Liu, Y., and Zheng, P. (2008). TSC-mTOR maintains quiescence and function of hematopoietic stem cells by repressing mitochondrial biogenesis and reactive oxygen species. J Exp Med *205*, 2397-2408.

Chen, Z., Carracedo, A., Lin, H.K., Koutcher, J.A., Behrendt, N., Egia, A., Alimonti, A., Carver, B.S., Gerald, W., Teruya-Feldstein, J.*, et al.* (2009). Differential p53-independent outcomes of p19(Arf) loss in oncogenesis. Science signaling *2*, ra44.

Chen, Z., Trotman, L.C., Shaffer, D., Lin, H.K., Dotan, Z.A., Niki, M., Koutcher, J.A., Scher, H.I., Ludwig, T., Gerald, W.*, et al.* (2005). Crucial role of p53-dependent cellular senescence in suppression of Pten-deficient tumorigenesis. Nature *436*, 725-730.

Cheshier, S., Morrison, S.J., Liao, X., and Weissman, I.L. (1999). In vivo proliferation and cell cycle kinetics of long-term self-renewing hematopoietic stem cells. Proceedings of the National Academy of Sciences USA *96*, 3120-3125.

Christensen, J.L., and Weissman, I.L. (2001). Flk-2 is a marker in hematopoietic stem cell differentiation: a simple method to isolate long-term stem cells. Proc Natl Acad Sci U S A *98*, 14541-14546.

Di Cristofano, A., and Pandolfi, P.P. (2000). The multiple roles of PTEN in tumor suppression. Cell *100*, 387-390.

Ema, H., Morita, Y., Yamazaki, S., Matsubara, A., Seita, J., Tadokoro, Y., Kondo, H., Takano, H., and Nakauchi, H. (2006). Adult mouse hematopoietic stem cells: purification and single-cell assays. Nat Protoc *1*, 2979-2987.

Fleming, W.H., Alpern, E.J., Uchida, N., Ikuta, K., Spangrude, G.J., and Weissman, I.L. (1993). Functional heterogeneity is associated with the cell cycle status of murine hematopoietic stem cells. Journal of Cell Biology *122*, 897-902.

Foudi, A., Hochedlinger, K., Van Buren, D., Schindler, J.W., Jaenisch, R., Carey, V., and Hock, H. (2009). Analysis of histone 2B-GFP retention reveals slowly cycling hematopoietic stem cells. Nature biotechnology *27*, 84-90.

Gan, B., Sahin, E., Jiang, S., Sanchez-Aguilera, A., Scott, K.L., Chin, L., Williams, D.A., Kwiatkowski, D.J., and DePinho, R.A. (2008). mTORC1-dependent and -independent regulation of stem cell renewal, differentiation, and mobilization. Proceedings of the National Academy of Sciences of the United States of America *105*, 19384-19389.

Gregorian, C., Nakashima, J., Le Belle, J., Ohab, J., Kim, R., Liu, A., Smith, K.B., Groszer, M., Garcia, A.D., Sofroniew, M.V.*, et al.* (2009). Pten deletion in adult neural stem/progenitor cells enhances constitutive neurogenesis. J Neurosci *29*, 1874-1886.

Groszer, M., Erickson, R., Scripture-Adams, D.D., Dougherty, J.D., Le Belle, J., Zack, J.A., Geschwind, D.H., Liu, X., Kornblum, H.I., and Wu, H. (2006). PTEN negatively regulates neural stem cell self-renewal by modulating G0-G1 cell cycle entry.

Proceedings of the National Academy of Sciences of the United States of America *103*, 111-116.

Groszer, M., Erickson, R., Scripture-Adams, D.D., Lesche, R., Trumpp, A., Zack, J.A., Kornblum, H.I., Liu, X., and Wu, H. (2001). Negative regulation of neural stem/progenitor cell proliferation by the Pten tumor suppressor gene in vivo. Science (New York, NY *294*, 2186-2189.

Guertin, D.A., and Sabatini, D.M. (2007). Defining the role of mTOR in cancer. Cancer cell *12*, 9-22.

Guertin, D.A., Stevens, D.M., Saitoh, M., Kinkel, S., Crosby, K., Sheen, J.H., Mullholland, D.J., Magnuson, M.A., Wu, H., and Sabatini, D.M. (2009). mTOR complex 2 is required for the development of prostate cancer induced by Pten loss in mice. Cancer cell *15*, 148-159.

Harrington, L.S., Findlay, G.M., Gray, A., Tolkacheva, T., Wigfield, S., Rebholz, H., Barnett, J., Leslie, N.R., Cheng, S., Shepherd, P.R.*, et al.* (2004). The TSC1-2 tumor suppressor controls insulin-PI3K signaling via regulation of IRS proteins. The Journal of cell biology *166*, 213-223.

Inoki, K., Li, Y., Zhu, T., Wu, J., and Guan, K.L. (2002). TSC2 is phosphorylated and inhibited by Akt and suppresses mTOR signalling. Nat Cell Biol *4*, 648-657.

Ito, K., Bernardi, R., Morotti, A., Matsuoka, S., Saglio, G., Ikeda, Y., Rosenblatt, J., Avigan, D.E., Teruya-Feldstein, J., and Pandolfi, P.P. (2008). PML targeting eradicates quiescent leukaemia-initiating cells. Nature *453*, 1072-1078.

Ito, K., Hirao, A., Arai, F., Matsuoka, S., Takubo, K., Hamaguchi, I., Nomiyama, K., Hosokawa, K., Sakurada, K., Nakagata, N.*, et al.* (2004). Regulation of oxidative stress by ATM is required for self-renewal of haematopoietic stem cells. Nature *431*, 997-1002.

Ito, K., Hirao, A., Arai, F., Takubo, K., Matsuoka, S., Miyamoto, K., Ohmura, M., Naka, K., Hosokawa, K., Ikeda, Y.*, et al.* (2006). Reactive oxygen species act through p38 MAPK to limit the lifespan of hematopoietic stem cells. Nat Med *12*, 446-451.

Jacks, T., Remington, L., Williams, B.O., Schmitt, E.M., Halachmi, S., Bronson, R.T., and Weinberg, R.A. (1994). Tumor spectrum analysis in p53-mutant mice. Curr Biol *4*, 1-7.

Jimenez, G.S., Khan, S.H., Stommel, J.M., and Wahl, G.M. (1999). p53 regulation by post-translational modification and nuclear retention in response to diverse stresses. Oncogene *18*, 7656-7665.

Kamijo, T., Zindy, F., Roussel, M.F., Quelle, D.E., Downing, J.R., Ashmun, R.A., Grosveld, G., and Sherr, C.J. (1997). Tumor suppression at the mouse INK4a locus mediated by the alternative reading frame product p19ARF. Cell *91*, 649-659.

Kharas, M.G., Okabe, R., Ganis, J.J., Gozo, M., Khandan, T., Paktinat, M., Gilliland, D.G., and Gritsman, K. Constitutively active AKT depletes hematopoietic stem cells and induces leukemia in mice. Blood *115*, 1406-1415.

Kiel, M.J., Yilmaz, O.H., Iwashita, T., Terhorst, C., and Morrison, S.J. (2005). SLAM Family Receptors Distinguish Hematopoietic Stem and Progenitor Cells and Reveal Endothelial Niches for Stem Cells. Cell *121*, 1109-1121.

Kiel, M.J., Yilmaz, O.H., and Morrison, S.J. (2008). CD150- cells are transiently reconstituting multipotent progenitors with little or no stem cell activity. Blood *111*, 4413-4414.

Kogan, S.C., Ward, J.M., Anver, M.R., Berman, J.J., Brayton, C., Cardiff, R.D., Carter, J.S., deCoronado, S., Downing, J.R., Fredrickson, T.N.*, et al.* (2002). Bethesda proposals for classification of nonlymphoid hematopoietic neoplasms in mice. Blood *100*, 238-245.

Krishnamurthy, J., Torrice, C., Ramsey, M.R., Kovalev, G.I., Al-Regaiey, K., Su, L., and Sharpless, N.E. (2004). Ink4a/Arf expression is a biomarker of aging. J Clin Invest *114*, 1299-1307.

Kuhn, R., Schwenk, F., Aguet, M., and Rajewsky, K. (1995). Inducible gene targeting in mice. Science *269*, 1427-1429.

Lee, C.H., Inoki, K., Karbowniczek, M., Petroulakis, E., Sonenberg, N., Henske, E.P., and Guan, K.L. (2007). Constitutive mTOR activation in TSC mutants sensitizes cells to energy starvation and genomic damage via p53. The EMBO journal *26*, 4812-4823.

Lin, A.W., Barradas, M., Stone, J.C., van Aelst, L., Serrano, M., and Lowe, S.W. (1998). Premature senescence involving p53 and p16 is activated in response to constitutive MEK/MAPK mitogenic signaling. Genes & development *12*, 3008-3019.

Lowe, S.W., and Sherr, C.J. (2003). Tumor suppression by Ink4a-Arf: progress and puzzles. Current Opinion in Genetics & Development *13*, 77-83.

Maehama, T., and Dixon, J.E. (1998). The tumor suppressor, PTEN/MMAC1, dephosphorylates the lipid second messenger, phosphatidylinositol 3,4,5-trisphosphate. J Biol Chem *273*, 13375-13378.

Manning, B.D., and Cantley, L.C. (2007). AKT/PKB signaling: navigating downstream. Cell *129*, 1261-1274.

Miyamoto, K., Araki, K.Y., Naka, K., Arai, F., Takubo, K., Yamazaki, S., Matsuoka, S., Miyamoto, T., Ito, K., Ohmura, M.*, et al.* (2007). Foxo3a is essential for maintenance of the hematopoietic stem cell pool. Cell Stem Cell *1*, 101-112.

Molofsky, A.V., He, S., Bydon, M., Morrison, S.J., and Pardal, R. (2005). Bmi-1 promotes neural stem cell self-renewal and neural development but not mouse growth

and survival by repressing the p16Ink4a and p19Arf senescence pathways. Genes Dev *19*, 1432-1437.

Molofsky, A.V., Pardal, R., Iwashita, T., Park, I.K., Clarke, M.F., and Morrison, S.J. (2003). Bmi-1 dependence distinguishes neural stem cell self-renewal from progenitor proliferation. Nature *425*, 962-967.

Molofsky, A.V., Slutsky, S.G., Joseph, N.M., He, S., Pardal, R., Krishnamurthy, J., Sharpless, N.E., and Morrison, S.J. (2006). Increasing p16INK4a expression decreases forebrain progenitors and neurogenesis during ageing. Nature *443*, 448-452.

Morse, H.C., Anver, M.R., Fredrickson, T.N., Haines, D.C., Harris, A.W., Harris, N.L., Jaffe, E.S., Kogan, S.C., MacLennan, I.C.M., Pattengale, P.K.*, et al.* (2002). Bethesda proposals for classification of lymphoid neoplasms in mice. Blood *100*, 246-258.

Nguyen, T., Nioi, P., and Pickett, C.B. (2009). The Nrf2-antioxidant response element signaling pathway and its activation by oxidative stress. The Journal of biological chemistry *284*, 13291-13295.

Paik, J.H., Ding, Z., Narurkar, R., Ramkissoon, S., Muller, F., Kamoun, W.S., Chae, S.S., Zheng, H., Ying, H., Mahoney, J.*, et al.* (2009). FoxOs cooperatively regulate diverse pathways governing neural stem cell homeostasis. Cell stem cell *5*, 540-553.

Renault, V.M., Rafalski, V.A., Morgan, A.A., Salih, D.A., Brett, J.O., Webb, A.E., Villeda, S.A., Thekkat, P.U., Guillerey, C., Denko, N.C.*, et al.* (2009). FoxO3 regulates neural stem cell homeostasis. Cell stem cell *5*, 527-539.

Sakai, A., Thieblemont, C., Wellmann, A., Jaffe, E.S., and Raffeld, M. (1998). PTEN gene alterations in lymphoid neoplasms. Blood *92*, 3410-3415.

Sarbassov, D.D., Ali, S.M., Sengupta, S., Sheen, J.H., Hsu, P.P., Bagley, A.F., Markhard, A.L., and Sabatini, D.M. (2006). Prolonged rapamycin treatment inhibits mTORC2 assembly and Akt/PKB. Molecular cell *22*, 159-168.

Serrano, M., Lee, H., Chin, L., Cordon-Cardo, C., Beach, D., and DePinho, R.A. (1996). Role of the INK4a locus in tumor suppression and cell mortality. Cell *85*, 27-37.

Serrano, M., Lin, A.W., McCurrach, M.E., Beach, D., and Lowe, S.W. (1997). Oncogenic ras provokes premature cell senescence associated with accumulation of p53 and p16INK4a. Cell *88*, 593-602.

Sharpless, N.E., Bardeesy, N., Lee, K.-H., Carrasco, D., Castrillon, D.H., Aguirre, A.J., Wu, E.A., Horner, J.W., and DePinho, R.A. (2001). Loss of p16Ink4a with retention of p19Arf predisposes mice to tumorigenesis. Nature *413*, 86-91.

Sherr, C.J. (2001). The INK4a/ARF network in tumour suppression. Nature Reviews Molecular Cell Biology *2*, 731-737.

Sherr, C.J. (2006). Divorcing ARF and p53: an unsettled case. Nature reviews *6*, 663-673.

Sun, H., Lesche, R., Li, D.-M., Liliental, J., Zhang, H., Gao, J., Gavrilova, N., Mueller, B., Liu, X., and Wu, H. (1999). PTEN modulates cell cycle progression and cell survival by regulating phosphatidylinositol 3,4,5-triphosphate and Akt/protein kinase B signaling pathway. Proc Natl Acad Sci USA *96*, 6199-6204.

Takagi, M., Absalon, M.J., McLure, K.G., and Kastan, M.B. (2005). Regulation of p53 translation and induction after DNA damage by ribosomal protein L26 and nucleolin. Cell *123*, 49-63.

Tang, E.D., Nunez, G., Barr, F.G., and Guan, K.L. (1999). Negative regulation of the forkhead transcription factor FKHR by Akt. The Journal of biological chemistry *274*, 16741-16746.

Tothova, Z., Kollipara, R., Huntly, B.J., Lee, B.H., Castrillon, D.H., Cullen, D.E., McDowell, E.P., Lazo-Kallanian, S., Williams, I.R., Sears, C.*, et al.* (2007). FoxOs are critical mediators of hematopoietic stem cell resistance to physiologic oxidative stress. Cell *128*, 325-339.

Wilson, A., Laurenti, E., Oser, G., van der Wath, R.C., Blanco-Bose, W., Jaworski, M., Offner, S., Dunant, C.F., Eshkind, L., Bockamp, E.*, et al.* (2008). Hematopoietic stem cells reversibly switch from dormancy to self-renewal during homeostasis and repair. Cell *135*, 1118-1129.

Wullschleger, S., Loewith, R., and Hall, M.N. (2006). TOR signaling in growth and metabolism. Cell *124*, 471-484.

Yalcin, S., Zhang, X., Luciano, J.P., Mungamuri, S.K., Marinkovic, D., Vercherat, C., Sarkar, A., Grisotto, M., Taneja, R., and Ghaffari, S. (2008). Foxo3 is essential for the regulation of ataxia telangiectasia mutated and oxidative stress-mediated homeostasis of hematopoietic stem cells. The Journal of biological chemistry *283*, 25692-25705.

Yilmaz, O.H., Valdez, R., Theisen, B.K., Guo, W., Ferguson, D.O., Wu, H., and Morrison, S.J. (2006). Pten dependence distinguishes haematopoietic stem cells from leukaemia-initiating cells. Nature *441*, 475-482.

You, M.J., Castrillon, D.H., Bastian, B.C., O'Hagan, R.C., Bosenberg, M.W., Parsons, R., Chin, L., and DePinho, R.A. (2002). Genetic analysis of Pten and Ink4a/Arf interactions in the suppression of tumorigenesis in mice. Proc Natl Acad Sci U S A *99*, 1455-1460.

Yuan, T.L., and Cantley, L.C. (2008). PI3K pathway alterations in cancer: variations on a theme. Oncogene *27*, 5497-5510.

Zhang, J., Grindley, J.C., Yin, T., Jayasinghe, S., He, X.C., Ross, J.T., Haug, J.S., Rupp, D., Porter-Westpfahl, K.S., Wiedemann, L.M.*, et al.* (2006). PTEN maintains

haematopoietic stem cells and acts in lineage choice and leukaemia prevention. Nature *441*, 518-522.

Zindy, F., Quelle, D.E., Roussel, M.F., and Sherr, C.J. (1997). Expression of the p16(INK4a) tumor suppressor versus other INK4 family members during mouse development and aging. Oncogene *15*, 203-211.

Zindy, F., Williams, R.T., Baudino, T.A., Rehg, J.E., Skapek, S.X., Cleveland, J.L., Roussel, M.F., and Sherr, C.J. (2003). Arf tumor suppressor promoter monitors latent oncogenic signals in vivo. Proceedings of the National Academy of Sciences of the United States of America *100*, 15930-15935.

CHAPTER 3

FIP200 IS REQUIRED FOR THE CELL-AUTONOMOUS MAINTENANCE OF FETAL HEMATOPOIETIC STEM CELLS[1]

SUMMARY

Little is known about whether autophagy is active in HSCs and whether they contribute to hematopoietic stem cell (HSC) maintenance. FIP200 plays important roles in mammalian autophagy and other cellular functions, but its role in hematopoiesis has not been examined. We found that conditional deletion of *FIP200* in hematopoietic cells led to impaired autophagy in the fetal liver, severe anemia, and perinatal lethality. FIP200 was also cell-autonomously required for the maintenance of fetal HSCs as *FIP200-*deleted HSCs were unable to reconstitute lethally irradiated recipients. *FIP200* ablation increased the rate of cell-cycling in HSCs, and *FIP200*-deleted HSCs exhibited increased mitochondrial mass and elevated reactive oxygen species levels. Our data identify FIP200 as a key intrinsic regulator of fetal HSCs and implicate a potential role for autophagy in the maintenance of fetal hematopoiesis and HSCs.

---

[1]A modified version of this work is currently in review as of June 2010 with authors listed as Liu, F., Lee, J.Y., Wei, H., Tanabe, O., Engel, J.D., Morrison, S.J., and Guan, J.L.

INTRODUCTION

Focal adhesion kinase family interacting protein of 200 kD (FIP200) was initially identified as a putative protein inhibitor of focal adhesion kinase and its related kinase Pyk2 (Ueda et al., 2000). Subsequent studies suggested that FIP200 regulates diverse cellular functions including cell size, survival, proliferation, spreading and migration through its interaction with multiple other proteins (Abbi et al., 2002; Chano et al., 2006; Gan et al., 2005; Gan et al., 2006; Melkoumian et al., 2005). FIP200 is widely expressed in various human and mouse tissues and is conserved throughout humans, mice, rats, frogs, flies and worms (Bamba et al., 2004), suggesting important functions for FIP200 throughout evolution. Consistent with this, germline deletion of *FIP200* in mice resulted in embryonic lethality at mid-to-late gestation associated with heart failure and liver degeneration (Gan et al., 2006).

Recent reports by several groups identified FIP200 as a component of the ULK-Atg13-FIP200 complex, prompting speculation that it acts as the mammalian counterpart of yeast Atg17, despite limited sequence homology. Without this complex, the ability of cells to form autophagosomes is severely impaired (Ganley et al., 2009; Hara and Mizushima, 2009; Hosokawa et al., 2009; Jung et al., 2009). Although autophagy was initially identified as a catabolic process to provide building blocks in response to starvation, it is now accepted that a basal level of autophagy occurs independently of nutrient stress which maintains cellular homeostasis. Consistent with an autophagic role for FIP200, neural-specific deletion of *FIP200* resulted in abnormal accumulation of ubiquitinated protein aggregates, increased accumulation of p62/sequestosome-1 (SQSTM1), increased apoptosis, and neurodegeneration (Hara et al., 2006; Komatsu et

al., 2006; Liang et al., 2010). It is not clear whether FIP200 or autophagy are also required for the maintenance of HSCs.

Here we report experiments in which *FIP200* was deleted from the hematopoietic system of mice through the use of Cre mediated excision. These results reveal a cell-autonomous requirement for FIP200 in fetal HSCs. Deletion of *FIP200* led to HSC depletion, loss of HSC reconstituting capacity, and a block in erythroid maturation. Within fetal HSCs, we observed an increased rate of cell cycling, increase in mitochondrial mass, and an increase in reactive oxygen species (ROS) levels. We also observed evidence for autophagic defects in fetal hematopoietic cells, consistent with a model in which impaired autophagy leads to abnormal accumulations in mitochondria and increases in ROS generation that depletes HSCs. These results illustrate the requirement for FIP200, perhaps through autophagy regulation, in the maintenance of fetal HSCs.

MATERIALS AND METHODS

Mice and blood cell counts

Floxed FIP200 and Tie2-Cre mice were described previously (Gan et al., 2006; Shen et al., 2005). Mx-1-Cre mice were obtained from The Jackson Laboratory (Bar Harbor, ME). All mice were backcrossed for at least six generations onto a C57BL/6 background. Mice were housed and handled according to local, state, and federal regulations and all experimental procedures were carried out according to the guidelines of Institutional Animal Care and Use Committee at University of Michigan. Mice genotyping for *FIP200* and *Cre* alleles were performed by PCR analysis of tail DNA, essentially as described previously (Gan et al., 2006). For analysis of blood counts, peripheral blood was collected in a heparinized microtube (SARSTEDT) and analyzed with a hematology analyzer (Advia 120 hematology system).

Protein extraction, SDS-PAGE, and Western blotting

The mouse fetal livers were collected from control or CKO mice at E14.5. The protein lysates were prepared by homogenization in CelLytic buffer (Sigma) supplemented with protease inhibitors (5 μg/ml leupeptin, 5 μg/ml aprotinin, and 1 mM phenylmethylsulfonyl fluoride). The protein extraction and western blotting procedures were performed as described previously (Liang et al., 2010).

Histology and in situ detection of apoptosis

Mice were euthanized using CO_2. E14.5 and E16.5 embryos were dissected out and fixed in freshly made, pre-chilled (4 °C) PBS-buffered formalin at 4 °C. The liver

tissues were sectioned and then embedded in paraffin, sectioned at 6 μm, and stained with hematoxylin and eosin for histological examination or left unstained for TUNEL assays. Hematoxylin and eosin stained sections were examined under a BX41 light microscope (Olympus America, Inc., Center Valley, PA), and images were captured with an Olympus digital camera (model DP70) using DP Controller software (Version 1.2.1.10 8). For TUNEL assays, fetal liver sections were deparaffinized, incubated in methanol containing 0.3% H_2O_2 for 30 min, washed, and incubated with proteinase K (20 μg/ml) in PBS for 15 min at room temperature. Apoptotic cells were detected as described in the ApopTag Peroxidase In Situ Apoptosis Detection Kit (Millipore, Billerica, MA). Sections were counterstained with methyl green.

Flow cytometry

Fetal livers were triturated with Hank's Buffered Salt Solution without calcium or magnesium, supplemented with 2% heat-inactivated bovine serum (Gibco, Grand Island, NY) and filtered through nylon screen (45 mm, Sefar America; Kansas City, MO) to obtain single cell suspensions. To examine the different lineages, whole fetal liver cells were incubated with conjugated monoclonal antibodies of lineage markers including Ter119(Ter119), B220(6B2), Mac1(M1/70), Gr1(8C5). For the analysis of erythroid maturation, whole fetal liver cells were incubated with anti-Ter119-FITC and anti-CD71-PE (BD Biosciences). For the detection of fetal liver hematopoietic stem cells, whole fetal liver cells were incubated with FITC-conjugated antibody to CD41 (MWReg30; BD PharMingen, San Diego, CA), CD48 (HM48-1; BioLegend, San Diego, CA), Ter119 (Ter119), PE conjugated antibody to CD150 (TC15-12F12.2, BioLegend), APC

104

conjugated Mac1 (M1/70), and biotin conjugated Sca1 (Ly6A/E-biotin), followed by staining with streptavidin conjugated to APC-Cy7 (Becton Dickinson, San Jose, CA). Sometimes, anti-c-Kit (2B8) was used in place of Mac1 (M1/70). Cells were resuspended in 2 µg/mL DAPI to distinguish live and dead cells.

In some experiments, BrdU (Sigma) was injected intraperitoneally into pregnant mice at 100 mg/kg 2 hrs before sacrificing the animals. BrdU staining was performed as suggested by the manufacturer. In other experiments, after labeling with various surface markers, cells were stained by MitoTracker (Invitrogen) at 20 nM for 15 min at $37^{o}C$, or by DCF-DA (Invitrogen) at 10 um for 15 min at $37^{o}C$, according to manufacturer's instructions. To detect apoptotic cells, fetal liver cells were stained with surface markers and followed by staining with DAPI and Annexin V (BD PharMingen) and Annexin V Binding Buffer as described by the manufacturer.

Blood cell staining

Dried blood smears were stained with Wright-Giemsa Stain (Sigma, WG16) as described by the manufacturer. For neutral benzidine staining, dried smears were fixed for 4 min in methanol, incubated in a 1% *o*-dianisidine (Sigma, D9143) in methanol for 2 min, and then in 0.9% H_2O_2 in 50% ethanol for 1.5 min, rinsed with water, and then air dried.

Long term competitive repopulation assay

Adult recipient mice (CD45.1) were irradiated using a Cesium137 GammaCell40 Exator Irradiator (MDS Nordia, Kanata, ON) delivering 110 rad/min in two equal doses

of 570 rad, delivered at least 2 hr apart. Cells were injected into the retro-orbital venous sinus of anesthetized recipients. Each recipient mouse received 500,000 CD45.1$^+$ bone marrow cells for radioprotection. Beginning 4 weeks after transplantation and continuing for at least 16 weeks, blood was obtained from the tail veins of recipient mice, subjected to ammonium-chloride potassium red cell lysis, and stained with directly conjugated antibodies to CD45.2 (104), B220 (6B2), Mac-1 (M1/70), CD3 (KT31.1), and Gr-1 (8C5) to monitor donor cell engraftment.

pIpC adminstration

Polyinosine-polycytidine (pIpC) (Amersham Pharmacia Biotech) was administered to mice as previously described (Yilmaz et al., 2006). Briefly, pIpC was resuspended in Dulbecco's phosphate buffered saline (D-PBS) at 50 ug/ml and mice were injected with 0.4 µg per gram of body weight every other day for 10 days.

RESULTS

FIP200 deletion leads to erythroblastic anemia and perinatal lethality

To test whether FIP200 might play a role in fetal hematopoiesis, we mated floxed FIP200 (*FIP200$^{fl/fl}$*) mice (Gan et al., 2006) with *Tie2-Cre$^+$* transgenic mice to generate *FIP200$^{fl/fl}$Tie2-Cre$^+$* mice (designated as CKO mice). *Tie2-Cre$^+$* mice express Cre recombinase in hematopoietic and endothelial cells during embryonic development (Ulyanova et al., 2005). As shown in Table 1, CKO and littermate controls (*FIP200$^{+/fl}$Tie2-Cre$^+$*, *FIP200$^{fl/fl}$*, and *FIP200$^{+/fl}$*; the latter two genotypes were used as controls in all experiments) were observed at normal Mendelian ratios at E14.5 and E16.5. There was a slight decrease in the observed fraction of CKO embryos at E17.5 and E18.5, and virtually all CKO mice died within the first week of birth.

To confirm the loss of FIP200 protein, we Western blotted protein lysates from the livers of E14.5 CKO and control embryos. A significantly reduced level of FIP200 was found in the fetal livers of CKO mice compared to control mice, indicating effective *FIP200* deletion (Fig. 3.1A). Next, we histologically examined fetal liver sections from CKO and control mice. At E14.5, no apparent differences were detected in CKO fetal liver sections as compared to control sections (Fig. 3.1B). In contrast, at E16.5 we observed robust erythropoiesis characterized by abundant sinuses filled with mature red blood cells (RBCs) in the fetal liver of control mice but not in CKO fetal liver sections, suggesting that *FIP200* deletion significantly impaired fetal erythropoiesis (Fig. 3.1B). At E18.5, we observed numerous mature RBCs within vascular structures of control fetal livers, but very few erythrocytes within vascular structures of CKO fetal livers (Fig. 3.1B). These histological features were consistent with the grossly paler appearance of

CKO fetal livers at E16.5 and E18.5 (but not E14.5) as compared to littermate control fetal livers (data not shown). Although *Tie2-Cre* is expressed in endothelial cells, we did not detect hemorrhaging or edema and immunochemical analysis also showed apparently normal vasculature density in the livers of CKO embryos (data not shown). There were no significant gross or histological defects in other major organs including the lungs and the heart in CKO embryos (Fig. 3.8). These results suggest disrupted fetal hematopoiesis as the major defect in CKO embryos.

To further characterize the consequences of defective erythropoiesis brought on by *FIP200* deletion, we analyzed the peripheral blood of CKO and control embryos at E18.5. Consistent with the reduced erythropoiesis observed in fetal livers, CKO embryos displayed dramatically reduced numbers of RBCs (Fig. 3.1C), decreased hemoglobin content (Fig. 3.1D), decreased hematocrit (Fig. 3.1E) and an elevation in the red blood cell distribution width (Fig. 3.1F) as compared to the circulating blood of control embryos, indicative of severe anemia. Analysis of the peripheral blood using the surface markers CD71 and Ter119 showed a significant decrease in frequency (Figs. 1G and 1H) and absolute number (Fig. 3.1I) of CD71^{low}Ter119^{+} mature red blood cells (R8 population) in CKO mice as compared to control mice, further confirming the presence of a profound anemia. Similar analysis of the fetal liver at E14.5 (when no histological defects were present) suggested compromised erythroid maturation in CKO embryos. We observed an increase in the frequency of immature erythroid cells (R4 population: CD71^{med}Ter119^{-} and R5 population: CD71^{high}Ter119^{-}) and a decrease in a maturing erythroid population (R6 population: CD71^{high}Ter119^{+}) in CKO embryos as compared to control embryos (Fig. 3.9). The anemia appeared to be erythroblastic as evidenced by the

significantly increased numbers of nucleated cells in the peripheral blood of E18.5 CKO mice by Wright-Giemsa staining (Fig. 3.1J). Indeed, differential counting identified 72% of the nucleated cells to be erythroblasts and 25% to be neutrophils. Erythroblast identity was further confirmed by Benzidine staining (Fig. 3.1K). Taken together, these results suggest a crucial role for FIP200 in fetal erythropoiesis and demonstrate that its loss in hematopoietic cells leads to perinatal lethality associated with severe erythroblastic anemia.

FIP200 deletion cell-autonomously leads to fetal HSC depletion

Although CKO fetal livers were histologically indistinguishable from control fetal livers at E14.5 (see Fig. 3.1B), we noted a decrease in total fetal liver cell number in CKO embryos at this stage and a more dramatic reduction at E18.5 as compared to control embryos (Fig. 3.2A). These data raised the possibility that an HSC defect might contribute to the anemia observed in CKO mice. We examined the frequency of $CD150^+CD48^-Lin^-Mac-1^+Sca-1^+$ cells in the E14.5 fetal liver of CKO and control mice. These cells include all fetal liver HSC activity and are highly enriched for HSCs (Kim et al., 2006). As shown in Figs. 2B and 2C, the frequency of immunophenotypic HSCs was 6-fold lower in CKO fetal livers as compared to control samples. Coupled with the overall decrease in fetal liver cellularity in CKO embryos, the absolute number of immunophenotypic HSCs was diminished roughly 10-fold in the fetal liver upon *FIP200* deletion. (Fig. 3.2D). We also confirmed this result with $CD150^+CD48^-CD41^-Lin^-c-Kit^+Sca-1^+$ HSCs (data not shown).

To address whether FIP200 loss impaired fetal HSC function and to exclude the possibility that HSCs simply changed their immunophenotype after *FIP200* deletion, we functionally assessed the repopulating capacity of fetal liver cells from CKO mice *in vivo*. Competitive reconstitution experiments were performed in which 200,000 E14.5 fetal liver cells from CD45.2[+] CKO or CD45.2[+] control donors were coinjected with 500,000 young adult bone marrow cells from congenic CD45.1[+] mice into lethally irradiated CD45.1[+] recipients (Fig 3A). We tracked donor cell reconstitution by analyzing the blood of recipients 4, 8, and 16 weeks after transplantation. Consistent with the relatively high proliferative potential of fetal liver cells (Morrison et al., 1995), 200,000 control fetal liver cells competed slightly better than 500,000 adult bone marrow cells in reconstituting the peripheral blood (Fig. 3.3B), and contributed to the myeloid, B cell and T cell lineages (Figs. 3C) throughout the length of the experiment. In contrast, *FIP200-*null fetal liver cells failed in multilineage reconstitution in all of the recipients, suggesting that FIP200 is indispensable for the repopulating ability of fetal HSCs.

Although these transplantation results were consistent with HSC maintenance defects *in vivo*, it was possible that the failure of fetal liver cells from CKO mice to repopulate recipients was due to their inability to home to the bone marrow after transplantation. Moreover, other extrinsic mechanisms could account for the failure of CKO cells in transplantation. For example, *FIP200* deletion in endothelial cells (as *Tie2-Cre* is also expressed in this tissue) could potentially cause irreversible damage to fetal HSCs by disrupting an important endothelial niche, which have been suggested, at least for adult HSCs (Butler et al.; Kiel and Morrison, 2006; Kiel et al., 2005). Even though no apparent defects in vascular development were observed in CKO mice, we nevertheless

wished to test these possibilities and to this end we generated mice from which we could inducibly delete *FIP200* in hematopoietic cells (*FIP200$^{fl/fl}$Mx-1-Cre$^+$* mice). We performed similar transplantation experiments as above by transplanting 200,000 fetal liver cells from E14.5 CD45.2$^+$ *FIP200$^{fl/fl}$Mx-1-Cre$^+$* or CD45.2$^+$ *FIP200$^{fl/fl}$* embryos along with 500,000 young adult bone marrow cells from congenic CD45.1$^+$ mice into lethally irradiated CD45.1$^+$ recipients (Fig. 3.4A). In one group of recipients, we administered 5 doses of polyinosine-polycytidine (pIpC) every other day to induce deletion of *FIP200* in transplanted cells from the *FIP200$^{fl/fl}$Mx-1-Cre$^+$* donors five days after transplantation, which is sufficiently long enough for homing (Kim et al., 2007b). The peripheral blood was then analyzed 4 to 18 weeks after transplantation to monitor donor cell reconstitution. Control donor cells successfully reconstituted all recipient mice in all lineages throughout the length of the experiment (Fig. 3.4B-C). In contrast, we noted a significantly reduced reconstitution in all lineages by *FIP200$^{fl/fl}$Mx-1-Cre$^+$* donor cells starting 4 weeks after transplantation. By 18 weeks, there was a complete loss of donor cell reconstitution from *FIP200$^{fl/fl}$Mx-1-Cre$^+$* cells in all hematopoietic lineages (Figs. 4B-C). Interestingly, we noticed that B-cell reconstitution by *FIP200$^{fl/fl}$Mx-1-Cre$^+$* cells decreased more gradually than myeloid cell reconstitution, suggesting that HSCs were particularly sensitive to *FIP200* deletion since myeloid cells are much shorter lived and must be regenerated frequently. In a second group of recipients, mice were not treated with pIpC and their peripheral blood was analyzed at 4 weeks after transplantation. Donor cell reconstitution levels from *FIP200$^{fl/fl}$Mx-1-Cre$^+$* cells (in the absence of Cre recombinase induction) were roughly equal to that of control cells at 4 weeks after transplantation (Fig. 3.4D), suggesting that reconstitution defects observed in

111

pIpC-treated *FIP200$^{fl/fl}$Mx-1-Cre$^+$* donor cells was indeed due to induced *FIP200* deletion.

Taken together, these results demonstrate that FIP200 is cell-autonomously required for the maintenance of fetal HSCs. This requirement is consistent with the phenotypic reduction in HSC frequency and number in E14.5 CKO embryos, prior to the onset of severe anemia, and with the functional defects in reconstitution ability of FIP200-deficient HSCs. It is likely that the loss of fetal HSC activity contributed significantly to the perinatal lethality and anemia in CKO mice.

Increased HSC cycling and myeloid expansion after *FIP200* deletion

Our previous studies showed that *FIP200* deletion led to increased apoptosis in several cell types in germline and conditional knockout mice (Gan et al., 2006; Liang et al., 2010). Thus, we wondered if increased apoptosis of HSCs upon *FIP200* deletion led to the depletion of HSCs in CKO mice. We measured apoptosis of fetal liver cells in CKO and control embryos at E14.5 and E16.5 by performing terminal deoxynucleotidyl transferase dUTP nick end labeling (TUNEL) assays on fetal liver sections. Low levels (~5%) of apoptotic cells were observed in the livers of both CKO and control embryos (Fig. 3.5A). These results were further confirmed in E14.5 fetal liver cells by staining for annexin V and analyzing by flow cytometry (Fig. 3.5B). We also examined CD150$^+$CD48$^-$CD41$^-$Lin$^-$c-Kit$^+$Sca-1$^+$ HSC cell death at E14.5 by annexin V staining and found that the levels of apoptosis in both CKO and control HSCs were, on average, comparably lower than in unfractionated fetal liver cells (Fig. 3.5C). These results suggest that *FIP200* deletion in hematopoietic cells did not appreciably increase

apoptosis of either unfractionated fetal liver cells or HSCs and that HSC depletion in CKO mice may not be caused by increased cell death.

We also evaluated the effect of *FIP200* deletion on the proliferation of CD150$^+$CD48$^-$CD41$^-$Lin$^-$c-Kit$^+$Sca-1$^+$ HSCs by BrdU incorporation assays. BrdU was administered intraperitoneally into pregnant mothers carrying E14.5 embryos two hours before sacrificing animals for analysis. Following this short pulse, we noted a slightly lower level of BrdU incorporation in the unfractionated fetal liver cells of CKO embryos compared to control embryos (Fig. 3.6A). Interestingly, a significant increase in BrdU incorporation was detected in FIP200-null HSCs ($37.3 \pm 9.9\%$) compared to control HSCs ($24.3 \pm 3.3\%$). These results suggest that FIP200 is required for cell cycle regulation in fetal HSCs.

Although HSC cycling was increased in FIP200-deficient animals, HSC number and function was depleted and an increase in cell death was not detectable. Therefore, FIP200-deficient HSCs were rapidly exiting the stem cell pool by other mechanisms. One mechanism by which increased cycling could immediately deplete HSCs is by tipping the balance towards differentiation at the expense of self-renewal. Therefore, we sought to examine the different lineages that were produced in E14.5 control and CKO fetal livers by flow cytometry. While slight changes were found for erythroid and B-cell lineages, a dramatic increase in the myeloid lineage (4-fold) was detected in the CKO fetal liver as compared to control mice (Fig. 3.6C). Despite the decrease in overall liver cellularity (see Fig. 3.2A) there was an increase in the absolute number of myeloid cells in CKO fetal livers compared to that of control fetal livers (Fig. 3.6D). The increase in frequency and absolute number of myeloid cells suggested that myelopoiesis was enhanced in the fetal

liver of CKO mice. Consistent with this, Wright-Giemsa staining of peripheral blood from E18.5 embryos displayed an increased presence of neutrophils in CKO embryos as compared to control embryos (Fig. 3.6E). Further analysis of the peripheral blood by flow cytometry indicated a 17-fold increase in Mac-1$^+$Gr-1$^+$ frequency (from about 0.03% to 0.52%) and an 8-fold increase in the number of Mac-1$^+$Gr-1$^+$ cells per microliter in CKO embryos as compared to control embryos (Fig. 3.6F). Taken together, these data demonstrate a significant expansion in the myeloid lineage in CKO mice.

Autophagy is disrupted in FIP200-deleted hematopoietic cells and mitochondrial mass and ROS levels increase in HSCs

Several recent studies identified FIP200 as an essential component of the ULK1-Atg13-FIP200 complex, which is involved in the generation of autophagosomes (Hara and Mizushima, 2009; Hara et al., 2008; Hosokawa et al., 2009; Jung et al., 2009; Nishida et al., 2009). Autophagy is thought to mediate the clearance of damaged and/or excess organelles including mitochondria, which are a major source of intracellular ROS (Beckman and Ames, 1998; Cumming et al., 2001; Ito et al., 2004). While normal HSCs contain low levels of ROS, an abnormal increase of ROS has been associated with increased cell cycle progression and depletion of adult HSCs (Chen et al., 2008; Ito et al., 2006; Tothova et al., 2007). Therefore, we investigated the possibility that autophagic defects in hematopoietic cells after *FIP200* deletion would cause an accumulation of mitochondria and increased ROS levels.

Consistent with a defect in autophagy, we observed an accumulation of p62/SQSTM1, a selective substrate for autophagy, in CKO fetal liver cells as compared

to control cells (Fig. 3.7A). Moreover, we observed an increase in mitochondrial mass in E14.5 CKO fetal liver cells as compared to control cells by staining cells with the cell-permeant MitoTracker Green probe and analyzing by flow cytometry (Fig. 3.7B). Lastly, we detected a 50% increase in ROS levels in CKO fetal liver cells by 2'-7'-dichlorofluorscein diacetate (DCFDA) staining (Fig. 3.7C), consistent with a model in which impaired autophagic clearance led to the accumulation of mitochondria and increased ROS levels. We also observed that mitochondrial mass (Fig. 3.7D) and ROS levels (Fig. 3.7E) increased in Mac-1$^+$Gr-1$^+$ cells in the E14.5 CKO fetal liver as compared to controls. Importantly, we detected greater increases in both mitochondrial content (Fig. 3.7F) and ROS levels (Fig. 3.7G) in E14.5 CKO fetal CD150$^+$CD48$^-$CD41$^-$ Lin$^-$c-Kit$^+$Sca-1$^+$ HSCs as compared to control fetal HSCs. Taken together, these results suggest that *FIP200* deletion results in the increased mitochondrial mass, perhaps through impaired mitochondrial autophagy, and thus results in increased ROS levels in hematopoietic cells, which could contribute to the various hematopoietic deficiencies in CKO embryos.

DISCUSSION

Compared to what is known about the regulation of adult HSCs (He et al., 2009), relatively little is known about the pathways that regulate fetal HSC maintenance. Here, we present data showing that deletion of *FIP200* in hematopoietic cells resulted in the depletion of fetal HSCs in a cell-autonomous manner. Decreased fetal liver cellularity was observed in CKO mice as early as E14.5 and hematopoietic perturbations became progressively worse, resulting in a profound anemia and the death of virtually all CKO mice by 1 week of age. A massive decrease in fetal HSC frequency and number was also found in CKO embryos. Fetal liver cells from CKO embryos completely lost their long-term multilineage reconstitution capacity when transplanted into wild-type recipient mice. We confirmed an intrinsic requirement for FIP200 in fetal HSCs by demonstrating HSC depletion in transplantation experiments where *FIP200* was deleted from donor cells after transplantation.

The mechanisms by which inactivation of FIP200 led to fetal HSC depletion are still not clear. Although *FIP200* deletion has been shown to increase apoptosis of cardiomyocytes, hepatocytes and neurons in previous studies (Gan et al., 2006; Liang et al., 2010), we were unable to detect increased cell death in CKO fetal HSCs. We did not find a decrease in the proliferation of fetal HSCs compared to the control HSCs, indicating that HSC depletion was not caused by reduced entry into cell-cycle. In fact, we actually observed a significant increase in the proliferation of *FIP200*-null fetal HSCs compared to control HSCs. At this point, we are unable to distinguish whether FIP200 deletion leads to the loss of fetal HSC quiescence or whether the increased cycling we observed was secondary to the dramatic reduction of fetal hematopoiesis.

We observed increased ROS levels and significantly increased myelopoiesis in CKO fetal livers. Loss of FoxO transcription factors, which normally promote the expression of various antioxidant enzymes, also leads to an ROS-mediated depletion of HSCs and a mild non-lethal myeloproliferative phenotype in adult mice (Tothova et al., 2007), suggesting that increased ROS levels may be linked with myeloid expansion. Consistent with this, a recent report showed that in *Drosophila*, ROS could function in signaling, and that increasing ROS in hematopoietic progenitors beyond their basal level triggers their premature differentiation into myeloid-like cells (Owusu-Ansah and Banerjee, 2009). This raises the possibility that increased ROS levels found in *FIP200*-deleted fetal HSCs increases their differentiation towards the myeloid lineage. This is consistent with the increased cell-cycling observed in *FIP200*-deleted HSCs that leads to HSC depletion. However, at this point, we do not know whether this lineage bias acts at the level of HSCs, or whether FIP200 deletion expands a currently uncharacterized fetal myeloid progenitor population.

Similar to several recent reports implicating a role of autophagy in erythropoiesis (Kundu et al., 2008; Mortensen et al., 2010; Sandoval et al., 2008; Zhang and Ney, 2008), we observed a significant decrease in erythroid maturation in CKO fetal livers. Though to a lesser extent than fetal HSCs, mitochondrial mass was increased in unfractionated fetal liver cells (which are mostly composed of erythrocytes) of CKO mice. Based on our observations of accumulated p62/SQSTM1 in fetal liver cells, it is possible that defects in autophagy to clear mitochondria in FIP200-null erythroid cells is responsible for their compromised maturation as observed in *Atg7*-deficient mice (Mortensen et al., 2010; Zhang et al., 2009). Erythroid cells also accumulate hemoglobin as they mature and thus

are highly prone to oxidative damage. Therefore, adequate antioxidant responses are required for the maintenance of erythrocyte survival (Tsantes et al., 2006). Disruptions in these protective responses, by FoxO3 deficiency for example, increases ROS levels and shortens erythrocyte lifespan (Marinkovic et al., 2007). Both an erythroid maturation defect, and the sensitivity of erythrocytes to oxidative damage likely contribute to the anemia observed in *FIP200*-deleted embryos.

Consistent with our prior observations in neurons (Liang et al., 2010), deletion of FIP200 in hematopoietic cells also led to increased accumulation of p62/SQSTM1, indicating impaired autophagic clearance. Moreover, we also observed increased mitochondrial mass in *FIP200*-null fetal liver cells, myeloid cells, and fetal HSCs, consistent with the accumulation of damaged mitochondria in FIP200-deficient Purkinje cells as visualized directly by electron microscopy (Liang et al., 2010). Autophagy defects and the associated accumulation of mitochondria often results in a harmful increase in intracellular ROS levels (Kim et al., 2007a; Sandoval et al., 2008; Tal et al., 2009). Furthermore, increased ROS levels have also been associated with increased cell cycle progression and depletion of adult HSCs (Chen et al., 2008; Tothova et al., 2007). Our data are consistent with a model in which defective autophagy leads to mitochondrial accumulation and increased generation of toxic ROS that deplete fetal HSCs.

FIP200 is also known to have numerous binding partners and thus impacts other cellular functions beyond autophagy. Disruptions in these interactions could also contribute to the hematopoietic phenotypes in CKO mice, warranting further investigation. Nevertheless, our study identifies FIP200 as a critical cell-autonomous regulator of fetal HSCs. Our results also suggest certain similarities between adult and

fetal HSCs in that loss of quiescence and increased ROS appear to be detrimental to both stem cell populations. Given the recently described function of FIP200 in autophagy, these results also provide the first suggestion for a potential role of autophagy in HSC maintenance. While several previous studies established a role for autophagy in hematopoiesis, particularly erythropoiesis (Kundu et al., 2008; Mortensen et al., 2010; Zhang and Ney, 2008), it is possible that stem cell defects also contribute to the phenotypes described in these mice.

	FIP200$^{+/fl}$	FIP200$^{+/fl}$ Tie2-Cre$^+$	FIP200$^{fl/fl}$	FIP200$^{fl/fl}$ Tie2-Cre$^+$
E14.5	39	37	38	41
E16.5	13	9	10	12
E17.5	13	17	10	8
E18.5	39	33	38	30
P7	32	26	31	3

Table 3.1: Genotypes of progeny from crosses between male *FIP200$^{fl/fl}$Tie2-Cre$^+$* and female *FIP200$^{fl/fl}$* mice.

All genotypes were present in Mendelian ratios at E14.5 and E16.5. *FIP200$^{fl/fl}$Tie2-Cre$^+$* mice declined slightly in number at E17.5 and E18.5 and the majority of these mice were dead by 7 days after birth.
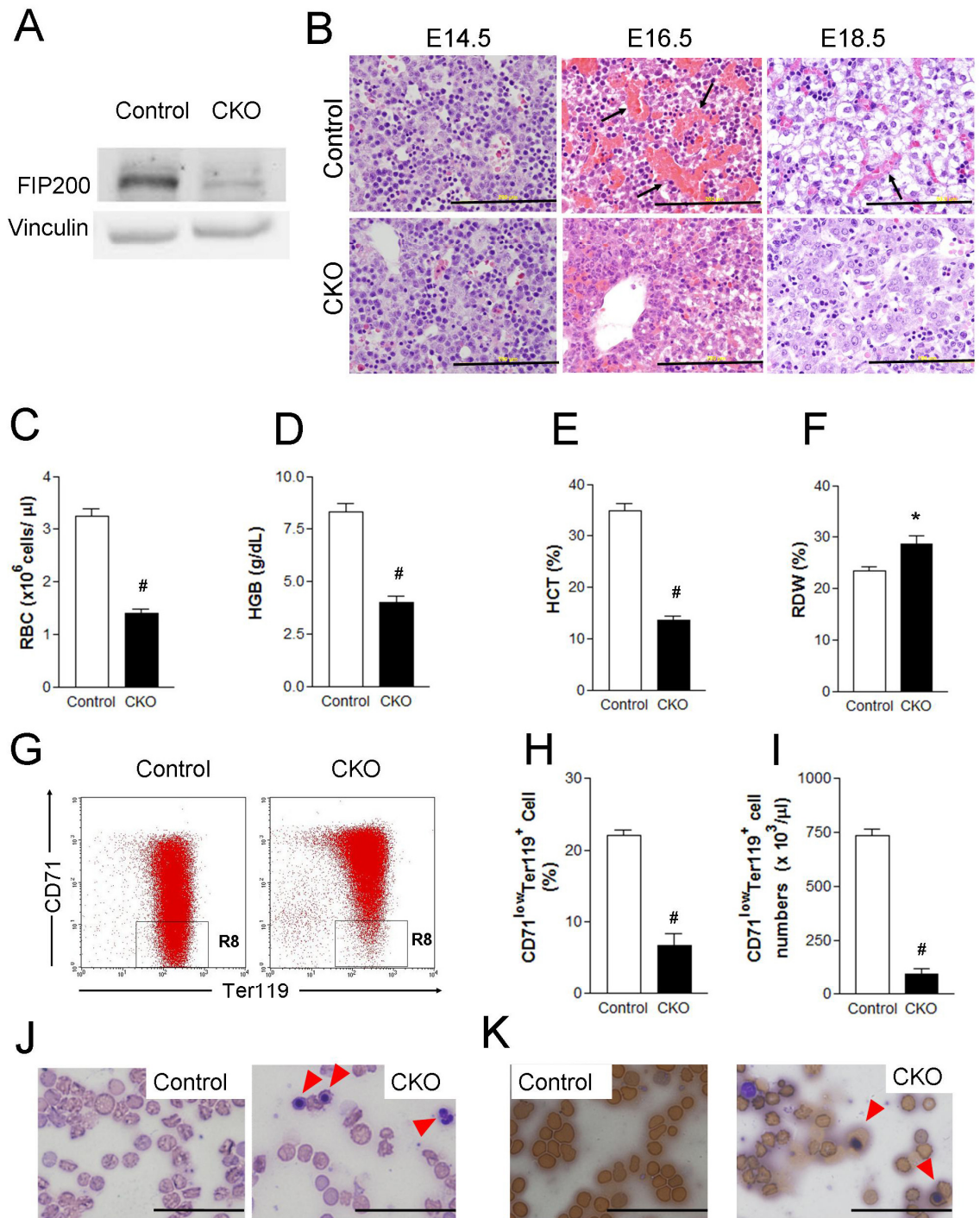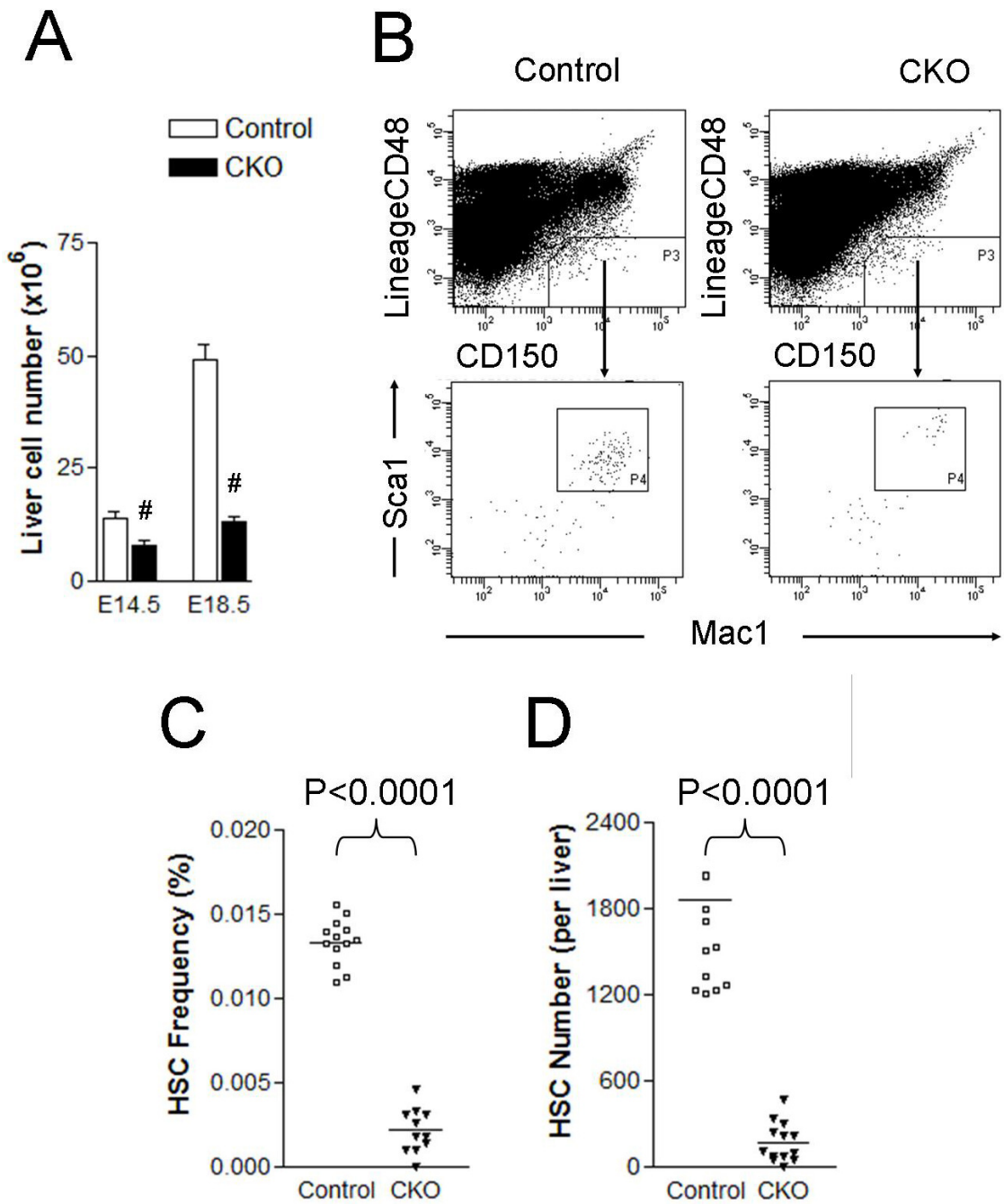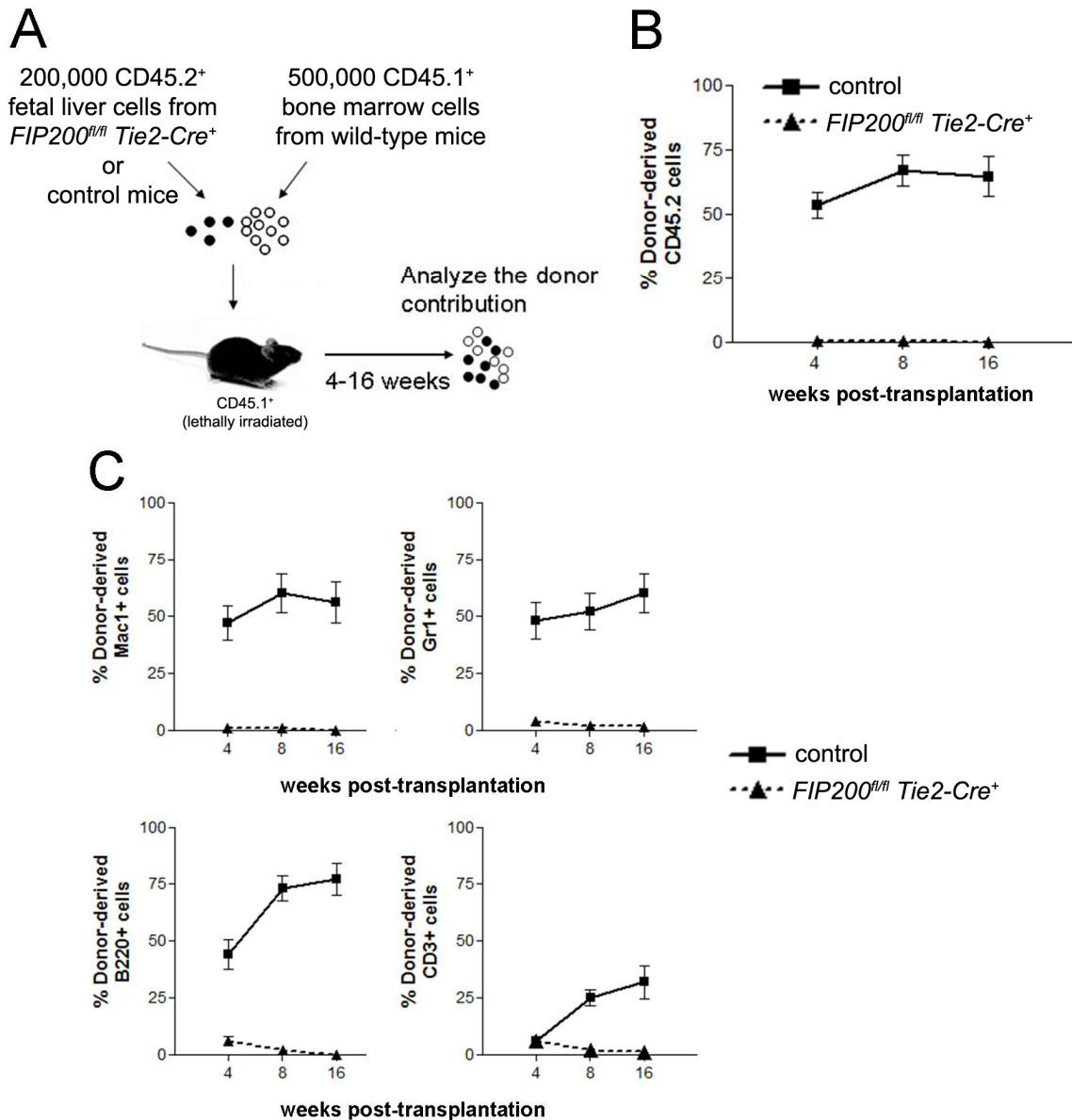
Figure 3.1

Figure 3.1: Conditional deletion of *FIP200* by Tie2-Cre results in severe anemia in developing embryos.

(A) Lysates were prepared from E14.5 livers of control or CKO mice and analyzed by Western blotting using anti-FIP200 (upper) or anti-vinculin (lower) antibodies. (B) H&E staining of E14.5, E16.5, E18.5 fetal livers from control and CKO mice. Arrows indicate enucleated red blood cells. Scale bars=200µm. (C-F) Red blood cell parameters of peripheral blood from E18.5 control and CKO mice: red blood cell numbers (C), hemoglobin (D), hematocrit (E), and red blood cell distribution width (F). n=7-17, #p<0.01, *p<0.05. Data are mean $\pm$ SE. (G) Representative FACS analysis of erythroid maturation in the peripheral blood of E18.5 control and CKO embryos. The cells were double labeled with anti-CD71 and anti-Ter119 antibodies. R8 represents the most mature population defined as $CD71^{low}Ter119^{+}$. (G) Representative flow cytometry plots showing the R8 population in control and CKO embryos. (H, I) Average values of R8 population frequency (H) and number (I) in control and CKO embryos. n=4-15, #p<0.01. Data are mean $\pm$ SE. (J) Wright-Giemsa staining of the blood smears from E18.5 control and CKO embryos. The arrowheads indicate the erythroblasts. (K) Benzidine staining of the blood smears as in (J). Arrowheads indicate the positively stained erythroblasts. Scale bars=100µm.

Figure 3.2: *FIP200* **deletion depletes fetal HSCs.**

(A) Cell numbers in E14.5 and E18.5 fetal livers of control and CKO mice. n=5-13, #p<0.01. Data are mean $\pm$ SE. (B) Representative flow cytometry plots of fetal liver cells from E14.5 control and CKO embryos. HSCs were gated as CD150$^+$CD48$^-$Lin$^-$Mac1$^+$Sca1$^+$ cells. (C, D) The frequency (C) and number (D) of fetal HSCs in control and CKO embryos shown in (B).

Figure 3.3: FIP200 is essential for the maintenance of fetal HSCs.

(A) Diagram of the competitive repopulation experimental design for data in (B) and (C). 200,000 fetal liver cells from CD45.2$^+$ control or *FIP200$^{fl/fl}$ Tie2-Cre$^+$* (CKO) mice were injected into lethally irradiated CD45.1$^+$ wild type recipients along with 500,000 CD45.1$^+$ bone marrow cells. Reconstitution of peripheral blood by donor cells was monitored for 16 weeks after transplantation. (B) Contribution of fetal liver-derived donor cells to all peripheral blood leukocytes in reconstituted mice. (C) Contribution of donor cells to the peripheral blood in different lineages, including myeloid (Mac1$^+$, Gr1$^+$), B-cell (B220$^+$), and T-cell (CD3$^+$). Data represent the average donor chimerism levels from three independent experiments with a total of 12 recipients per genotype.
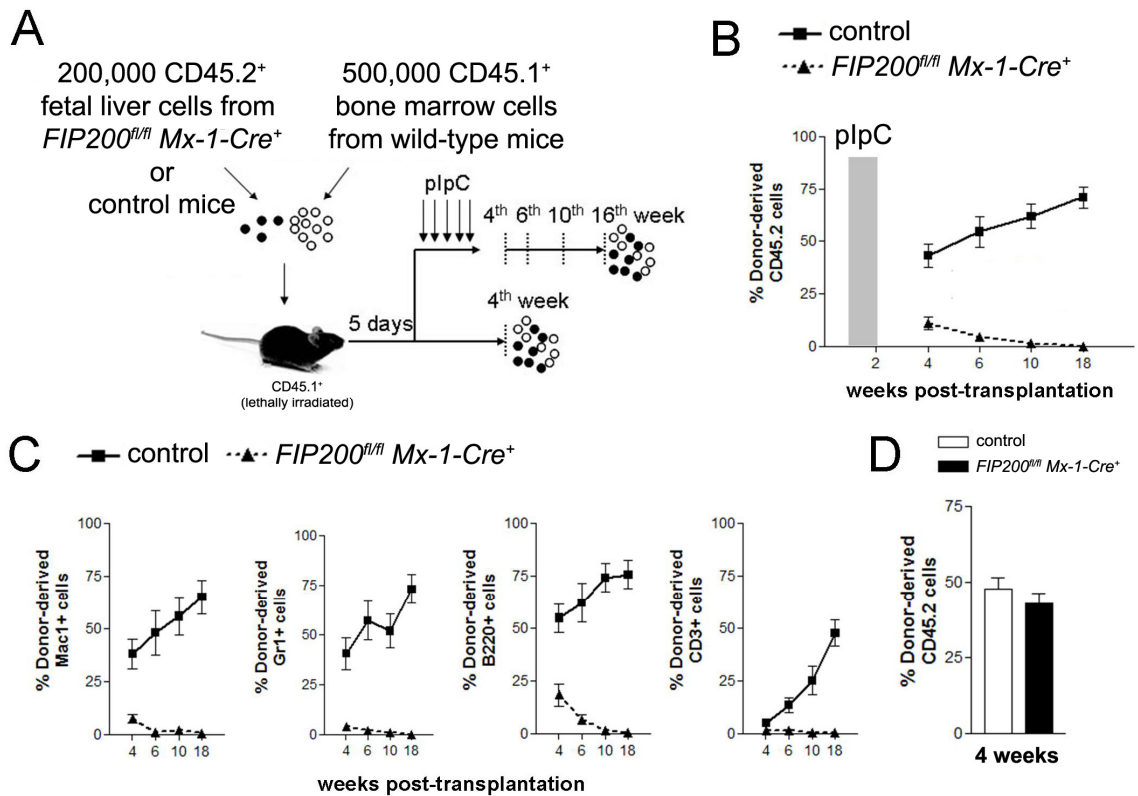
Figure 3.4: FIP200 is cell-autonomously required for the maintenance of fetal HSCs.

(A) Diagram of the competitive repopulation experimental design for data in (B) and (C). 200,000 fetal liver cells from CD45.2$^+$ *FIP200$^{fl/fl}$Mx-1-Cre$^+$* or control mice were injected into lethally irradiated CD45.1$^+$ wild type recipients along with 500,000 CD45.1$^+$ bone marrow cells. Five pIpC injections were administrated to one set of recipients every other day beginning 5 days after transplantation. Reconstitution of peripheral blood by donor cells was then monitored for an additional 16 weeks (at the 4th, 6th, 10th, and 18th weeks after transplantation). No pIpC was administrated to another set of recipients. Reconstitution of peripheral blood by donor cells was examined at the 4th week after transplantation. (B) Contribution of fetal liver-derived donor cells to all peripheral blood leukocytes in reconstituted mice in the group treated with pIpC. The shaded bar in B indicates pIpC administration. (C) Contribution of donor cells to the peripheral blood in different lineages, including myeloid (Mac1$^+$, Gr1$^+$), B-cell (B220$^+$), and T-cell (CD3$^+$) in the group treated with pIpC. (D) Contribution of donor cells to peripheral blood leucocytes in reconstituted mice in the group without pIpC treatment. Data represent the average donor chimerism levels from two independent experiments with a total of 9 recipients per genotype.
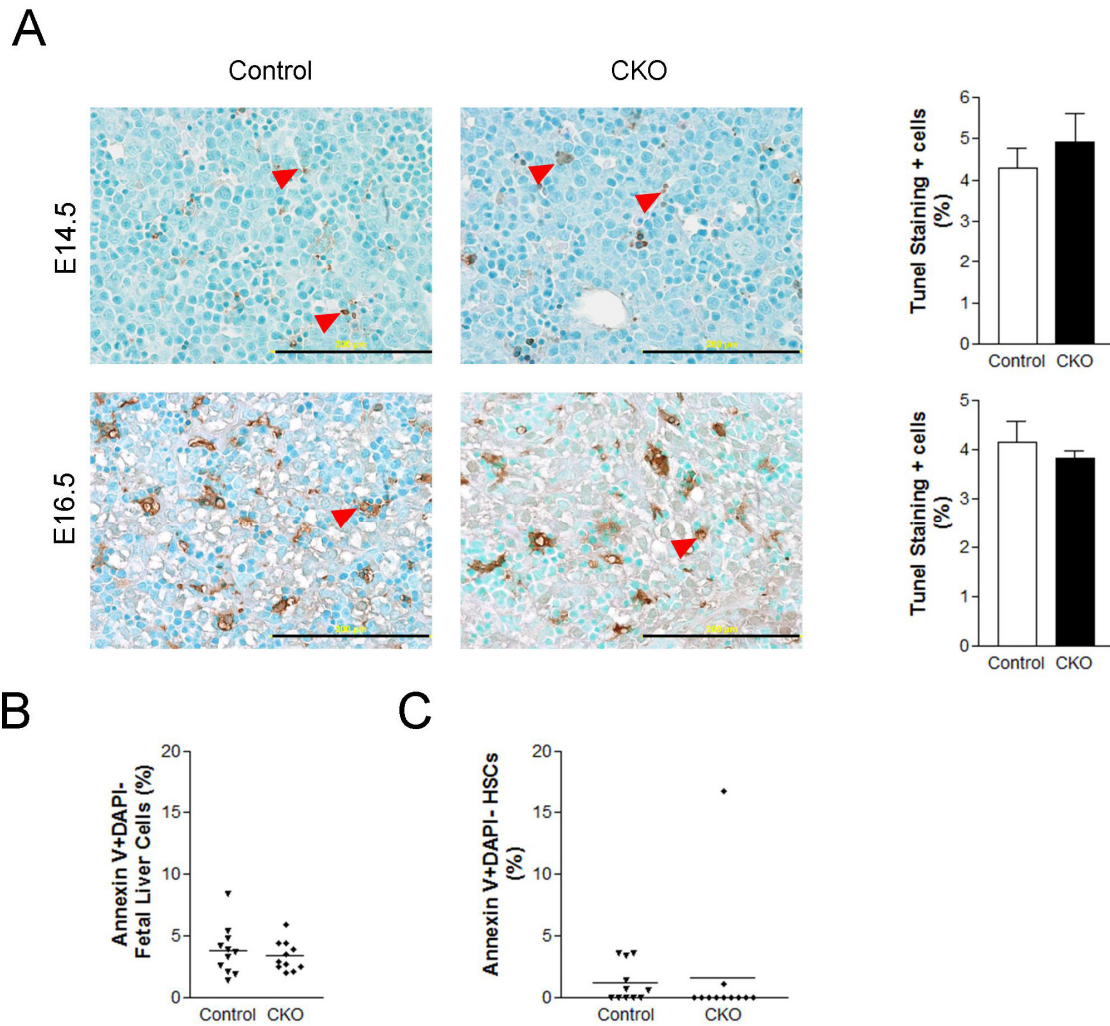
Figure 3.5: *FIP200* **deletion did not affect fetal liver cell apoptosis.**

(A) Fetal liver tissue sections from control and CKO mice at E14.5 and E16.5 were analyzed by TUNEL assays. Arrowheads indicate positively stained apoptotic cells. Graphs on the right are mean $\pm$ SE. n=4-5. Scale bars=200µm. (B, C) Annexin V labeling of fetal liver cells (B) or fetal $CD150^+CD48^-CD41^-Lin^-c\text{-}Kit^+Sca\text{-}1^+$ HSCs (C) from E14.5 control and CKO embryos. Data are mean $\pm$ SE.
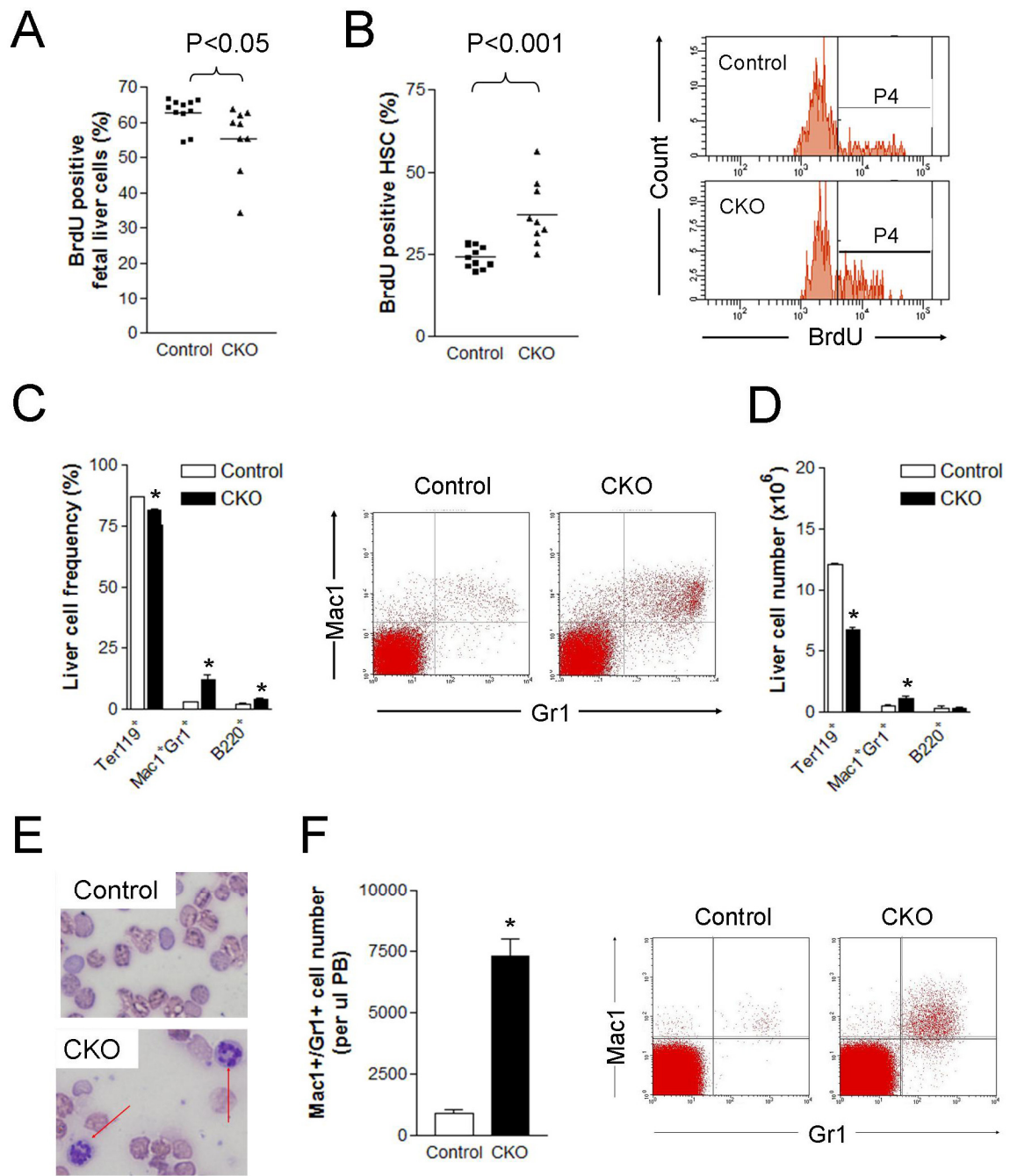
Figure 3.6

Figure 3.6: *FIP200* deletion led to increased HSC cell cycling and myeloid expansion

(A, B) The percentage of BrdU$^+$ fetal liver cells (A) and fetal CD150$^+$CD48$^-$CD41$^-$Lin$^-$c-Kit$^+$Sca-1$^+$ HSCs (B) in E14.5 control and CKO mice after a two hour BrdU pulse. Representative flow cytometry plots of fetal HSCs are shown to the right of (B). P4 represents the BrdU$^+$ population. (C, D) Frequency (C) and number (D) of fetal liver cells in various lineages from E14.5 control and CKO mice. Representative flow cytometry plots of the Mac1$^+$Gr1$^+$ population is shown to the right of (C). n=6-13, *p<0.05. Data are mean $\pm$ SE. (E) Wright-Giemsa staining of blood smears from E18.5 control and CKO embryos. The arrows indicate neutrophils. (F) Number of Mac1$^+$Gr1$^+$ cells per µl peripheral blood of E18.5 control and CKO embryos. These numbers were calculated by multiplying the frequency data obtained by flow cytometry with complete blood count data from hematology analyzer data. Representative flow cytometry plots are shown to the right of (F). n=3-15, *p<0.05. Data are mean $\pm$ SE.
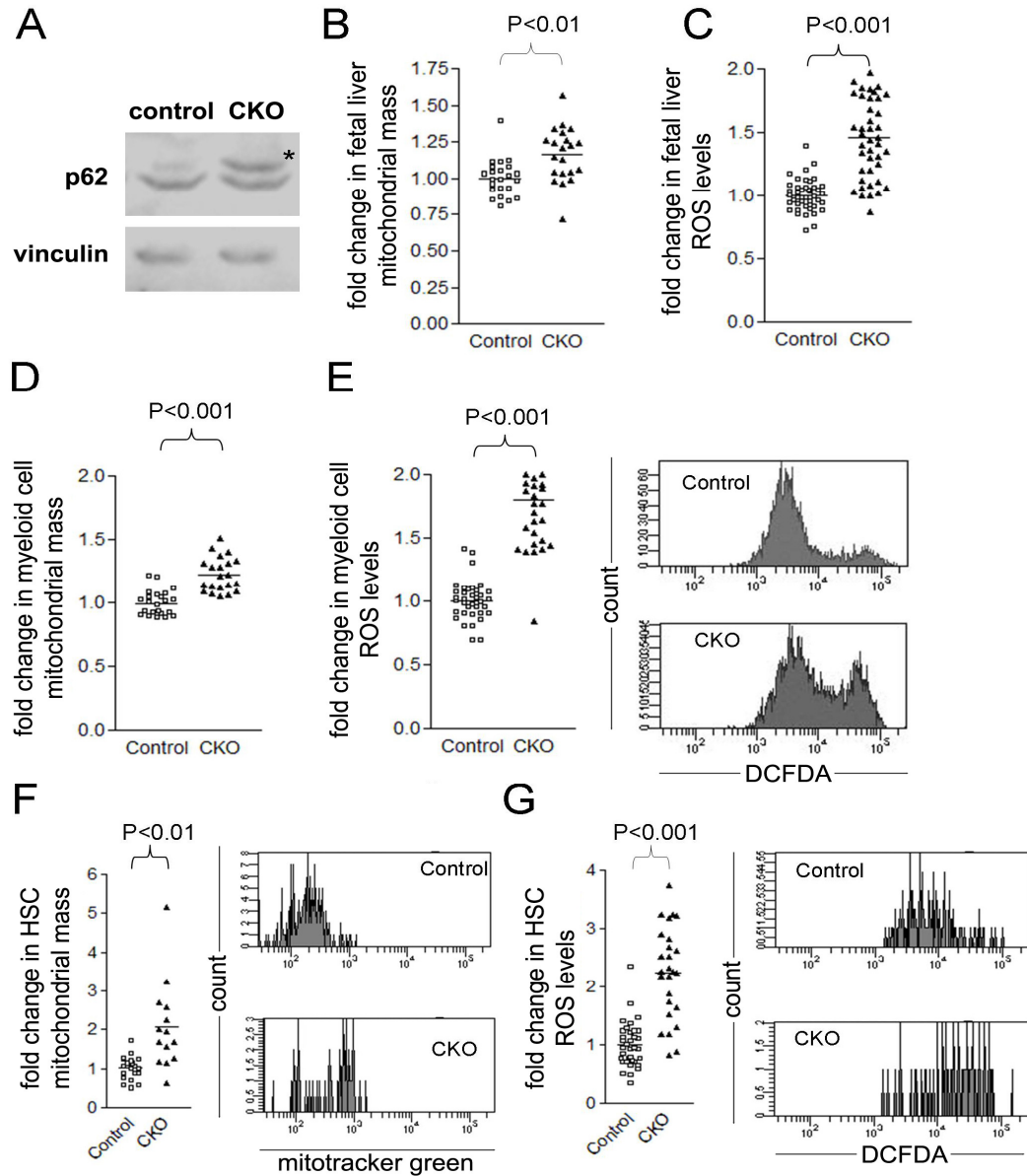
Figure 3.7: Autophagy is disrupted in FIP200-deleted hematopoietic cells and mitochondrial mass and ROS levels increase in HSCs

(A) Lysates from E14.5 liver of control or CKO mice were analyzed by Western blotting using anti-p62 (upper) or anti-vinculin (lower) antibodies. (*) indicates the p62 band. (B, C) Relative mitochondrial mass (B) and ROS levels (C) of E14.5 fetal liver cells as measured by mean fluorescence intensities of Mito-Tracker Green staining and DCFDA staining, respectively. (D, E) Relative mitochondrial mass (D) and ROS levels (E) in myeloid cells from E14.5 fetal liver. Representative flow cytometry plots of DCFDA staining are shown to the right of (E). (F, G) Relative mitochondrial mass (F) and ROS levels (G) of fetal CD150$^+$CD48$^-$CD41$^-$Lin$^-$c-Kit$^+$Sca-1$^+$ HSCs from E14.5 embryos. Representative flow cytometry plots of Mito-Tracker Green staining and DCFDA staining are shown to the right of the graphs.
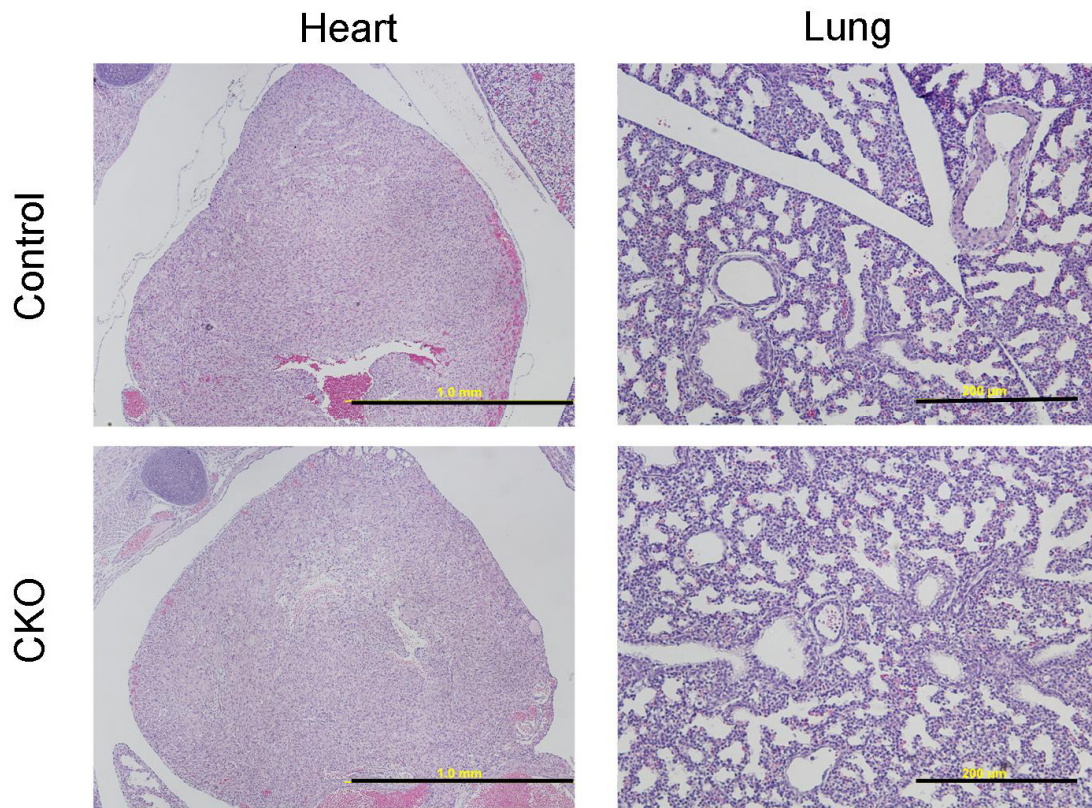
Figure 3.8: Histological analysis of fetal heart and lungs of CKO mice.

H&E staining of E18.5 fetal heart (left panels) and lung (right panels) sections from control and CKO mice. Scale bars=1 mm (left panels) and 200µm (right panels).
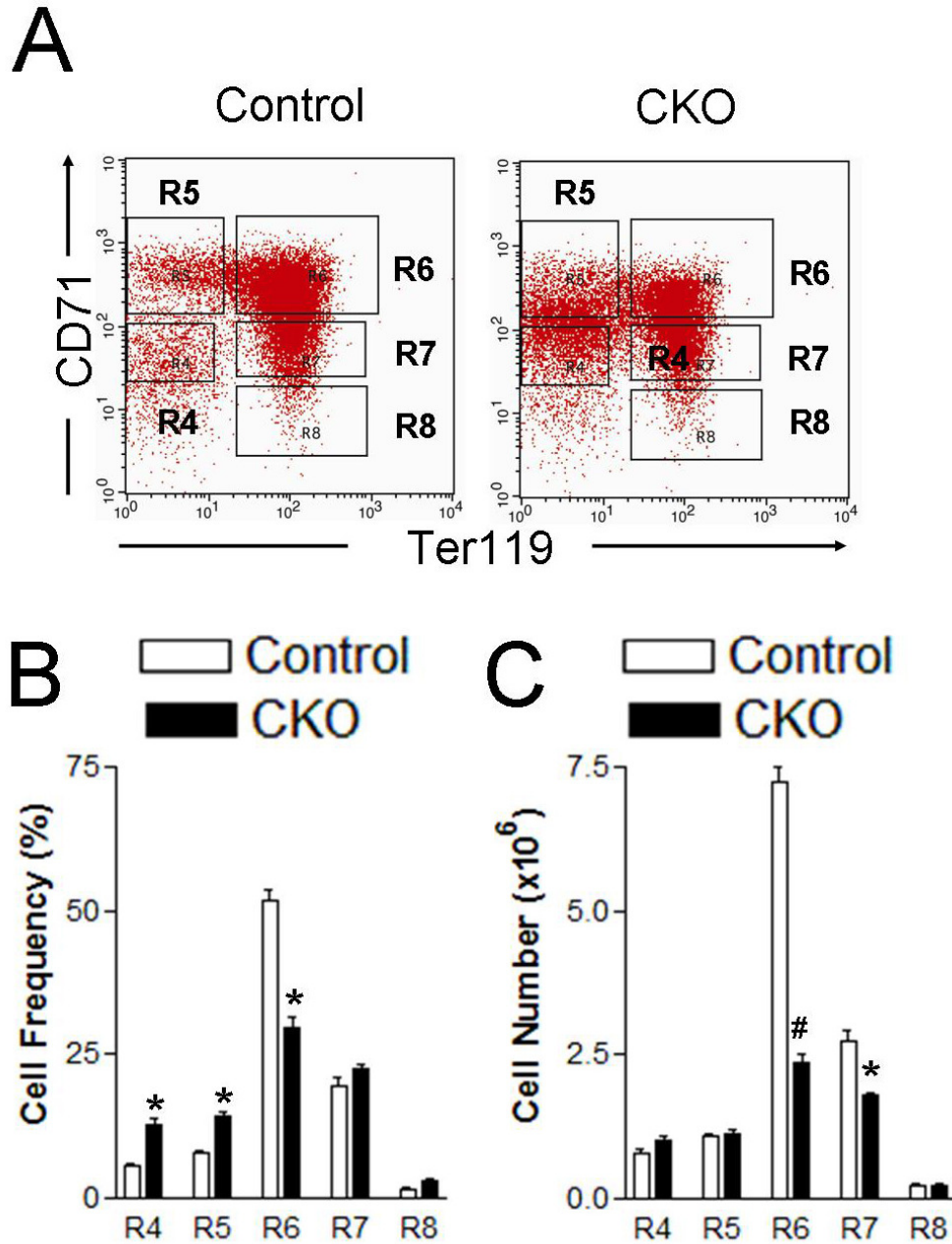
Figure 3.9: Impaired erythroid maturation in the fetal livers of CKO mice.

(A) Representative flow cytometry plot of erythroid maturation in E14.5 fetal liver of control and CKO embryos. The cells were stained for CD71 and Ter119. Regions R4 to R8 are defined by the characteristic staining pattern of cells, and represent increasingly mature populations from R4 to R8. (B, C) The cell frequency (B) and number (C) of the R4-R8 populations. Note that there were increases in immature populations (R4 and R5) and decreases in more mature populations (R6 and R7) in CKO mice. n=5-8, *p<0.05. Data are mean $\pm$ SE.

ACKNOWLEDGEMENTS

AUTHOR CONTRIBUTIONS

F.L. learned transplantation experiments, flow cytometric assessments of HSC frequency, lineage analysis, Annexin V staining, and BrdU analysis from J.Y.L, and repeated multiple replicates of these experiments initially performed by J.Y.L. Experiments characterizing the anemic phenotype were initiated by J.Y.L. and completed by F.L. All histological examinations and genotyping were performed by F.L. Both F.L. and J.Y.L. contributed to the design and interpretation of all experiments with J.L.G. and S.J.M. The paper was written by F.L., J.Y.L., and J.L.G.

BIBLIOGRAPHY

Abbi, S., Ueda, H., Zheng, C., Cooper, L.A., Zhao, J., Christopher, R., and Guan, J.L. (2002). Regulation of focal adhesion kinase by a novel protein inhibitor FIP200. Mol Biol Cell *13*, 3178-3191.

Bamba, N., Chano, T., Taga, T., Ohta, S., Takeuchi, Y., and Okabe, H. (2004). Expression and regulation of RB1CC1 in developing murine and human tissues. Int J Mol Med *14*, 583-587.

Beckman, K.B., and Ames, B.N. (1998). The free radical theory of aging matures. Physiol Rev *78*, 547-581.

Butler, J.M., Nolan, D.J., Vertes, E.L., Varnum-Finney, B., Kobayashi, H., Hooper, A.T., Seandel, M., Shido, K., White, I.A., Kobayashi, M.*, et al.* Endothelial cells are essential for the self-renewal and repopulation of Notch-dependent hematopoietic stem cells. Cell Stem Cell *6*, 251-264.

Chano, T., Saji, M., Inoue, H., Minami, K., Kobayashi, T., Hino, O., and Okabe, H. (2006). Neuromuscular abundance of RB1CC1 contributes to the non-proliferating enlarged cell phenotype through both RB1 maintenance and TSC1 degradation. Int J Mol Med *18*, 425-432.

Chen, C., Liu, Y., Liu, R., Ikenoue, T., Guan, K.L., Liu, Y., and Zheng, P. (2008). TSC-mTOR maintains quiescence and function of hematopoietic stem cells by repressing mitochondrial biogenesis and reactive oxygen species. J Exp Med *205*, 2397-2408.

Cumming, R.C., Lightfoot, J., Beard, K., Youssoufian, H., O'Brien, P.J., and Buchwald, M. (2001). Fanconi anemia group C protein prevents apoptosis in hematopoietic cells through redox regulation of GSTP1. Nat Med *7*, 814-820.

Gan, B., Melkoumian, Z.K., Wu, X., Guan, K.L., and Guan, J.L. (2005). Identification of FIP200 interaction with the TSC1-TSC2 complex and its role in regulation of cell size control. J Cell Biol *170*, 379-389.

Gan, B., Peng, X., Nagy, T., Alcaraz, A., Gu, H., and Guan, J.L. (2006). Role of FIP200 in cardiac and liver development and its regulation of TNFalpha and TSC-mTOR signaling pathways. J Cell Biol *175*, 121-133.

Ganley, I.G., Lam du, H., Wang, J., Ding, X., Chen, S., and Jiang, X. (2009). ULK1.ATG13.FIP200 complex mediates mTOR signaling and is essential for autophagy. J Biol Chem *284*, 12297-12305.

Hara, T., and Mizushima, N. (2009). Role of ULK-FIP200 complex in mammalian autophagy: FIP200, a counterpart of yeast Atg17? Autophagy *5*, 85-87.

Hara, T., Nakamura, K., Matsui, M., Yamamoto, A., Nakahara, Y., Suzuki-Migishima, R., Yokoyama, M., Mishima, K., Saito, I., Okano, H.*, et al.* (2006). Suppression of basal autophagy in neural cells causes neurodegenerative disease in mice. Nature *441*, 885-889.

Hara, T., Takamura, A., Kishi, C., Iemura, S., Natsume, T., Guan, J.L., and Mizushima, N. (2008). FIP200, a ULK-interacting protein, is required for autophagosome formation in mammalian cells. J Cell Biol *181*, 497-510.

Hosokawa, N., Hara, T., Kaizuka, T., Kishi, C., Takamura, A., Miura, Y., Iemura, S., Natsume, T., Takehana, K., Yamada, N.*, et al.* (2009). Nutrient-dependent mTORC1 association with the ULK1-Atg13-FIP200 complex required for autophagy. Mol Biol Cell *20*, 1981-1991.

Ito, K., Hirao, A., Arai, F., Matsuoka, S., Takubo, K., Hamaguchi, I., Nomiyama, K., Hosokawa, K., Sakurada, K., Nakagata, N.*, et al.* (2004). Regulation of oxidative stress by ATM is required for self-renewal of haematopoietic stem cells. Nature *431*, 997-1002.

Ito, K., Hirao, A., Arai, F., Takubo, K., Matsuoka, S., Miyamoto, K., Ohmura, M., Naka, K., Hosokawa, K., Ikeda, Y.*, et al.* (2006). Reactive oxygen species act through p38 MAPK to limit the lifespan of hematopoietic stem cells. Nat Med *12*, 446-451.

Jung, C.H., Jun, C.B., Ro, S.H., Kim, Y.M., Otto, N.M., Cao, J., Kundu, M., and Kim, D.H. (2009). ULK-Atg13-FIP200 complexes mediate mTOR signaling to the autophagy machinery. Mol Biol Cell *20*, 1992-2003.

Kiel, M.J., and Morrison, S.J. (2006). Maintaining hematopoietic stem cells in the vascular niche. Immunity *25*, 862-864.

Kiel, M.J., Yilmaz, O.H., Iwashita, T., Yilmaz, O.H., Terhorst, C., and Morrison, S.J. (2005). SLAM family receptors distinguish hematopoietic stem and progenitor cells and reveal endothelial niches for stem cells. Cell *121*, 1109-1121.

Kim, I., He, S., Yilmaz, O.H., Kiel, M.J., and Morrison, S.J. (2006). Enhanced purification of fetal liver hematopoietic stem cells using SLAM family receptors. Blood *108*, 737-744.

Kim, I., Rodriguez-Enriquez, S., and Lemasters, J.J. (2007a). Selective degradation of mitochondria by mitophagy. Arch Biochem Biophys *462*, 245-253.

Kim, I., Saunders, T.L., and Morrison, S.J. (2007b). Sox17 dependence distinguishes the transcriptional regulation of fetal from adult hematopoietic stem cells. Cell *130*, 470-483.

Komatsu, M., Waguri, S., Chiba, T., Murata, S., Iwata, J., Tanida, I., Ueno, T., Koike, M., Uchiyama, Y., Kominami, E.*, et al.* (2006). Loss of autophagy in the central nervous system causes neurodegeneration in mice. Nature *441*, 880-884.

Kundu, M., Lindsten, T., Yang, C.Y., Wu, J., Zhao, F., Zhang, J., Selak, M.A., Ney, P.A., and Thompson, C.B. (2008). Ulk1 plays a critical role in the autophagic clearance of mitochondria and ribosomes during reticulocyte maturation. Blood *112*, 1493-1502.

Liang, C.C., Wang, C., Peng, X., Gan, B., and Guan, J.L. (2010). Neural-specific deletion of FIP200 leads to cerebellar degeneration caused by increased neuronal death and axon degeneration. J Biol Chem *285*, 3499-3509.

Marinkovic, D., Zhang, X., Yalcin, S., Luciano, J.P., Brugnara, C., Huber, T., and Ghaffari, S. (2007). Foxo3 is required for the regulation of oxidative stress in erythropoiesis. J Clin Invest *117*, 2133-2144.

Melkoumian, Z.K., Peng, X., Gan, B., Wu, X., and Guan, J.L. (2005). Mechanism of cell cycle regulation by FIP200 in human breast cancer cells. Cancer Res *65*, 6676-6684.

Morrison, S.J., Hemmati, H.D., Wandycz, A.M., and Weissman, I.L. (1995). The purification and characterization of fetal liver hematopoietic stem cells. Proc Natl Acad Sci U S A *92*, 10302-10306.

Mortensen, M., Ferguson, D.J., Edelmann, M., Kessler, B., Morten, K.J., Komatsu, M., and Simon, A.K. (2010). Loss of autophagy in erythroid cells leads to defective removal of mitochondria and severe anemia in vivo. Proc Natl Acad Sci U S A *107*, 832-837.

Nishida, Y., Arakawa, S., Fujitani, K., Yamaguchi, H., Mizuta, T., Kanaseki, T., Komatsu, M., Otsu, K., Tsujimoto, Y., and Shimizu, S. (2009). Discovery of Atg5/Atg7-independent alternative macroautophagy. Nature *461*, 654-658.

Owusu-Ansah, E., and Banerjee, U. (2009). Reactive oxygen species prime Drosophila haematopoietic progenitors for differentiation. Nature *461*, 537-541.

Sandoval, H., Thiagarajan, P., Dasgupta, S.K., Schumacher, A., Prchal, J.T., Chen, M., and Wang, J. (2008). Essential role for Nix in autophagic maturation of erythroid cells. Nature *454*, 232-235.

Shen, T.L., Park, A.Y., Alcaraz, A., Peng, X., Jang, I., Koni, P., Flavell, R.A., Gu, H., and Guan, J.L. (2005). Conditional knockout of focal adhesion kinase in endothelial cells reveals its role in angiogenesis and vascular development in late embryogenesis. J Cell Biol *169*, 941-952.

Tal, M.C., Sasai, M., Lee, H.K., Yordy, B., Shadel, G.S., and Iwasaki, A. (2009). Absence of autophagy results in reactive oxygen species-dependent amplification of RLR signaling. Proc Natl Acad Sci U S A *106*, 2770-2775.

Tothova, Z., Kollipara, R., Huntly, B.J., Lee, B.H., Castrillon, D.H., Cullen, D.E., McDowell, E.P., Lazo-Kallanian, S., Williams, I.R., Sears, C.*, et al.* (2007). FoxOs are critical mediators of hematopoietic stem cell resistance to physiologic oxidative stress. Cell *128*, 325-339.

Tsantes, A.E., Bonovas, S., Travlou, A., and Sitaras, N.M. (2006). Redox imbalance, macrocytosis, and RBC homeostasis. Antioxid Redox Signal *8*, 1205-1216.

Ueda, H., Abbi, S., Zheng, C., and Guan, J.L. (2000). Suppression of Pyk2 kinase and cellular activities by FIP200. J Cell Biol *149*, 423-430.

Ulyanova, T., Scott, L.M., Priestley, G.V., Jiang, Y., Nakamoto, B., Koni, P.A., and Papayannopoulou, T. (2005). VCAM-1 expression in adult hematopoietic and nonhematopoietic cells is controlled by tissue-inductive signals and reflects their developmental origin. Blood *106*, 86-94.

Yilmaz, O.H., Valdez, R., Theisen, B.K., Guo, W., Ferguson, D.O., Wu, H., and Morrison, S.J. (2006). Pten dependence distinguishes haematopoietic stem cells from leukaemia-initiating cells. Nature *441*, 475-482.

Zhang, J., and Ney, P.A. (2008). NIX induces mitochondrial autophagy in reticulocytes. Autophagy *4*, 354-356.

Zhang, J., Randall, M.S., Loyd, M.R., Dorsey, F.C., Kundu, M., Cleveland, J.L., and Ney, P.A. (2009). Mitochondrial clearance is regulated by Atg7-dependent and - independent mechanisms during reticulocyte maturation. Blood *114*, 157-164.

CHAPTER 4

CONCLUSION

This dissertation investigates the function of signaling pathways in HSC maintenance. Chronic activation of the PI-3kinase/Akt/mTOR pathway by genetic *Pten* ablation resulted in HSC depletion through the induction of a tumor suppressor response involving p16$^{\text{Ink4a}}$ and p53 in HSCs. Loss of FIP200 resulted in the rapid depletion of fetal HSCs, potentially due to autophagic defects that resulted in an accumulation of mitochondria that increased ROS levels in HSCs.

The results in Chapter 2 demonstrated that a tumor suppressor response was activated in hematopoietic cells after *Pten* deletion. In unfractionated spleen cells, the levels of p19$^{\text{Arf}}$, p53, and p21$^{\text{Cip1}}$ increased after *Pten* deletion in a manner dependent on activated mTOR signaling, but p16$^{\text{Ink4a}}$ was not induced. This tumor suppressor response was activated in order to suppress the development of leukemias, as further loss of p19$^{\text{Arf}}$, p16$^{\text{Ink4a}}$/p19$^{\text{Arf}}$, or p53 (but not p16$^{\text{Ink4a}}$) accelerated *Pten*-deleted leukemogenesis. Interestingly, a similar but slightly different tumor suppressor response was also activated in HSCs. Specifically, p16$^{\text{Ink4a}}$ and p53 was induced in *Pten*-deleted HSCs, although p19$^{\text{Arf}}$ was not. Consistent with this, further deleting p16$^{\text{Ink4a}}$, p16$^{\text{Ink4a}}$/p19$^{\text{Arf}}$, or p53 (but not p19$^{\text{Arf}}$) prolonged the reconstituting capacity of *Pten*-deleted HSCs. The restoration of reconstituting potential appeared to function at the level of HSCs, as p16$^{\text{Ink4a}}$ or p53

deficiency reversed the depletion of *Pten*-deleted HSCs in primary recipients. These data are in contrast to observations that after *Pten* deletion, FoxO transcription factors are not inactivated, ROS levels do not increase, and NAC fails to rescue HSC function. Therefore, these results demonstrate there are multiple distinct mechanisms by which increased PI-3kinase pathway signaling can lead to stem cell depletion, including an mTOR-mediated tumor suppressor response that occurs in HSCs after *Pten* deletion.

Pten and FoxO transcription factors

The results in Chapter 2 raise many questions for the future. For example, why are FoxO transcription factors not inactivated in *Pten*-deleted HSCs, despite increased Akt activation? One possibility is that the physiologic level of Akt activation after *Pten* deletion is not sufficient to induce significant FoxO inactivation. Consistent with this possibility, we were able to observe cytoplasmic sequestration and decreases in FoxO3a levels in HSCs that were stimulated with SCF and TPO *in vitro*, but not in HSCs obtained freshly from mice. Furthermore, phosphorylation by Akt only represents a fraction of the regulatory inputs that modulate the activities of FoxOs. Many other kinases also negatively regulate FoxOs by phosphorylation, and FoxOs are also subject to regulation by acetylation and ubiquitylation (Tothova and Gilliland, 2007; van der Horst and Burgering, 2007). A second non-mutually exclusive possibility is that other signals that also regulate FoxO function simply override the increased activation of Akt found in *Pten*-deleted HSCs. For example, the stabilization and activation of FoxOs by stress signals through Jun N-terminal kinase (JNK) or the sirtuin SIRT1 are thought to be more influential than inactivation by pro-survival signals through Akt (Brunet et al., 2004;

Wang et al., 2005). Therefore, instead of *Pten* deletion resulting in the inactivation of FoxOs, it is possible that stressful stimuli activate FoxOs in *Pten*-deleted HSCs in an attempt to confer stress resistance (including resistance to oxidative stress) to HSCs after *Pten* deletion. This may help to explain why ROS levels were increased in *Pten*-deleted T-cells but not in HSCs. The activation of stress resistance pathways may simply be more robust in HSCs than in lymphocytes. It is currently unknown whether such stress signaling pathways are activated in *Pten*-deleted HSCs, but inactivation of these pathways might result in demonstrable FoxO exclusion from the nucleus, much more rapid depletion of HSCs, perhaps with dramatic elevations in ROS levels.

HSC fates after inducing a tumor suppressor response

The activation of some combination of p16^{Ink4a}, p19^{Arf}, and/or p53 has now been genetically demonstrated to deplete multiple stem cell populations in a variety of settings including *Bmi-1* deficiency (Akala et al., 2008; Molofsky et al., 2005; Oguro et al., 2006), *Hmga2* deficiency (Nishino et al., 2008), physiologic aging (Janzen et al., 2006; Krishnamurthy et al., 2006; Molofsky et al., 2006), and *Cited2* deficiency (Kranc et al., 2009). After *Pten*-deletion, both p16^{Ink4a} and p53 are induced through activation of mTOR signaling. However, in all of these examples, it is still unclear exactly what happens to HSCs or neural stem cells upon activation of tumor suppressor pathways. Two of the most common consequences of tumor suppressor activation: senescence and apoptosis, have been reproducibly demonstrated in non stem cell populations, but current evidence is lacking that these fates are assumed by stem cells *in vivo*. Part of this may be reflected in the insensitivity of assays used to detect these events. In the case of *Pten*

139

deletion, HSCs are depleted over weeks, suggesting an asynchronous depletion such that only a small subset of HSCs undergoes cell death or senescence at any given time. Detecting rare events in a rare population may not be possible, implying that the failure to detect these events does not rigorously exclude these fates for HSCs.

Alternatively, HSCs may assume fates other than senescence or cell death upon p16^{Ink4a} or p53 induction. In support of this possibility, we have observed increased cell-cycling in *Pten*-deleted HSCs that is rescued by rapamycin treatment, but overall, these cell divisions do not maintain self-renewal, as these HSCs were lost in recipients and were unable to provide long-term multilineage reconstitution. Therefore, the combination of increased PI-3kinase/Akt/mTOR activity and the increased expression of p16^{Ink4a} or p53 in *Pten*-deleted HSCs may promote their exit from the stem cell pool, perhaps by causing them to differentiate into downstream progenitors.

This model offers a more precise definition for the term "stem-cell exhaustion" or the phenomenon of HSC depletion associated with the loss of quiescence. Examples of this phenomenon are plentiful (see Introduction), and recent evidence implicates PI-3kinase pathway activation in differentiation. BCR-ABL, which is known to potently activate the PI-3kinase pathway (Kharas and Fruman, 2005), appears to induce the differentiation of HSCs. In mice expressing BCR-ABL under inducible control of the stem cell leukemia (SCL) enhancer, the MPP:HSC ratio increases dramatically (Schemionek et al., 2010), and BCR-ABL^{+} marrow displays reduced reconstituting activity, similar to what is observed in *Pten*-deleted mice. Offering clues into which lineages may be favored by PI-3kinase/Akt-induced differentiation, transplantation of

CD34$^+$ human progenitor cells expressing constitutively active AKT results in the expansion of myeloid cells at the expense of B-lymphocytes (Buitenhuis et al., 2008).

Both p53 and p16^{Ink4a} may also play roles in the progressive restriction of self-renewal capacity as immature cells become more committed. The correlation of increasing p53 protein levels with increasing differentiation has been known for some time in human hematopoietic cells (Kastan et al., 1991). Similarly, in human umbilical cord blood, the CD34$^+$ HSC-containing fraction expresses very low levels of *p16^{INK4A}* and *p15^{INK4B}* whereas expression of these genes increases dramatically in the mature CD34$^-$ fraction (Kheradmand Kia et al., 2009). Erythroblasts cultured from human fetal liver tissue also upregulates p16^{INK4A} and p15^{INK4B} as they differentiate (Kheradmand Kia et al., 2009). In mouse embryonic stem cells, p53 directly suppresses *Nanog* expression and thus induces differentiation at the expense of self-renewal (Lin et al., 2005). This is consistent with the role of p53 in limiting the reprogramming of induced pluripotent stem (iPS) cells (Hong et al., 2009; Kawamura et al., 2009; Li et al., 2009; Marion et al., 2009; Utikal et al., 2009), although inactivation of senescence also mediates this increase in reprogramming efficiency (Banito et al., 2009). Finally, combined loss of p16^{Ink4a}, p19^{Arf}, and p53 results in increased HSC frequency and confers long-term multilineage reconstituting potential to multipotent progenitors, which are normally only capable of transient reconstitution. Thus, increased expression of p16^{Ink4a} and p53 in dividing HSCs after *Pten* deletion may deplete HSCs by reinforcing the normal maturation process of HSCs to more restricted progenitors.

Although rapamycin completely rescues *Pten*-deleted HSC depletion (Yilmaz et al., 2006), p16^{Ink4a} or p53 deficiency did not. This implies that rapamycin, in addition to

suppressing p16^{Ink4a} and p53 activation in HSCs, must also do other things to prevent HSC depletion. Genome-wide transcriptional analyses in HSCs may illuminate additional pathways that are perturbed upon *Pten*-deletion, and normalized by additional rapamycin treatment. It is possible that transcriptional programs that induce differentiation are activated. Also, pathways downstream of mTORC2 are promising candidates in mediating HSC depletion, since mTORC2 can also be indirectly inhibited by rapamycin (Sarbassov et al., 2006) and is required for the development of prostate cancer after *Pten* deletion (Guertin et al., 2009).

***Pten*-deficient leukemogenesis and therapeutic implications**

Loss of p53 and p16^{Ink4a} significantly restored *Pten*-deleted HSC function, and loss of p53 and p19^{Arf} significantly accelerated *Pten*-deleted leukemogenesis. At face value, these results suggest that leukemias might arise from rare HSC clones that manage to inactivate these tumor suppressor responses before becoming depleted. However, evidence that HSCs are the leukemic cell-of-origin is lacking, and transplantation of a non-HSC (c-Kit^{mid}CD3^{+}Lin^{-}) population can transfer T-ALL (Guo et al., 2008). Moreover, *Pten*-deletion in mature T-cells with Lck-Cre or in mature myeloid cells with LysM-Cre can give rise to lymphoid and myeloid neoplasms respectively (Suzuki et al., 2001; Yu et al., 2010). However, longer leukemic latencies are observed with Lck-Cre and LysM-Cre mediated deletion as compared to Mx-1-Cre deletion, which deletes *Pten* from all hematopoietic cells, including HSCs. Thus, it is possible that some *Pten*-deficient leukemias originate from a transformed HSC, but this does not represent the only path towards tumorigenesis.

The accumulation of p53 was involved in both the inhibition of leukemogenesis and the depletion of HSCs after *Pten* deletion. One important therapeutic implication of this observation is that attempts to suppress leukemia formation by enhancing p53 function would also have the unfortunate side effect of depleting HSCs. However, stem cells and cancer cells may exhibit differential sensitivities to p53, presenting a therapeutic window of p53 stabilization that affords tumor suppression without HSC depletion. A conceptually similar approach has been demonstrated with Pml inhibition by arsenic trioxide (Ito et al., 2008). Although maintenance of both normal HSCs and BCR-ABL leukemia-initiating cells are dependent on Pml, moderate inhibition with arsenic trioxide results in selective eradication of leukemia-initiating cells. Small molecule agonists that stabilize p53 exist, such as Nutlin-3, and have been demonstrated to be useful in a pro-senescence therapeutic approach to treat *Pten*-deleted prostate cancer (Alimonti et al., 2010). Such compounds, in moderate doses, may also inhibit *Pten*-deleted leukemogenesis without severely compromising HSC function.

We have also uncovered subtle differences in the tumor suppressor responses that may be exploited in the future. Whereas *Pten*-deleted HSCs were also depleted through the induction of p16$^{\text{Ink4a}}$, *Pten*-deleted leukemogenesis was inhibited by increased p19$^{\text{Arf}}$ levels. This raises the interesting possibility that the specific stabilization of p19$^{\text{Arf}}$ may selectively promote tumor suppression without facilitating stem cell depletion. Conversely, p16$^{\text{Ink4a}}$ inhibition, perhaps through RNA interference, would be predicted to prolong stem cell activity without significantly accelerating leukemogenesis. Nutlin-3 may substitute for the role of p19$^{\text{Arf}}$ with respect to p53 stabilization, but future small molecule stabilizers of p19$^{\text{Arf}}$ may illuminate further p53-independent tumor suppressive

functions of $p19^{Arf}$. These approaches are distinct from the inhibition of leukemogenesis by rapamycin, since mTOR inhibition reversed the induction of tumor suppressors. Thus, the approaches outlined above represent alternative strategies that may be useful for neoplasms refractory to mTOR inhibition, and perhaps more clinically useful than rapamycin alone. Even leukemias that originate in *Pten*-deleted mice sustain multiple genetic hits (Guo et al., 2008) and become rapamycin-resistant over time (Yilmaz et al., 2006).

FIP200 and fetal HSC maintenance

The second half of this thesis examined the consequences of disrupting the FIP200 signaling node on fetal HSC maintenance. The loss of FIP200 resulted in a severe anemia during embryonic development, perinatal death, and a cell-autonomous depletion of HSCs (Chapter 3). The impact of FIP200 deletion on its numerous binding partners (Gan and Guan, 2008) in the fetal liver has not been examined and warrants future investigation. However, confirming the role of FIP200 in autophagosome synthesis (Ganley et al., 2009; Hara and Mizushima, 2009; Hara et al., 2008; Hosokawa et al., 2009; Jung et al., 2009), defects in autophagy were present in the fetal liver. Additionally, *FIP200*-deleted HSCs displayed increased mitochondrial mass and ROS levels, consistent with a model in which defects in autophagy led to the accumulation of damaged mitochondria that increased toxic ROS. However, we do not conclusively know whether autophagy is impaired in *FIP200*-deleted HSCs. Due to the dramatic depletion of an already rare fetal HSC population, traditional detection of autophagosome components

by western blotting in this population has proven difficult. Novel methods to assess autophagy *in vivo* may shed further light as outlined below.

Approaches to study autophagy in stem cell biology

The most widely used marker to monitor autophagy is microtubule-associated protein light chain 3 (LC3) (Mizushima and Yoshimori, 2007), the mammalian homolog of yeast Atg8. Processed LC3 exists in two forms, and during autophagy induction, phosphatidylethanolamine (PE) is conjugated to LC3-I to form LC3-II which is then targeted to autophagic membranes (Mizushima, 2007). Transgenic mice which ubiquitously express a fusion GFP-LC3 protein have been generated and used to demonstrate active autophagy in various tissues during the neonatal starvation period immediately after birth, and in response to starvation in adult mice (Kuma et al., 2004; Mizushima et al., 2004). In cells that induce autophagy, GFP-LC3 staining patterns appear punctate, and these dots represent autophagosomes. The GFP-LC3 transgene could be crossed into FIP200 mutant mice and HSCs could be examined to test whether autophagosomes form in fetal HSCs of control mice but not in *FIP200*-deleted mice. However, this experiment has not yet been done.

Autophagosomes ultimately fuse with lysosomes to degrade their contents, and this has made it difficult to monitor the later stages of autophagy with GFP-LC3 since its fluorescence is extinguished in acidic environments (Kuma et al., 2007). To address this, transgenic mice harboring mCherry-LC3, which is resistant to lysosomal degradation, have also been created and used to measure autophagy in the heart (Iwai-Kanai et al., 2008). Furthermore, injection of mice with the fluorescent label monodansylcadaverine

(MDC) specifically labels autophagosomes, with tight correlation to mCherry-LC3 staining (Iwai-Kanai et al., 2008). Double transgenic mice harboring both GFP-LC3 and mCherry-LC3 have also been generated, and allow for the monitoring of autophagosomes fusing with lysosomes as puncta change color from yellow to red (Terada et al., 2010). Further analysis of these mice could also illuminate the role of autophagy in numerous additional tissues, including stem cells. Chemical library screens are rapidly identifying both mTORC1-dependent and mTORC1-independent inducers of autophagy (Renna et al., 2010), many of which are currently used therapeutically and could be used for autophagy rescue experiments.

The combination of LC3 indicator mice, techniques to label autophagosomes *in vivo* with MDC, and chemical inducers of autophagy represent powerful tools offering unprecedented opportunities to investigate the role of autophagy in stem cell biology. To date, there are no reports characterizing any stem cell population utilizing these mice, and fundamental questions regarding stem cell properties and their regulation could be addressed. Furthermore, mice from which essential autophagy genes (Atg5 and Atg7) can be conditionally deleted display significant neural phenotypes (Hara et al., 2006; Komatsu et al., 2006), and in the case of Atg7, fatal hematopoietic phenotypes (Mortensen et al., 2010). However, it is unknown whether these neural and hematopoietic defects reflect defects in stem cell function in these mice. In addition to testing stem cell function in Atg5-deficient or Atg7-deficient mice, these mice could also be crossed with LC3 indicator mice to directly visualize autophagic defects in stem cells. In fact, LC3 indicator mice could be crossed with any mutants that display stem cell phenotypes, particularly those impacting mTORC1 function, to test if autophagy is involved. With

146

respect to *Pten*-deleted HSCs, it is possible that autophagic defects also contribute to their depletion, since activation of mTORC1 results in the inhibition of autophagy (Codogno and Meijer, 2005). Treatment with rapamycin, a known inducer of autophagy (Ravikumar et al., 2004), may be exerting its rescue partially through restoration of autophagy.

In closing, the work described in this thesis provides further mechanistic insight into how Pten maintains adult HSCs, and demonstrates the critical role for FIP200 in the maintenance of fetal HSCs. Young, adult, and old HSCs show different characteristics with respect to cell-cycle kinetics (Cheshier et al., 1999; Kiel et al., 2007; Morrison et al., 1995; Morrison et al., 1996), and use of different self-renewal mechanisms (Levi and Morrison, 2009). Future work will shed further light on how HSCs are differentially regulated throughout age by determining the consequences PI-3kinase hyperactivation on young HSCs, and whether FIP200 is involved in the maintenance of adult HSCs.

BIBLIOGRAPHY

Akala, O.O., Park, I.K., Qian, D., Pihalja, M., Becker, M.W., and Clarke, M.F. (2008). Long-term haematopoietic reconstitution by Trp53-/-p16Ink4a-/-p19Arf-/- multipotent progenitors. Nature *453*, 228-232.

Alimonti, A., Nardella, C., Chen, Z., Clohessy, J.G., Carracedo, A., Trotman, L.C., Cheng, K., Varmeh, S., Kozma, S.C., Thomas, G.*, et al.* A novel type of cellular senescence that can be enhanced in mouse models and human tumor xenografts to suppress prostate tumorigenesis. J Clin Invest *120*, 681-693.

Banito, A., Rashid, S.T., Acosta, J.C., Li, S., Pereira, C.F., Geti, I., Pinho, S., Silva, J.C., Azuara, V., Walsh, M.*, et al.* (2009). Senescence impairs successful reprogramming to pluripotent stem cells. Genes Dev *23*, 2134-2139.

Brunet, A., Sweeney, L.B., Sturgill, J.F., Chua, K.F., Greer, P.L., Lin, Y., Tran, H., Ross, S.E., Mostoslavsky, R., Cohen, H.Y.*, et al.* (2004). Stress-dependent regulation of FOXO transcription factors by the SIRT1 deacetylase. Science *303*, 2011-2015.

Buitenhuis, M., Verhagen, L.P., van Deutekom, H.W., Castor, A., Verploegen, S., Koenderman, L., Jacobsen, S.E., and Coffer, P.J. (2008). Protein kinase B (c-akt) regulates hematopoietic lineage choice decisions during myelopoiesis. Blood *111*, 112-121.

Cheshier, S.H., Morrison, S.J., Liao, X., and Weissman, I.L. (1999). In vivo proliferation and cell cycle kinetics of long-term self-renewing hematopoietic stem cells. Proc Natl Acad Sci U S A *96*, 3120-3125.

Codogno, P., and Meijer, A.J. (2005). Autophagy and signaling: their role in cell survival and cell death. Cell Death Differ *12 Suppl 2*, 1509-1518.

Gan, B., and Guan, J.L. (2008). FIP200, a key signaling node to coordinately regulate various cellular processes. Cell Signal *20*, 787-794.

Ganley, I.G., Lam du, H., Wang, J., Ding, X., Chen, S., and Jiang, X. (2009). ULK1.ATG13.FIP200 complex mediates mTOR signaling and is essential for autophagy. J Biol Chem *284*, 12297-12305.

Guertin, D.A., Stevens, D.M., Saitoh, M., Kinkel, S., Crosby, K., Sheen, J.H., Mullholland, D.J., Magnuson, M.A., Wu, H., and Sabatini, D.M. (2009). mTOR complex 2 is required for the development of prostate cancer induced by Pten loss in mice. Cancer Cell *15*, 148-159.

Guo, W., Lasky, J.L., Chang, C.J., Mosessian, S., Lewis, X., Xiao, Y., Yeh, J.E., Chen, J.Y., Iruela-Arispe, M.L., Varella-Garcia, M.*, et al.* (2008). Multi-genetic events collaboratively contribute to Pten-null leukaemia stem-cell formation. Nature *453*, 529-533.

Hara, T., and Mizushima, N. (2009). Role of ULK-FIP200 complex in mammalian autophagy: FIP200, a counterpart of yeast Atg17? Autophagy *5*, 85-87.

Hara, T., Nakamura, K., Matsui, M., Yamamoto, A., Nakahara, Y., Suzuki-Migishima, R., Yokoyama, M., Mishima, K., Saito, I., Okano, H.*, et al.* (2006). Suppression of basal autophagy in neural cells causes neurodegenerative disease in mice. Nature *441*, 885-889.

Hara, T., Takamura, A., Kishi, C., Iemura, S., Natsume, T., Guan, J.L., and Mizushima, N. (2008). FIP200, a ULK-interacting protein, is required for autophagosome formation in mammalian cells. J Cell Biol *181*, 497-510.

Hong, H., Takahashi, K., Ichisaka, T., Aoi, T., Kanagawa, O., Nakagawa, M., Okita, K., and Yamanaka, S. (2009). Suppression of induced pluripotent stem cell generation by the p53-p21 pathway. Nature *460*, 1132-1135.

Hosokawa, N., Hara, T., Kaizuka, T., Kishi, C., Takamura, A., Miura, Y., Iemura, S., Natsume, T., Takehana, K., Yamada, N.*, et al.* (2009). Nutrient-dependent mTORC1 association with the ULK1-Atg13-FIP200 complex required for autophagy. Mol Biol Cell *20*, 1981-1991.

Ito, K., Bernardi, R., Morotti, A., Matsuoka, S., Saglio, G., Ikeda, Y., Rosenblatt, J., Avigan, D.E., Teruya-Feldstein, J., and Pandolfi, P.P. (2008). PML targeting eradicates quiescent leukaemia-initiating cells. Nature *453*, 1072-1078.

Iwai-Kanai, E., Yuan, H., Huang, C., Sayen, M.R., Perry-Garza, C.N., Kim, L., and Gottlieb, R.A. (2008). A method to measure cardiac autophagic flux in vivo. Autophagy *4*, 322-329.

Janzen, V., Forkert, R., Fleming, H.E., Saito, Y., Waring, M.T., Dombkowski, D.M., Cheng, T., DePinho, R.A., Sharpless, N.E., and Scadden, D.T. (2006). Stem-cell ageing modified by the cyclin-dependent kinase inhibitor p16INK4a. Nature *443*, 421-426.

Jung, C.H., Jun, C.B., Ro, S.H., Kim, Y.M., Otto, N.M., Cao, J., Kundu, M., and Kim, D.H. (2009). ULK-Atg13-FIP200 complexes mediate mTOR signaling to the autophagy machinery. Mol Biol Cell *20*, 1992-2003.

Kastan, M.B., Radin, A.I., Kuerbitz, S.J., Onyekwere, O., Wolkow, C.A., Civin, C.I., Stone, K.D., Woo, T., Ravindranath, Y., and Craig, R.W. (1991). Levels of p53 protein increase with maturation in human hematopoietic cells. Cancer Res *51*, 4279-4286.

Kawamura, T., Suzuki, J., Wang, Y.V., Menendez, S., Morera, L.B., Raya, A., Wahl, G.M., and Belmonte, J.C. (2009). Linking the p53 tumour suppressor pathway to somatic cell reprogramming. Nature *460*, 1140-1144.

Kharas, M.G., and Fruman, D.A. (2005). ABL oncogenes and phosphoinositide 3-kinase: mechanism of activation and downstream effectors. Cancer Res *65*, 2047-2053.

Kheradmand Kia, S., Solaimani Kartalaei, P., Farahbakhshian, E., Pourfarzad, F., von Lindern, M., and Verrijzer, C.P. (2009). EZH2-dependent chromatin looping controls INK4a and INK4b, but not ARF, during human progenitor cell differentiation and cellular senescence. Epigenetics Chromatin *2*, 16.

Kiel, M.J., He, S., Ashkenazi, R., Gentry, S.N., Teta, M., Kushner, J.A., Jackson, T.L., and Morrison, S.J. (2007). Haematopoietic stem cells do not asymmetrically segregate chromosomes or retain BrdU. Nature *449*, 238-242.

Komatsu, M., Waguri, S., Chiba, T., Murata, S., Iwata, J., Tanida, I., Ueno, T., Koike, M., Uchiyama, Y., Kominami, E.*, et al.* (2006). Loss of autophagy in the central nervous system causes neurodegeneration in mice. Nature *441*, 880-884.

Kranc, K.R., Schepers, H., Rodrigues, N.P., Bamforth, S., Villadsen, E., Ferry, H., Bouriez-Jones, T., Sigvardsson, M., Bhattacharya, S., Jacobsen, S.E.*, et al.* (2009). Cited2 is an essential regulator of adult hematopoietic stem cells. Cell Stem Cell *5*, 659-665.

Krishnamurthy, J., Ramsey, M.R., Ligon, K.L., Torrice, C., Koh, A., Bonner-Weir, S., and Sharpless, N.E. (2006). p16INK4a induces an age-dependent decline in islet regenerative potential. Nature *443*, 453-457.

Kuma, A., Hatano, M., Matsui, M., Yamamoto, A., Nakaya, H., Yoshimori, T., Ohsumi, Y., Tokuhisa, T., and Mizushima, N. (2004). The role of autophagy during the early neonatal starvation period. Nature *432*, 1032-1036.

Kuma, A., Matsui, M., and Mizushima, N. (2007). LC3, an autophagosome marker, can be incorporated into protein aggregates independent of autophagy: caution in the interpretation of LC3 localization. Autophagy *3*, 323-328.

Levi, B.P., and Morrison, S.J. (2009). Stem Cells Use Distinct Self-renewal Programs at Different Ages. Cold Spring Harb Symp Quant Biol.

Li, H., Collado, M., Villasante, A., Strati, K., Ortega, S., Canamero, M., Blasco, M.A., and Serrano, M. (2009). The Ink4/Arf locus is a barrier for iPS cell reprogramming. Nature *460*, 1136-1139.

Lin, T., Chao, C., Saito, S., Mazur, S.J., Murphy, M.E., Appella, E., and Xu, Y. (2005). p53 induces differentiation of mouse embryonic stem cells by suppressing Nanog expression. Nat Cell Biol *7*, 165-171.

Marion, R.M., Strati, K., Li, H., Murga, M., Blanco, R., Ortega, S., Fernandez-Capetillo, O., Serrano, M., and Blasco, M.A. (2009). A p53-mediated DNA damage response limits reprogramming to ensure iPS cell genomic integrity. Nature *460*, 1149-1153.

Mizushima, N. (2007). Autophagy: process and function. Genes Dev *21*, 2861-2873.

Mizushima, N., Yamamoto, A., Matsui, M., Yoshimori, T., and Ohsumi, Y. (2004). In vivo analysis of autophagy in response to nutrient starvation using transgenic mice expressing a fluorescent autophagosome marker. Mol Biol Cell *15*, 1101-1111.

Mizushima, N., and Yoshimori, T. (2007). How to interpret LC3 immunoblotting. Autophagy *3*, 542-545.

Molofsky, A.V., He, S., Bydon, M., Morrison, S.J., and Pardal, R. (2005). Bmi-1 promotes neural stem cell self-renewal and neural development but not mouse growth and survival by repressing the p16Ink4a and p19Arf senescence pathways. Genes Dev *19*, 1432-1437.

Molofsky, A.V., Slutsky, S.G., Joseph, N.M., He, S., Pardal, R., Krishnamurthy, J., Sharpless, N.E., and Morrison, S.J. (2006). Increasing p16INK4a expression decreases forebrain progenitors and neurogenesis during ageing. Nature *443*, 448-452.

Morrison, S.J., Hemmati, H.D., Wandycz, A.M., and Weissman, I.L. (1995). The purification and characterization of fetal liver hematopoietic stem cells. Proc Natl Acad Sci U S A *92*, 10302-10306.

Morrison, S.J., Wandycz, A.M., Akashi, K., Globerson, A., and Weissman, I.L. (1996). The aging of hematopoietic stem cells. Nature Medicine *2*, 1011-1016.

Mortensen, M., Ferguson, D.J., Edelmann, M., Kessler, B., Morten, K.J., Komatsu, M., and Simon, A.K. Loss of autophagy in erythroid cells leads to defective removal of mitochondria and severe anemia in vivo. Proc Natl Acad Sci U S A *107*, 832-837.

Nishino, J., Kim, I., Chada, K., and Morrison, S.J. (2008). Hmga2 promotes neural stem cell self-renewal in young but not old mice by reducing p16Ink4a and p19Arf Expression. Cell *135*, 227-239.

Oguro, H., Iwama, A., Morita, Y., Kamijo, T., van Lohuizen, M., and Nakauchi, H. (2006). Differential impact of Ink4a and Arf on hematopoietic stem cells and their bone marrow microenvironment in Bmi1-deficient mice. J Exp Med *203*, 2247-2253.

Ravikumar, B., Vacher, C., Berger, Z., Davies, J.E., Luo, S., Oroz, L.G., Scaravilli, F., Easton, D.F., Duden, R., O'Kane, C.J.*, et al.* (2004). Inhibition of mTOR induces autophagy and reduces toxicity of polyglutamine expansions in fly and mouse models of Huntington disease. Nat Genet *36*, 585-595.

Renna, M., Jimenez-Sanchez, M., Sarkar, S., and Rubinsztein, D.C. Chemical inducers of autophagy that enhance the clearance of mutant proteins in neurodegenerative diseases. J Biol Chem *285*, 11061-11067.

Sarbassov, D.D., Ali, S.M., Sengupta, S., Sheen, J.H., Hsu, P.P., Bagley, A.F., Markhard, A.L., and Sabatini, D.M. (2006). Prolonged rapamycin treatment inhibits mTORC2 assembly and Akt/PKB. Mol Cell *22*, 159-168.

Schemionek, M., Elling, C., Steidl, U., Baumer, N., Hamilton, A., Spieker, T., Gothert, J.R., Stehling, M., Wagers, A., Huettner, C.S.*, et al.* BCR-ABL enhances differentiation of long-term repopulating hematopoietic stem cells. Blood *115*, 3185-3195.

Suzuki, A., Yamaguchi, M.T., Ohteki, T., Sasaki, T., Kaisho, T., Kimura, Y., Yoshida, R., Wakeham, A., Higuchi, T., Fukumoto, M.*, et al.* (2001). T cell-specific loss of Pten leads to defects in central and peripheral tolerance. Immunity *14*, 523-534.

Terada, M., Nobori, K., Munehisa, Y., Kakizaki, M., Ohba, T., Takahashi, Y., Koyama, T., Terata, Y., Ishida, M., Iino, K.*, et al.* Double transgenic mice crossed GFP-LC3 transgenic mice with alphaMyHC-mCherry-LC3 transgenic mice are a new and useful tool to examine the role of autophagy in the heart. Circ J *74*, 203-206.

Tothova, Z., and Gilliland, D.G. (2007). FoxO transcription factors and stem cell homeostasis: insights from the hematopoietic system. Cell Stem Cell *1*, 140-152.

Utikal, J., Polo, J.M., Stadtfeld, M., Maherali, N., Kulalert, W., Walsh, R.M., Khalil, A., Rheinwald, J.G., and Hochedlinger, K. (2009). Immortalization eliminates a roadblock during cellular reprogramming into iPS cells. Nature *460*, 1145-1148.

van der Horst, A., and Burgering, B.M. (2007). Stressing the role of FoxO proteins in lifespan and disease. Nat Rev Mol Cell Biol *8*, 440-450.

Wang, M.C., Bohmann, D., and Jasper, H. (2005). JNK extends life span and limits growth by antagonizing cellular and organism-wide responses to insulin signaling. Cell *121*, 115-125.

Yilmaz, O.H., Valdez, R., Theisen, B.K., Guo, W., Ferguson, D.O., Wu, H., and Morrison, S.J. (2006). Pten dependence distinguishes haematopoietic stem cells from leukaemia-initiating cells. Nature *441*, 475-482.

Yu, H., Li, Y., Gao, C., Fabien, L., Jia, Y., Lu, J., Silberstein, L.E., Pinkus, G.S., Ye, K., Chai, L.*, et al.* Relevant mouse model for human monocytic leukemia through Cre/lox-controlled myeloid-specific deletion of PTEN. Leukemia *24*, 1077-1080.